NUREG/CR-5169
PNL-7154

Mobilization and Transport of Uranium at Uranium Mill Tailings Disposal Sites

Application of a Chemical Transport Model

Prepared by R. L. Erikson, C. J. Hostetler, M. L. Kemner

Mobilization and Transport of Uranium at Uranium Mill Tailings Disposal Sites

Application of a Chemical Transport Model

Prepared by
R. L. Erikson, C. J. Hostetler, M. L. Kemner

Pacific Northwest Laboratory
Richland, WA 99352

ABSTRACT

The geochemical processes of aqueous specification, precipitation, dissolution, and adsorption influence the transport of uranium at uranium mill tailings disposal sites. Traditional transport models involve the use of a single parameter, the retardation factor, to simulate the effects of these geochemical processes. Single parameter models are most applicable to field situations exhibiting no changes in major element chemistry along the flow path. Because of the changes in major element chemistry that occur when acidic leachate contacts a neutralizing soil, a single parameter transport model cannot accurately capture the details of uranium migration at a number of disposal sites. We have used a chemical transport model to qualitatively describe the effects of geochemical mechanisms on uranium transport. The result is a generalized conceptual model that can reproduce the features observed at a number of uranium mill tailings disposal sites.

SUMMARY

The purpose of our study is the development of a qualitative model of geochemical processes controlling uranium migration at uranium mill tailings disposal sites. Knowledge of operative mechanisms and their effects is important in assessing the environmental impact of a disposal site and in evaluating potential remedial actions. Our primary approach is to infer the identity of geochemical mechanisms from observations of contaminant plumes at existing disposal sites. We have supplemented this approach with information gathered from laboratory experiments and geochemical modeling. The result of this approach is a generalized conceptual model of geochemical mechanisms operating at uranium mill tailings disposal sites.

In order to use this conceptual model to make calculations of uranium transport, a mathematical transport model must be employed. Traditional transport models involve the use of a single parameter, the retardation factor, to simulate the effects of geochemical processes. Single parameter models are most applicable to field situations exhibiting no changes in major element chemistry along the flow path. Because of the changes in major element chemistry that occur when acidic leachate contacts a neutralizing soil, a single parameter transport model cannot accurately capture the details of uranium migration at a number of disposal sites. We have used a chemical transport model to calculate the effects of geochemical mechanisms on uranium transport. The result is an implementation of the generalized conceptual model that can be used to calculate the transport of uranium under a variety of field conditions.

The generalized conceptual model can be used to estimate uranium transport at individual field sites if sufficient site characterization data are available. The geochemical interactions at the field sites we examined in this report were dominated by acid/base reactions. For these sites, the most important site-specific geochemical parameters required are the buffering capacity of the soil, the adsorptive capacity of the soil, and an analysis of the leachate composition. The interaction of the leachate with

the soil governs the migration of the neutralization front. Migration of the uranium front is influenced both by the acid/base geochemistry and by the presence of complexing ligands in the leachate. Given this site specific information, the chemical transport model can be used to investigate the environmental impact of an existing uranium mill tailings disposal site, and estimate the consequences of proposed remedial actions.

ACKNOWLEDGMENTS

CONTENTS

FIGURES

TABLES

1.0 INTRODUCTION

The mining and milling of uranium requires chemical treatments that use strong acids and sometimes alkaline solutions to extract uranium from the ore. These uranium extraction procedures produce large quantities of uranium mill tailings (UMT) solids and tailings leachates. Approximately 1.8×10^8 metric tons of uranium mill tailings are disposed of in a number of facilities in the United States (Peterson et al. 1986). Of the total disposal sites, 24 have been officially designated inactive under the Uranium Mill Tailings Radiation Control Act (UMTRCA). These sites have been scheduled for clean-up under the U.S. Department of Energy's (DOE) Uranium Mill Tailings Remedial Action Project (UMTRAP, Matthews 1985; Wright and Turner 1987). UMTRCA-associated regulations for the inactive sites include 40 CFR 192 (USEPA 1988) and 10 CFR 40, Appendix A (USNRC 1984). These regulations require that the waste be stabilized for not less than 200 years (but preferably 1000 years) and that the planned actions should ensure that the U.S. Environmental Protection Agency (EPA) groundwater standards are met.

Amendments to UMTRCA allow DOE to conduct the remediation process as a two-step program. The program first requires the stabilization of the uranium mill tailings and then subsequent clean-up of groundwater contamination. The tailings are commonly moved and stabilized and the groundwater standards must be met at any new site. Leachate plumes are commonly found in the groundwater systems at these sites and the existing contamination must be reduced to meet the applicable groundwater standards. In addition, there are many sites that have not been designated for remedial action under UMTRAP. These sites were permitted facilities that are either still in operation, or had ceased operation after 1983. These sites must also be brought into compliance with EPA standards. Plans to meet these requirements are currently being developed and submitted to the U.S. Nuclear Regulatory Commission (NRC) for approval.

FACTORS AFFECTING CONTAMINANT MIGRATION

Potential environmental impacts at unstabilized UMT disposal sites
include release of radon gas into the atmosphere and release of leachate into
surface and groundwater systems. Although all transport pathways must be
considered in evaluating the environmental effects of these UMT disposal
sites, the assessment of groundwater quality impacts is the particular
concern of this project. The results of this project are also applicable to
the assessment of the impacts of in situ solution mining of uranium.

UMT disposal sites are potential sources of groundwater contamination
because subsurface water movement through the disposal site can result in the
mobilization and release of contaminants into groundwater systems. Depending
on the hydrologic and geochemical characteristics of the site, groundwater
concentrations of radionuclides, trace metals, cations, and anions introduced
from UMT leachate can exceed drinking water standards at considerable
distances away from the source.

Contaminant migration at disposal sites is governed by both hydrologic
and geochemical factors. The physical properties of the subsurface soils
control the velocity and dispersion of solutes transported through the media.
The porosity, saturated hydraulic conductivity, and relative permeability/
water retention relationships all influence moisture movement in variably
saturated soils. The boundary conditions of the groundwater system also
affect the flow paths from the disposal site. Hydrodynamic dispersion, which
results in the spreading of a contaminant plume, acts to attenuate the
movement of contaminants.

The geochemical factors influencing solute concentrations include
aqueous speciation, reduction/oxidation, solubility, ion-exchange, and
specific-ion adsorption reactions. Aqueous speciation and
reduction/oxidation reactions do not affect total solute concentrations but
can control the distribution of species in solution and their thermodynamic
activities. Interactions between groundwater or leachate with soil minerals
and mineral surfaces alter the composition of the pore water through

1.2

adsorption, ion-exchange, and solubility reactions. These mass-transfer reactions also retard solute velocities and attenuate their concentrations relative to a conservative tracer. Thus, the spatial and temporal distribution of contaminants at disposal sites are a complex function of both hydrologic and geochemical variables.

Uses of Transport Models

Transport models offer a quantitative description of solute migration. Thus, computer codes containing mathematical models that represent the hydrologic and geochemical processes are required to obtain a quantitative understanding of the subsurface transport of solutes in porous media. The simplest approach utilizes the one-dimensional advection/dispersion equation. Transport processes are described through an average groundwater velocity and coefficient of hydrodynamic dispersion. The effects of chemical reactions for those species that exhibit a retardation relative to a conservative tracer can be included using a constant retardation factor that approximates the attenuation behavior. However, chemical attenuation is a function of both solution and soil interactions that can more accurately be described using thermodynamic mass-action and mass-transfer reactions. A constant retardation mechanism cannot accurately describe the resulting nonlinear transport behavior in geologically complex systems of variable chemical composition.

Recent advances in modeling solute transport have included incorporating mass-transfer reactions with the advective/dispersive description of solute transport. These reactions have been incorporated into codes that are divided into one-step and two-step coupled codes depending on the numerical technique used to couple the geochemical reactions with solute transport. In one-step codes, the chemical and transport equations are combined into a set of coupled, nonlinear partial differential equations and are solved numerically. Geochemical attenuation mechanisms in these models have included ion-exchange reactions (Rubin and James 1973; Valocchi et al. 1981), ion-exchange reactions with solute complexation (Miller and Benson 1983), specific-ion adsorption reactions with solute complexation (Jennings et al.

1.3

1982), and adsorption and solubility reactions with solute complexation (Kirkner and Reeves 1988).

In two-step codes, time is treated as a discrete variable and the solute movement calculation is separated from the chemical reaction calculation at each time increment. Two-step codes have commonly employed a finite elements method to solve the transport calculation and either a direct iteration method (Grove and Wood 1979) or the Newton-Raphson method (Walsh et al. 1982; Kirkner et al. 1984; Cederberg et al. 1985; Narasimhan et al. 1986) to solve the chemical reaction calculation. Geochemical attenuation mechanisms included in two-step codes also have included solute complexation, ion-exchange, surface adsorption, and solubility equilibria.

PURPOSE OF STUDY

The first phase of this project emphasized the determination of conceptual models for geochemical attenuation reactions relevant to contaminant migration from the disposal of uranium mill tailings in earthen pits. The geochemical code MINTEQ (Felmy et al. 1984) was used to test the accuracy of the conceptual models using both laboratory column data and field site data. The conceptual model developed (Peterson et al. 1986) included solubility reactions involving the neutralization of acidic leachate by calcareous soils, and the adsorption of several trace metals onto amorphous iron oxyhydroxides present in the soil. The model was capable of qualitatively predicting effluent concentrations of several of the major constituents and trace elements for successive pore volumes of leachate reacting with soils in column experiments and in the field. One limitation of this approach is the neglect of transport processes. The evolution of solute profiles as explicit functions of space and time cannot be modeled using geochemical codes alone because of the advective/dispersive nature of solute transport.

In this phase of the project, we used the two-step coupled transport code CTM described in Erikson and Hostetler (1989) to examine geochemical processes affecting contaminant mobility at uranium mill tailings disposal

1.4

sites. A simplified geohydrochemical conceptual model was developed to represent contaminant migration of acidic leachate from waste disposal ponds. In particular, the focus of the model is on the transport of uranium and other aqueous species that affect the transport of uranium. Our model is not site-specific; because of spatial and temporal gaps in hydrologic and geochemical field data at many disposal sites, it is difficult to derive comprehensive site-specific initial and boundary conditions. Therefore, quantitative comparisons of model calculations with approximated field conditions is unwarranted. Instead, we examined the attenuation behavior of solutes involved in two types of mass-transfer reactions; precipitation/dissolution, and specific-ion adsorption reactions. Both types of reactions are particularly relevant to the observed behavior of uranium in low-temperature solutions associated with uranium ore deposits (Langmuir 1978a,b; Hsi and Langmuir 1985). The relative importance of these mass-transfer reactions is controlled by the chemical composition of the leachate and the chemical properties of the soil.

The geohydrochemical conceptual model developed in this study for uranium transport at uranium mill tailings disposal sites is divided into separate hydrologic and geochemistry models. The hydrologic parameters (groundwater velocity, dispersivity) were assumed constant and were set equal to values typical of sandy or silty soils. The geochemistry model was formulated from previous work on this project as summarized in Peterson et al. (1986) and a review of lixiviant chemical compositions and soil properties typical of UMT disposal sites. The soil chemical properties important in the attenuation process included the soil acid buffering capacity and specific-ion adsorption capacity. The acid buffering capacity controls the neutralization of the acidic leachate by the soil, the advance of the pH front, and thus will buffer the pH of the soil solution. The adsorption capacity refers to the quantity of adsorptive surface sites in the soil available for the specific-ion adsorption of a number of adsorbing solutes.

Using the geohydrochemical conceptual model that contains the mechanistic speciation/solubility/adsorption reactions, we investigated

1.5

solute profiles as a function of time and space for the different attenuation mechanisms. In addition, the model results were used to calculate local distribution coefficients and retardation factors for the transport of uranium. The results of the transport simulations are qualitatively compared to solute profiles that were interpolated from field data obtained from the Federal American Partners and Riverton sites in Wyoming, and the L-Bar site in New Mexico. The simulations illustrate the sensitivity of groundwater transport times and distances traveled to the geochemical factors affecting contaminant mobility and the limitations of using a constant retardation model to describe the migration of some reactive solutes. The use of a coupled model for transport may assist in ranking the relative importance of the types of mass-transfer reactions for attenuating the transport of contaminants.

In Chapter 2.0 of this report, we discuss observations of solute migration at four UMT disposal sites. Also in this chapter, the generic model developed by Sheppard and Brown (1982) to describe solute transport at UMT field sites is reviewed. The chemical transport model CTM is discussed in Chapter 3.0 of this report. The CTM code is used in conjunction with the geohydrological conceptual model described in Chapter 4.0 to calculate solute transport under several scenarios. The results of these calculations are discussed in Chapter 5.0. Chapter 6.0 summarizes the observations and calculations made in this report, and presents recommendations for site characterization work at UMT disposal sites.

2.0 CONSTRAINTS FROM FIELD MEASUREMENTS

Field observations of contaminant plumes are of two types. The first type is an observation of spatial contaminant distribution in the aqueous phase obtained from a network of monitoring wells at a point in time. The second type is an observation of spatial contaminant distribution in the vadose zone obtained from a series of soil cores taken at a point in time. The relationship between the two types of observations is complementary: the aqueous phase distribution shows the mobile portion of the contaminant, while the solid phase distribution shows the immobile portion. Although environmental regulation focuses particularly on the aqueous phase distribution (e.g., through drinking water standards, maximum concentration limits, etc.) the solid phase distribution can also be of concern because of plant uptake and remobilization. The primary geochemical factors involved in remobilization are changes in pH and Eh. For example, passage of a pH front can cause adsorbed constituents to be released into the aqueous phase.

Supplementary information on the field setting is required for the interpretation of plume distributions in terms of geochemical mechanisms. This information includes the chemical composition of leachate entering the subsurface and the chemical and mineralogic composition of the subsurface material. Of particular interest are the pH buffering capacity and the adsorptive capacity of the subsurface material. The pH buffering capacity and the acidity of the leachate will act together to govern the pH in the plume. Acid/base chemistry plays an important role in determining the stability of solid phases which can remove contaminants from solution. In addition, the pH together with the adsorptive capacity of the subsurface material determines the degree to which adsorption can immobilize contaminants from the plume.

A brief literature review was performed to collate field data for several UMT disposal sites. Site data were reviewed for the Federal American Partners (FAP), Riverton, L-Bar, and Lucky Mc Pathfinder sites. The review of field data for all sites examined suggested both the subsurface material properties and the plume distributions can exhibit large amounts of spatial

variation, and can be difficult to quantify through point measurements. Often, soil characterization is performed only for a single sample of material taken from the site. The spatial distribution of monitoring wells is generally not designed to estimate spatial variability (especially the vertical variability) in plume distributions. In addition, a limited number of soil cores may be analyzed for contaminant distribution.

Based on our review, we concluded that insufficient site characterization information exists at any individual UMT disposal site to allow the use of a multidimensional geohydrochemical transport model to predict contaminant distributions with any degree of certainty. In addition, field observations of contaminant distributions are insufficient to allow a quantitative test of such a predictive model. Uncertainties in subsurface properties, leachate production (as a function of time), and plume distributions led us to develop a generalized model for contaminant transport at UMT disposal sites that captures the major geochemical features observed at these sites. We feel that the proper use of geohydrochemical transport modeling is as an aid in identifying the geochemical mechanisms influencing solute migration at UMT field sites.

GENERIC MODEL OF GEOCHEMICAL PROCESSES AT UMT SITES

In order to apply a geohydrochemical transport code to identify geochemical mechanisms at UMT field sites, a conceptual model of the important geochemical and hydrological aspects of the problem must be developed. We have adopted the generic model of Sheppard and Brown (1982) as a starting point for our analysis. Sheppard and Brown (1982) identified acid/base reactions as the predominant geochemical process controlling leachate migration at UMT disposal sites. In particular, their generic model focuses on the neutralization of acidic leachate by calcareous soil. Because a common procedure used to extract uranium from ore involves processing the crushed ore with sulfuric acid and oxidizing agents, leachates at UMT disposal sites are typically highly acidic and oxidizing. UMT disposal sites are commonly located over subsurface materials containing carbonate minerals, which have the capacity to neutralize the acidity of the leachate.

As will be discussed in detail in Chapter 4.0, the partitioning of uranium among the aqueous, solid, and surface phases is particularly sensitive to pH. In general, uranium is strongly partitioned into the mobile aqueous phase at low pH, and prefers the solid and surface phases at high pH. Thus, as neutralization of the acidic leachate occurs, uranium tends to become immobilized by precipitation and adsorption reactions. Sheppard and Brown (1982) claim that this pattern of behavior is observed for most heavy metals, transition metals, toxic non-metals, and radionuclides.

Sheppard and Brown (1982) use water quality information to divide the contaminant plume at UMT sites into three zones. Chloride is assumed to behave as a conservative tracer, so chloride concentrations reflect the hydrologic processes of advection and dispersion. The concentrations of other species are affected by geochemical reactions in addition to advection and dispersion. The pH distribution in the plume is used to define the extent of neutralization. Sulfate concentrations in the plume are governed by precipitation of sulfate minerals and the adsorption of sulfate on mineral surfaces. Trace metal concentrations are also governed by precipitation and adsorption reactions.

The three zones in the contaminant plume are illustrated in Figure 2.1. In the acid zone, closest to the disposal impoundment, the pH is similar to the pH of the leachate because in this zone the acid buffering capacity of the soil has been consumed. The concentrations of chloride, sulfate, and trace metals are high, similar to those in the leachate. The second zone out from the impoundment is the neutralization zone. This zone is characterized by an increase in the pH from the acidic influent values to near neutral. The buffering capacity of the soil is lower in this zone than in uncontacted soil. Chloride concentrations are not affected by the neutralization reactions, and remain at the influent values. Sulfate concentrations are controlled by the precipitation of sulfate minerals. There is a decrease

2.3
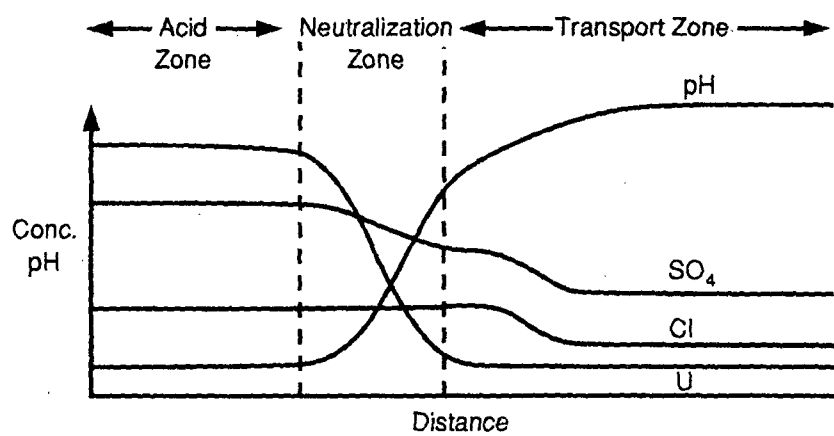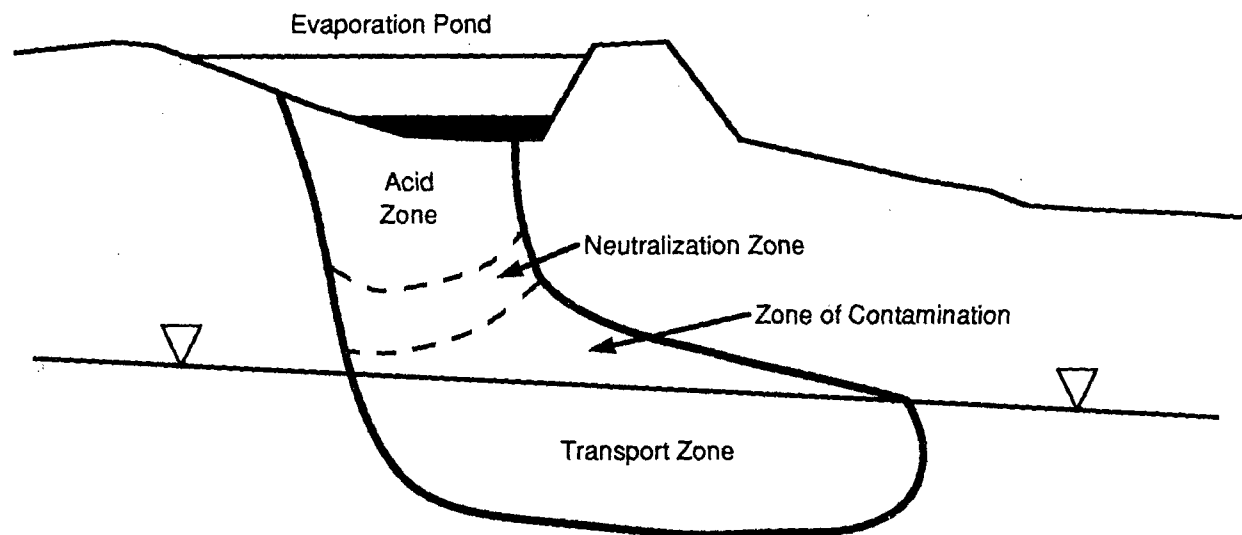
FIGURE 2.1. The Generic Model of Sheppard and Brown (1982) for the Transport of Solutes at UMT Disposal Sites.

2.4

in trace metal and radionuclide concentrations in zone 2. The third zone in the plume in the model of Sheppard and Brown (1982) is the neutral pH zone. The pH in this zone increases from neutral to alkaline values typical of carbonate sediments. The buffering capacity of the soil is essentially unaffected by the leachate. Chloride, sulfate, and trace metal concentrations decrease with distance from the impoundment in this zone as the hydrologic processes of advection and dispersion dominate. In this report we refer to this zone as the transport zone (Figure 2.1) which combines the properties of the neutral zone and the background water composition zone defined in the model of Sheppard and Brown (1982).

For any particular UMT site, the location and velocity of migration of the three zones depends on the hydrologic and geochemical conditions at the site. The location of the transport zone is governed by hydrologic processes. The location of the neutralization zone is governed primarily by the relationship between the acidity of the influent and the acid buffering capacity of the soil. The acid zone migrates behind the neutralization zone until leachate stops leaving the impoundment.

The breakthrough location of the transport zone can easily be obtained by multiplying the total time by the pore water velocity. The location of the center of mass of the neutralization zone relative to the impoundment is called the neutralization length by Sheppard and Brown (1982). They suggest that the neutralization length can be calculated by dividing the total acid content that has seeped into the subsurface (up to a given time, through a given area) by the soil buffering capacity (per volume of soil).

In summary, the major features of the generic model of Sheppard and Brown (1982) are:

- three distinct zones in the plume can be identified by water quality data,

- the location of the outermost zone, the transport zone, is governed primarily by hydrologic processes and can be calculated from the pore

water velocity,

• the location of the second zone, the neutralization zone, is governed primarily by acid/base reactions and can be calculated from the acidity of the leachate and the buffering capacity of the soil,

• the acid zone follows the neutralization zone until the leachate stops leaving the impoundment.

In the remainder of this chapter, we will discuss the application of the generic model of Sheppard and Brown (1982) to the field data for the four field sites identified in the literature review. Our attention will focus on identifying the zones of contamination and estimating the frontal velocities from the site characterization data. In the following sections of this report, we will express the model of Sheppard and Brown (1982) in more quantitative terms using a chemical transport model.

DESCRIPTION OF INDIVIDUAL SITES

Four field sites were selected for this study: the Sohio L-Bar site in Cebola County, New Mexico (Longmire and Brookins 1982), the Riverton, Wyoming site (White et al. 1984), the Federal American Partners uranium mill in central Wyoming (Dames and Moore 1981), and the Lucky Mc Pathfinder Mill in Gas Hills, Wyoming (Erikson and Sherwood 1982). Water quality data obtained from monitoring wells were available for the first three sites, and trace metal concentrations obtained from soil corings were available for the last site. These sites were selected because of the site characterization data and because they appear to span a range of soil buffering capacities.

Sohio L-Bar Site

The SOHIO L-Bar site is located in Cebola County, New Mexico. The L-Bar site contains a tailings basin of approximately 40 acres in which uranium mill tailings were disposed of from 1976 to 1982 (Longmire and Brookins

1982). The tailings and pore waters are contained by dams on the west and northeast side. The tailings have a maximum thickness of 5 m. The tailings are the residue from a sulfuric acid leaching process, and have a highly acidic character.

The hydrogeology of the area around the tailings basin consists of alluvial material overlying the Tres Hermanos sandstone. The alluvial material contains an unconfined aquifer that is hydraulically connected to a deeper aquifer located in the sandstone. Infiltration from the tailings basin has supplied recharge to the alluvial aquifer. In the deeper aquifer, groundwater flow is to the north-northwest.

The underlying sediments and groundwater are alkaline in character; calcite is present as an interstitial precipitate in the alluvial material. The buffering capacity of the alluvium is at least 3 wt. % (as calcium carbonate). No data was presented for the adsorptive capacity of the sediment or aquifer material.

The major element composition of the L-Bar leachate is given in Table 2.1. A speciation analysis showed that 0.4M of excess hydrogen (i.e., hydrogen not obtained from dissociation of water) were required to reproduce the measured pH of 0.98. The L-Bar leachate is predominately sulfuric acid. We performed a second calculation in which the leachate was allowed to dissolve calcite and precipitate gypsum until both minerals were in equilibrium simultaneously. This calculation was designed to simulate neutralization of the tailings solution by carbonate containing sediments (e.g., Erikson and Sherwood 1982). Our calculation showed that each kilogram of the tailings solution could dissolve up to 29.2 grams of calcite and precipitate up to 39.3 grams of gypsum. The neutralized pH was 5.97.

Water quality data from the site are presented as a function of distance from the tailings pond in Figures 2.2, 2.3, 2.4, and 2.5. The monitoring wells do not fall along a single groundwater flow line, and no attempt has been made to spatially represent a plume in these figures. Rather, this

2.7

TABLE 2.1.   The Chemical Compositions of Leachates (in molal) from the
              SOHIO L-Bar Site (Longmire and Brookins 1982), the Riverton
              Site (White et al. 1984), the FAP Site (Dames and Moore 1981)
              and the Lucky Mc Site (Erikson and Sherwood 1982).

	L-Bar	Riverton	FAP	Lucky Mc
pH	0.98	1.4	2.2	1.2
Al	4.1e-2	4.3e-1	5.6e-3	3.8e-2
Ca	8.8e-3	3.5e-3	1.3e-2	1.5e-2
Fe	-	7.7e-1	7.3e-3	5.0e-2
K	-	5.6e-6	2.4e-3	4.0e-3
Mg	5.2e-2	7.8e-2	1.3e-2	5.0e-2
Na	4.0e-2	8.7e-4	2.5e-2	7.1e-2
SO_4	3.8e-1	5.7e-1	1.4e-1	2.7e-1
Cl	1.0e-2	2.6e-3	1.1e-2	3.1e-2

representation of the data can be compared with the generic model of Sheppard
and Brown (1982) in a purely qualitative sense.

In Figure 2.2, the chloride concentration in the groundwater is shown as
a function of distance. The error bars represent the range of variation
measured in different wells located at the same distance from the tailings
pond. The diamond symbol represents the chloride concentration in the
leachate, and the square symbol represents the chloride concentration in an
upgradient (and presumably uncontaminated) well. Chloride is not strongly
affected by retardation mechanisms, and thus should act as a geochemically
conservative tracer. These data suggest that leachate has migrated at least
200 m from the tailings pond.

In Figure 2.3, the pH of the groundwater is shown as a function of
distance. The error bars represent the range of variation measured in
different wells located at the same distance from the tailings pond. The
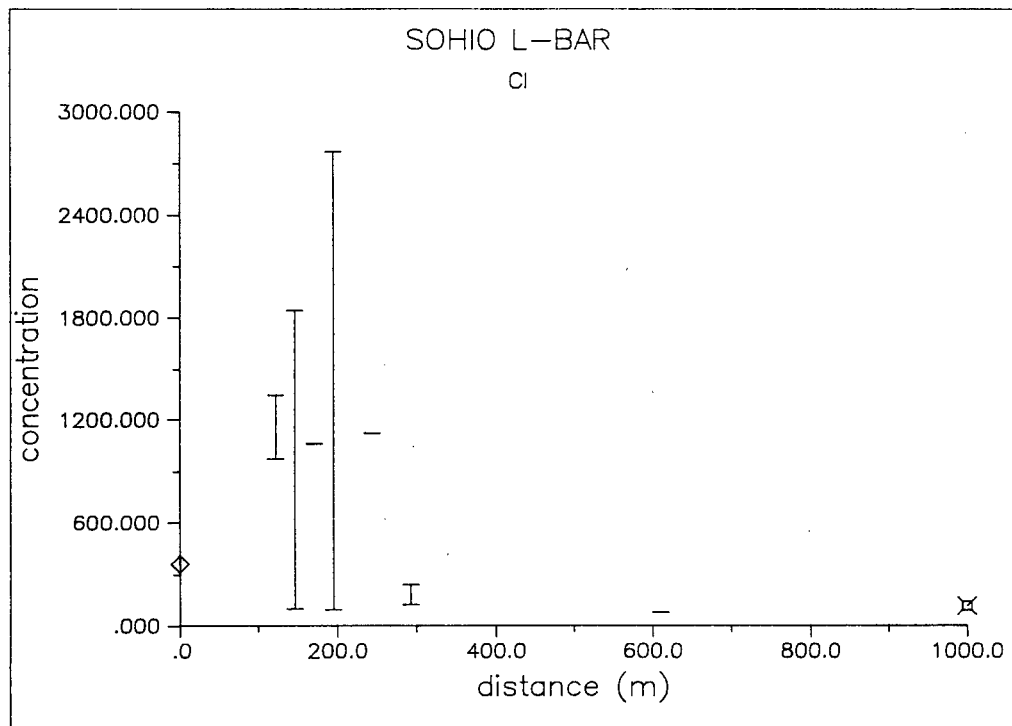
FIGURE 2.2. Water Quality Data for Chloride (mg/L) from the SOHIO L-Bar Site (Longmire and Brookins 1982).
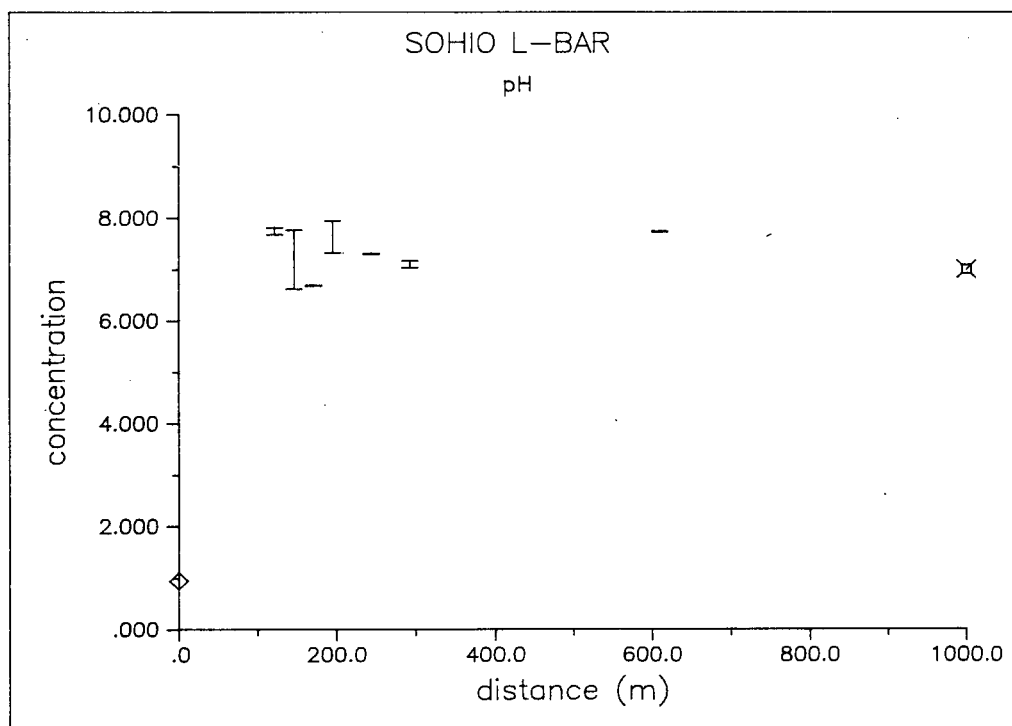
FIGURE 2.3. Water Quality Data for pH from the SOHIO L-Bar Site (Longmire and Brookins 1982).

SOHIO L—BAR

SO4
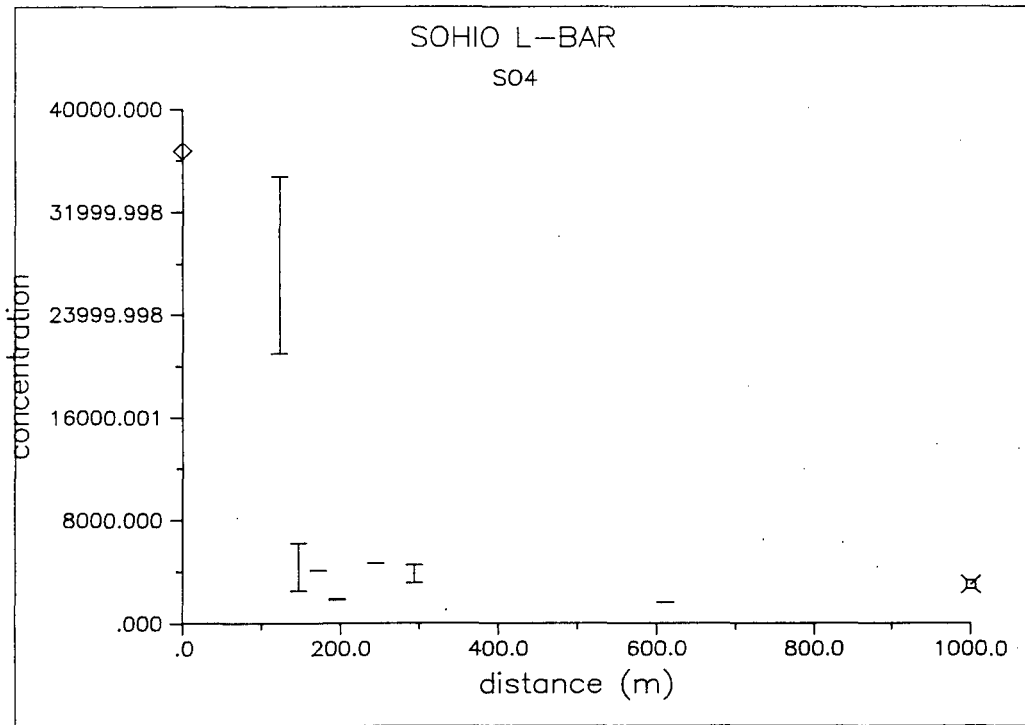
FIGURE 2.4. Water Quality Data for Sulfate (mg/L) from the SOHIO L-Bar
Site (Longmire and Brookins 1982).

SOHIO L—BAR

Utot
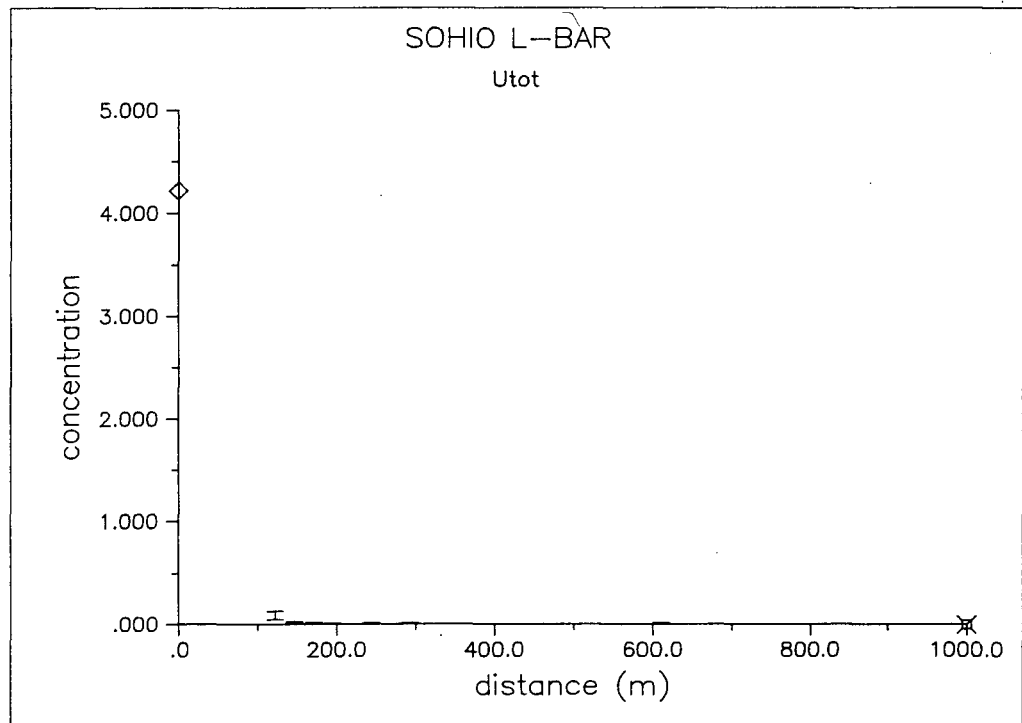
FIGURE 2.5. Water Quality Data for Total Uranium (mg/L) from the SOHIO
L-Bar Site (Longmire and Brookins 1982).

diamond symbol represents the pH of the leachate, and the square symbol represents the pH of an upgradient well. Note that due to the buffering capacity of the soil, the acidic leachate has been neutralized before reaching the closest monitoring well.

Sulfate shows some mobility at the L-Bar site (Figure 2.4). Sulfate concentrations in the leachate are extremely high, and the first monitoring wells (120 m from the tailings pond) also exhibit elevated sulfate concentrations. Sulfate levels in the second set of wells (145 m from the tailings pond) have essentially dropped to background.

Finally, total dissolved uranium is shown as a function of distance in Figure 2.5. The influent concentration is approximately 4.2 mg/L. The total dissolved uranium in the closest set of monitoring wells is slightly above background (47 to 130 μg/L, background <10 μg/L).

Only one of the three zones in the contaminant plume proposed by Sheppard and Brown (1982) can be identified at the L-Bar site. The transport zone, characterized by neutral pH and decreasing chloride values is located outwards of 120 m from the tailings basin. If the inner two zones do exist, they must be present inside the innermost monitoring wells. Thus, an upper bound on the neutralization length at the L-Bar site is 120 m.

Riverton Site

The Riverton tailings pile is located in central Wyoming (White et al. 1984). Tailings were disposed of at Riverton from 1958 to 1963. The tailings pile is approximately 20 m thick, of which 15 m are above the original land surface. Pore waters from the tailings exhibit a highly acidic character, the result of the sulfuric acid leach process used at the mill.

The tailings are primarily in the vadose zone, although groundwater does reach the base of the tailings pile during rainy periods. The tailings pile overlies alluvial sediments in which a shallow aquifer is located. A deeper

aquifer at the site located in the Wind River formation is probably not hydraulically connected to the shallow aquifer.

Analyses of ambient groundwater in the shallow aquifer suggest saturation with carbonate minerals. However, the buffering capacity of the sediment was not measured. The adsorptive capacity of the sediments is also undetermined.

The major element composition of the Riverton tailings pore waters is given in Table 2.1. A speciation analysis showed that 0.1 M of excess hydroxide (i.e., hydroxide not obtained from dissociation of water) were required to reproduce the measured pH of 1.4. Acidity in the Riverton leachate is provided predominately by aluminum and iron sulfates. Our neutralization calculation showed that each kilogram of the tailings solution could dissolve up to 88.7 grams of calcite and precipitate up to 76.1 grams of gypsum. The neutralized pH was 4.39. Thus, the total acidity of the Riverton leachate is greater than that the L-Bar leachate.

Some of the groundwater quality data is shown as a function of distance in Figures 2.6, 2.7, 2.8, and 2.9. In viewing these figures, it should be kept in mind that the monitoring wells are not located on a single flow pathline and that our intent is to represent a qualitative picture of the trends in concentration with distance.

In Figure 2.6, the chloride concentration in the groundwater is shown as a function of distance. The error bars represent the range of variation measured in different wells located at the same distance from the tailings pond. The diamond symbol represents the chloride concentration in the leachate, and the square symbol represents the chloride concentration in an upgradient well. These data suggest that leachate has moved at least 900 m from the tailings pond.

In Figure 2.7, the pH of the groundwater is shown as a function of distance. The error bars represent the range of variation measured in different wells located at the same distance from the tailings pond. The

2.12
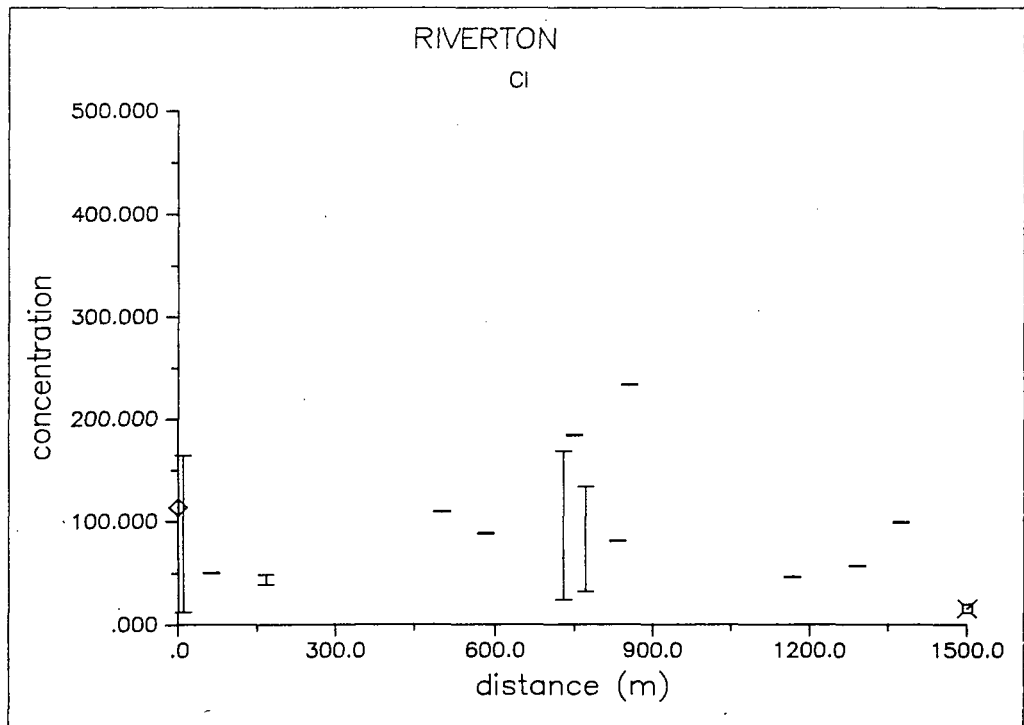
FIGURE 2.6. Water Quality Data for Chloride (mg/L) from the Riverton
Site (White et al. 1984).
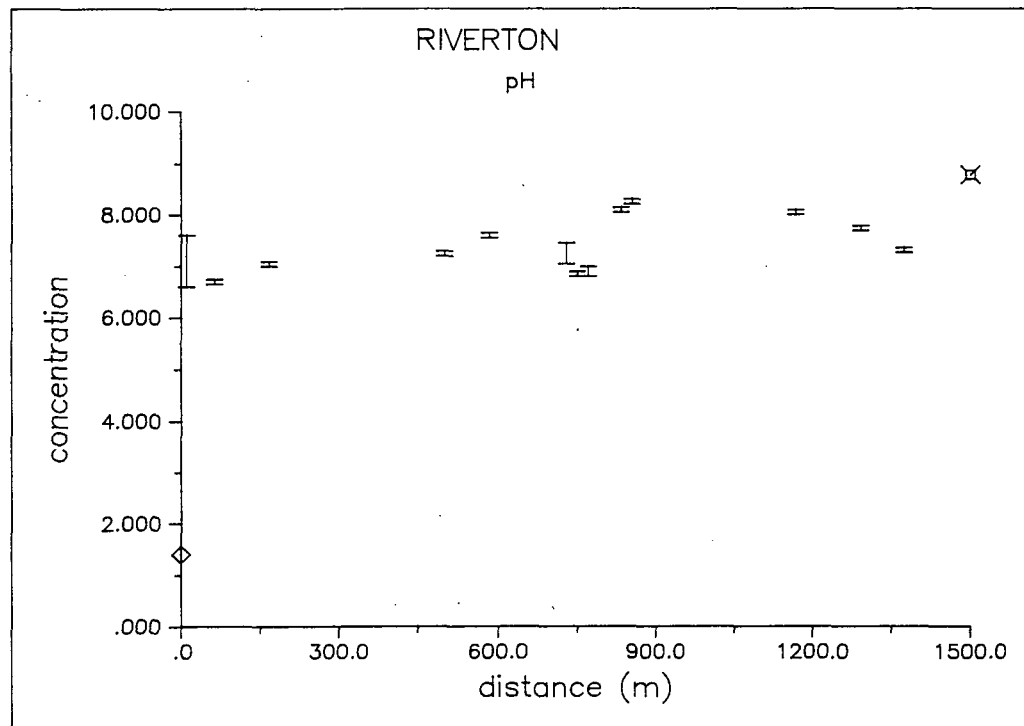
FIGURE 2.7. Water Quality Data for pH from the Riverton Site (White et
al. 1984).

2.13
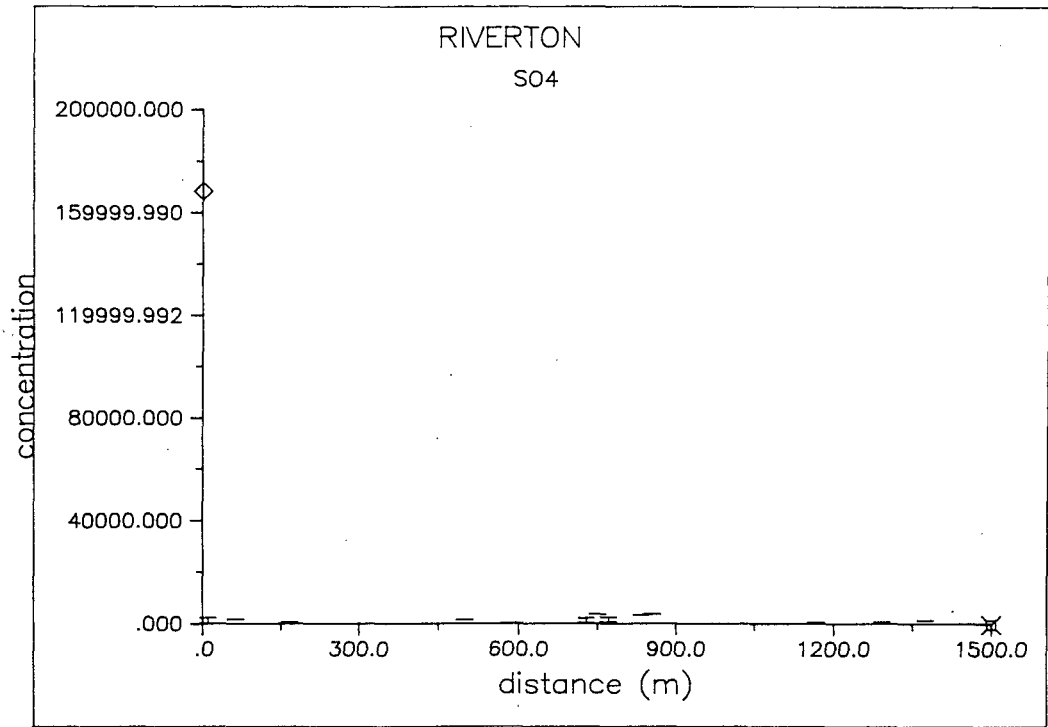
FIGURE 2.8. Water Quality Data for Sulfate (mg/L) from the Riverton Site (White et al. 1984).
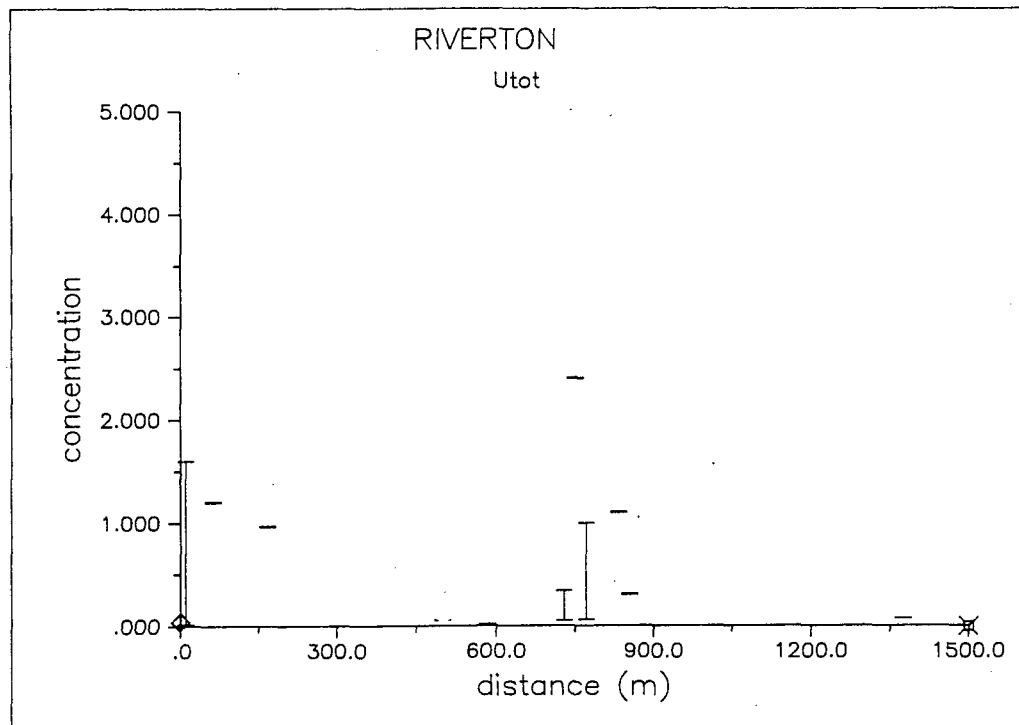
FIGURE 2.9. Water Quality Data for Total Uranium (mg/L) from the Riverton Site (White et al. 1984).

diamond symbol represents the pH of the leachate, and the square symbol represents the pH of an upgradient well. Note that because of the buffering capacity of the soil, the acidic leachate has been neutralized before reaching the closest monitoring well, only 60 m from the tailings pond.

Sulfate shows almost no mobility at the Riverton site (Figure 2.8). Sulfate concentrations in the leachate are extremely high, and the first monitoring wells (60 m from the tailings pond) show sulfate concentrations at background.

Finally, total dissolved uranium is shown as a function of distance in Figure 2.9. The influent concentration is approximately 54 μg/L (U concentrations up to 138 mg/L have been measured in tailings pore waters). The total dissolved uranium in the monitoring wells inside of 900 m range up to 2.4 mg/L. Therefore, although the pH appears to be buffered by carbonate minerals even close to the tailings pile, U appears fairly mobile at the Riverton site.

Only one of the three zones in the contaminant plume proposed by Sheppard and Brown (1982) can be identified at the Riverton site. The transport zone, characterized by neutral pH and decreasing chloride values is located outwards of 10 m from the tailings basin. If the inner two zones do exist, they must be present inside the innermost monitoring wells that are located at the edge of the tailings pile. Thus, an upper bound on the neutralization length at the Riverton site is 10 m. In contrast to the Sheppard and Brown (1982) model, U concentrations remain relatively high in the plume past the neutralization front.

Federal American Partners Site

The Federal American Partners (FAP) uranium mill is located in the Gas Hills region of central Wyoming approximately 50 miles west of Casper. Conventional uranium milling operations took place at the mill from about 1960 to 1983 (Dames and Moore 1981). The method used to extract uranium from the ore during processing required a highly acidic leaching solution. The

liquid portion of the waste from this operation was routed to an evaporation pond for disposal. In the pond, evaporation, precipitation, rainfall, and seepage out of the pond into the shallow groundwater environment modified the concentration of the raffinate. The raffinate initially had a low pH value (<2), and high concentrations of total dissolved solids, SO_4^{2-}, and radionuclides left from the extraction process of the uranium ore. Liquid from the evaporation pond seeped into the groundwater system during a 20-year period.

The chemical characteristics of ground water in the shallow aquifer immediately below the evaporation pond were not determined prior to the emplacement of the evaporation pond, but is assumed to be similar to that of the lower uncontaminated aquifers at the site. Groundwater data collected in 1979 indicated that seepage of raffinate had migrated into the shallow aquifer to a distance of about 1,000 feet to the north (downgradient) of the evaporation pond (Dames and Moore 1981).

The FAP site was constructed on the Wind River formation and Quaternary alluvial material in the stream valleys. The Wind River formation consists of an upper and lower unit in the vicinity of the FAP site. An upper arkosic unit occurs at the surface where not covered by the alluvial material. The lower Wind River unit consists of siltstones, mudstones, and claystones (Dames and Moore 1981). The regional dip of the Wind River formation is to the southeast at between 1 and 3 degrees.

The site hydrology consists of two main aquifers which underlie the evaporation pond at the FAP site. A shallow, perched aquifer exists from the surface to a depth elevation of about 6340 feet (Dames and Moore 1981) and has been contaminated by site operations. This aquifer exists primarily in the Quaternary alluvial fill material directly underlying the evaporation pond and dam, and downgradient of the evaporation pond. The second and deeper aquifer lies in the Upper Wind River formation and is an unconfined, uncontaminated aquifer that exists below the top of the lower Wind River formation, and is separated from the Upper Wind River formation by about 20 feet of claystone (Dames and Moore 1981). The regional gradient of the

2.16

shallow, perched aquifer is generally toward the northwest. The presence of the evaporation pond overlies and superposes upon the regional gradient, and affects the hydrologic condition of the aquifer.

The major element composition of evaporation pond water at the FAP site is given in Table 2.1. A speciation analysis showed that 0.032 M of excess hydrogen (i.e., hydrogen not obtained from dissociation of water) were required to reproduce the measured pH of 2.16. Acidity in the FAP pond water is provided predominately by sulfuric acid. Our neutralization calculation showed that each kilogram of the tailings solution could dissolve up to 5.26 grams of calcite and precipitate up to 7.68 grams of gypsum. The neutralized pH was 6.51. This leachate has the lowest total acidity of the leachates from the four sites discussed in this chapter.

Because of the quantity of data from the monitoring well network at the FAP site, we initially attempted to analyze the transport of chloride in somewhat more detail than at the L-Bar and Riverton sites. The four most complete sets of field chemical data were initially studied to determine an appropriate transport model. Chloride was chosen as the constituent to use in this determination, because of the conservative nature of its transport. Data gathered by Dames and Moore (1981) on October 1981, January 1982, April 1982, and July 1982 provided the most complete sets of chemical analyses for chloride at the FAP site. Eighteen wells had information on chloride concentrations in October 1981 and January 1982, 15 wells had analyses that included chloride in April 1982, and 9 wells reported chloride data in July 1982.

A set of X-Y coordinates describing the location of the wells was hand-derived and combined with each set of chloride data as input to a computer program that computed chloride concentrations for points along a selected one-dimensional streamtube. The streamtubes used in this study were chosen based in part upon the three zones used in the model developed by Dames and Moore (1981). Points along the streamtube correspond to piezometric surface contours from the 1979 map included in the Dames and Moore (1981) report, and are directed perpendicular to the contour at that point. Streamtubes were

2.17

derived for distances up to the farthest point for which chemical and
hydraulic data existed. Interpolation of the chloride concentration was
accomplished by taking a weighted average of the concentration of all actual
chloride data points as an inverse function of distance from the point of
interest along the streamtube. Figures 2.10 through 2.13 show the gridded
area in which streamtubes A, B, and C lie along the chloride concentration
surface. The chloride data were interpolated and extrapolated from the data
set to compute a surface representing chloride concentration in the area.
The sparse data set forced the concentration surface to the mean of the
entire data set at greater distances from the actual known concentration
points. Kriging or moving-neighborhood methods and closest-neighbor
weighting schemes did not produce a more accurate or intuitively more
reasonable surface. These data show the difficulty of constructing a
detailed transport model for the FAP site which would have to be based on a
two-dimensional transient flow analysis.

The solution for a one-dimensional advective dispersive equation from
van Genuchten and Alves (1982) was used in a computer program to fit an
advective-dispersive transport curve to the interpolated field data for each
streamtube using the October 1981 data. The velocity of the conservative
tracer (chloride) was determined from the distance of the breakthrough front
(C/C_O equals 50% of initial influent) divided by the years of operation of
the evaporation pond prior to the chemical data collection date. The
velocities of streamtubes A, B, and C were determined to be 130, 97.05, and
179.4 ft/yr respectively. A common coefficient of dispersivity of 55 feet
was derived by repeated application of the interpolation program and fits of
the analytical solution to the interpolated field data from October 1981.
The relatively constant level of chloride in streamtube A and lack of a
definite breakthrough front made determination of the transport parameters
more difficult. We attempted to use the derived parameters for each
streamtube to predict the chloride distributions observed at later times with
little success. In light of the spatial and temporal variations in the data
and the relative sparseness of the data set, a more detailed transport model
of the FAP site cannot be reasonably constructed.
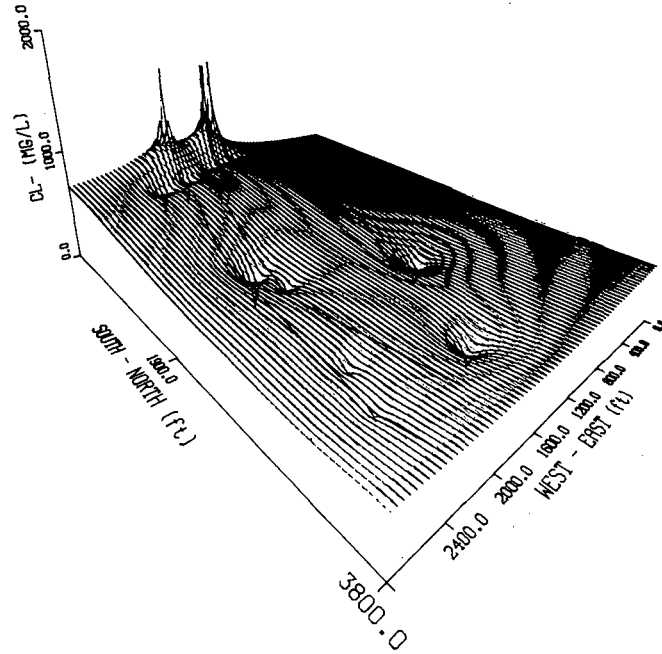
FIGURE 2.10. Surface for Chloride Concentrations at the FAP Site Using Data Measured in October 1981.
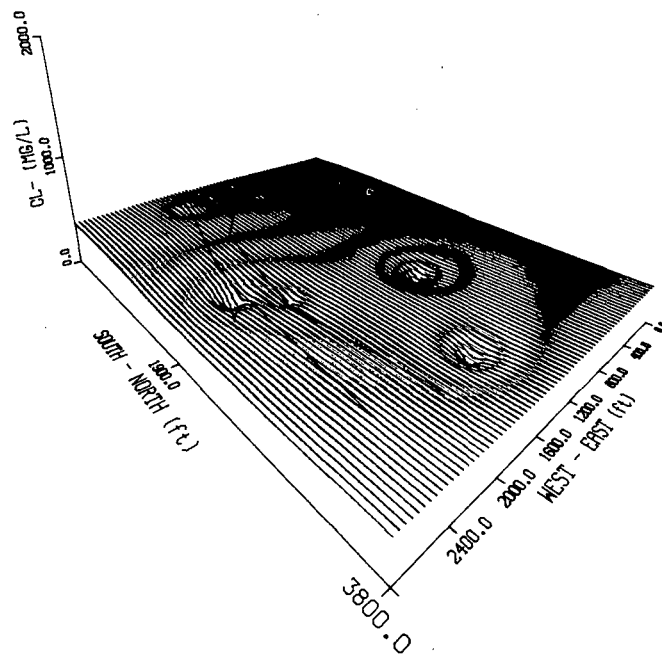
FIGURE 2.11. Surface for Chloride Concentrations at the FAP Site Using Data Measured in July 1982.
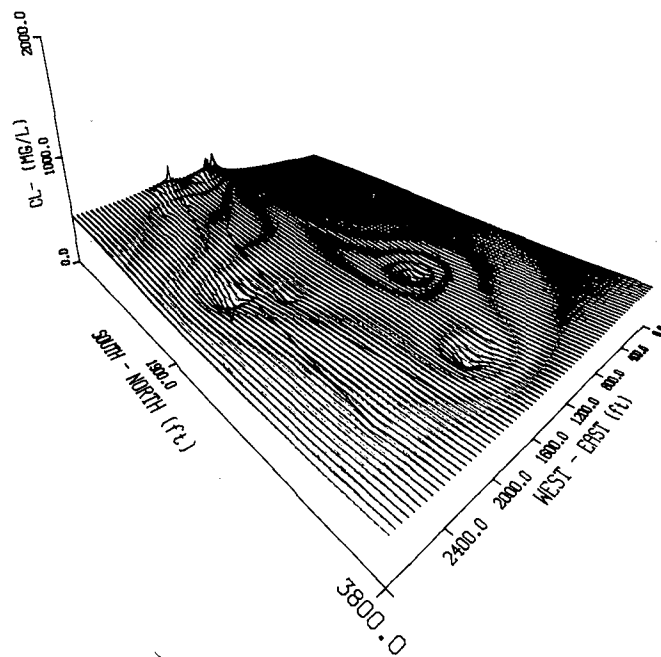
FIGURE 2.12. Surface for Chloride Concentrations at the FAP Site Using Data Measured in April 1982.
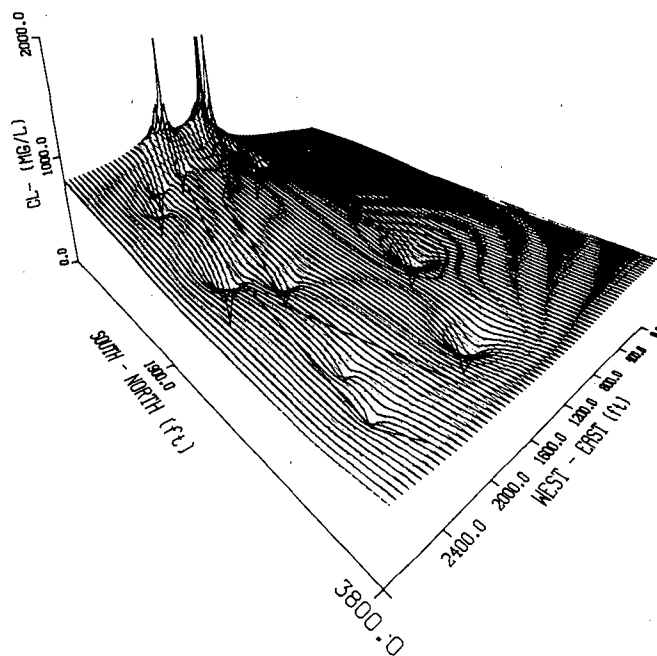
FIGURE 2.13. Surface for Chloride Concentrations at the FAP Site Using Data Measured in January 1982.

Some of the groundwater quality data at the FAP site are shown as a function of distance in Figures 2.14, 2.15, 2.16, and 2.17. These figures are based on the October 1981 data set and are shown for comparison with the L-Bar and Riverton sites as well as the generic model of Sheppard and Brown (1982). In viewing these figures, it should be kept in mind that the monitoring wells are not located on a single flow pathline and that our intent is to represent a qualitative picture of the trends in concentration with distance.

In Figure 2.14, the chloride concentration in the groundwater is shown as a function of distance. The error bars represent the range of variation measured in the same well over a one year monitoring period. The diamond symbol represents the chloride concentration in the leachate, and the square symbol represents the chloride concentration in an upgradient well. These data suggest that leachate has moved at least 1000 m from the tailings pond, as discussed above.

In Figure 2.15, the pH of the groundwater is shown as a function of distance. The error bars represent the range of variation measured in the same well over a one year monitoring period. The diamond symbol represents the pH of the leachate, and the square symbol represents the pH of an upgradient well. The groundwater pH does not reach the background pH of 8.0 until 500 m from the pond, the approximate neutralization length at FAP. Note that this observation is roughly consistent with the Kd of 0.44 fit by Dames and Moore (1981) to the pH plume data using a two-dimensional transport model.

Sulfate is highly mobile at the FAP site (Figure 2.16). All of the sulfate concentrations measured from the monitoring network in the shallow aquifer at the FAP site are above the sulfate concentration measured in the deep aquifer.

Finally, total dissolved uranium is shown as a function of distance in Figure 2.17. The influent concentration is approximately 13 mg/L. The total dissolved uranium in the monitoring wells in the shallow aquifer are in the
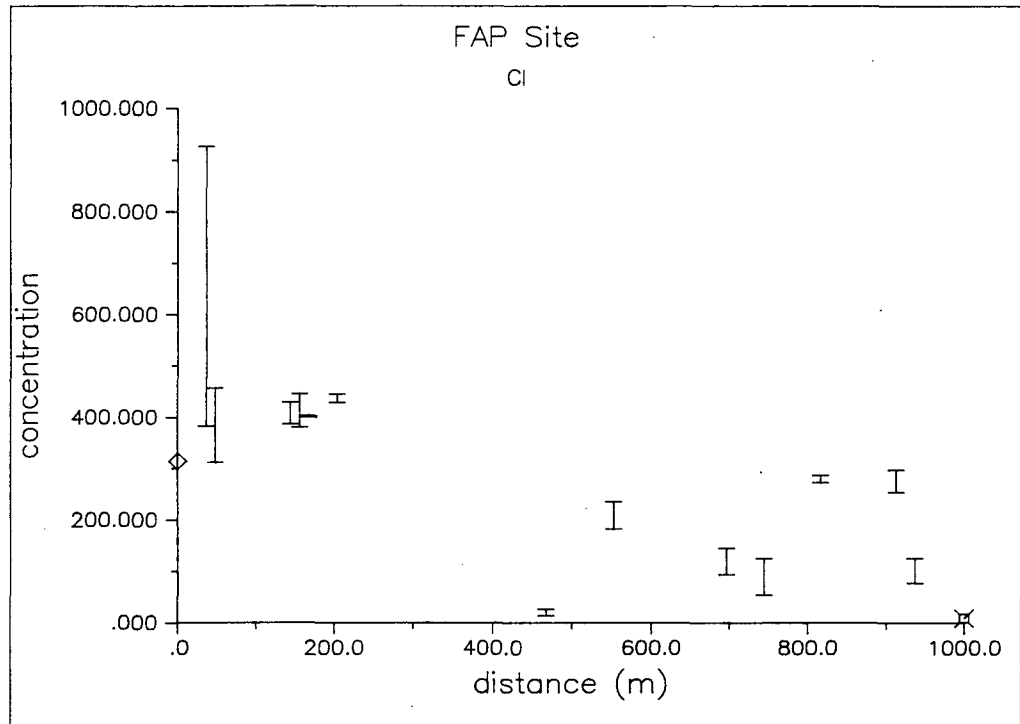
FIGURE 2.14.   Water Quality Data for Chloride (mg/L) from the FAP Site
(Dames and Moore 1981).
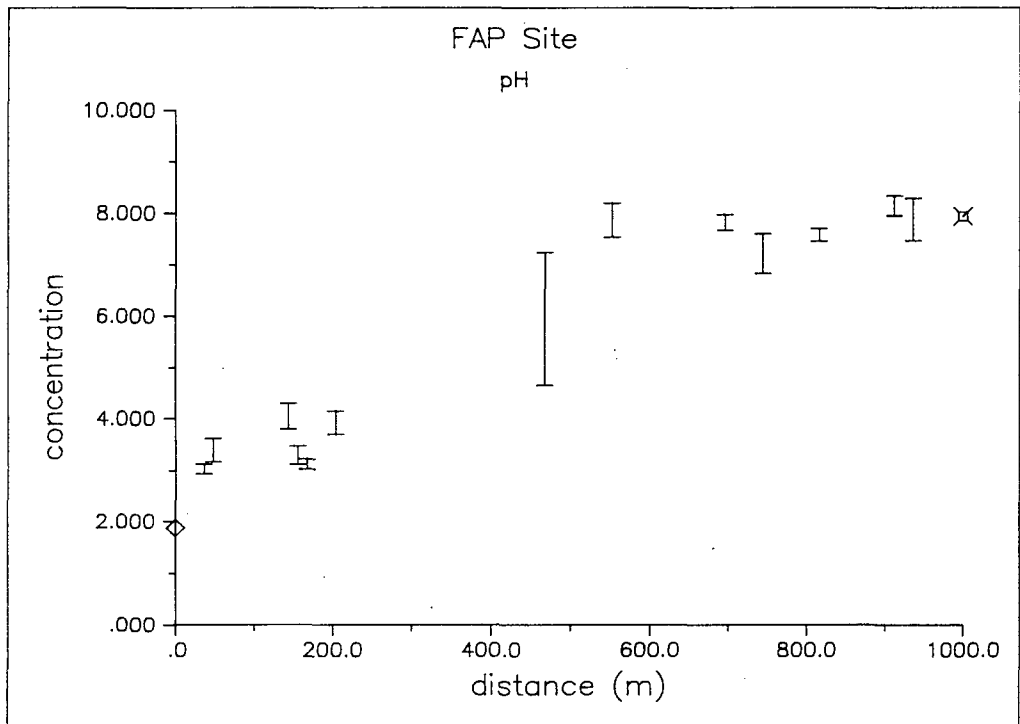
FIGURE 2.15.   Water Quality Data for pH from the FAP Site (Dames and
Moore 1981).

2.22
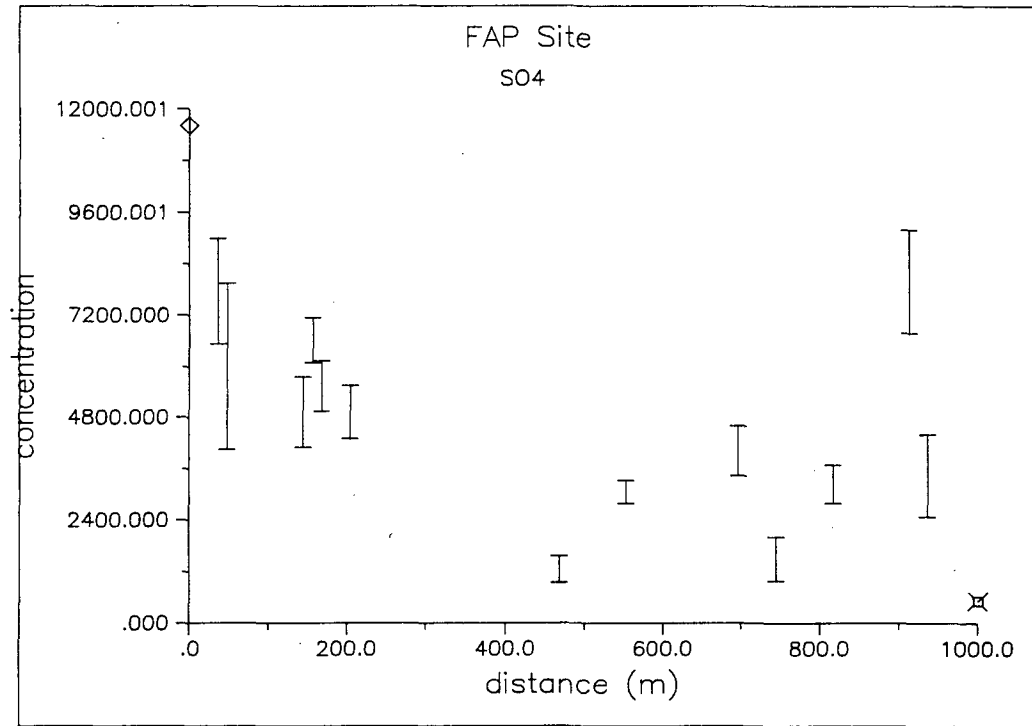
FIGURE 2.16. Water Quality Data for Sulfate (mg/L) from the FAP Site
(Dames and Moore 1981).
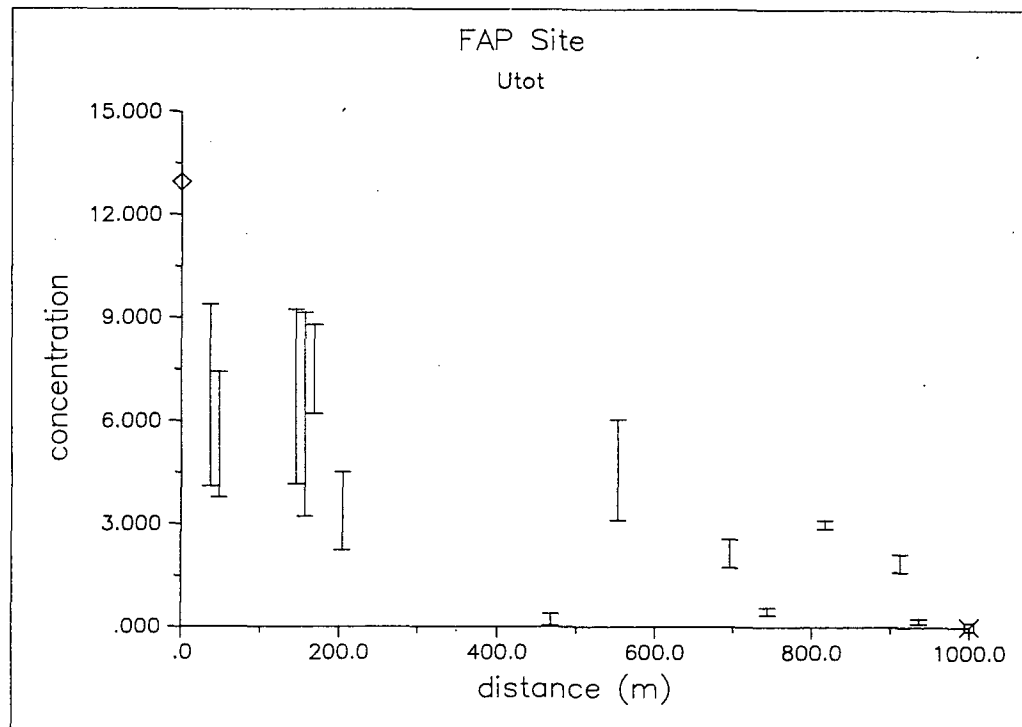
FIGURE 2.17. Water Quality Data for Total Uranium (mg/L) from the FAP
Site (Dames and Moore 1981).

2.23

hundreds of μg/L to mg/L range. Note that even beyond the 500 m neutralization length, U concentrations of several mg/L were measured.

The FAP site exhibits most of the features of the generic model of Sheppard and Brown (1982). Inside of 200 m, low pH values, high sulfate concentrations, and high uranium concentrations characterize the acid zone. The neutralization zone extends from 200 m to 500 m. The transport zone, characterized by neutral pH and decreasing chloride values is located outwards of 500 m from the tailings basin. In contrast to the Sheppard and Brown (1982) model, U concentrations do remain relatively high in the plume beyond the neutralization front.

Lucky Mc Site

The Lucky Mc Mill, located in the Gas Hills of central Wyoming, contains five tailings ponds (Erikson and Sherwood 1982). The largest evaporation pond covers approximately 90 acres. The estimated depth of liquid in the pond was 3.5 m. The evaporation pond was in operation for 10 years, during which acidic tailings solution was discharged and allowed to seep into the subsurface.

The evaporation pond was constructed over an alluvial sediment that is a member of the Forelle-Patent Association soil series. The total carbonate content of the alluvium was qualitatively estimated to be 20% to 40% using an XRD technique (Erikson and Sherwood 1982). The clay minerals illite, smectite, and kaolinite were also identified in this soil.

The leachate pH of 1.2 reflects the sulfuric acid leaching process used at the mill. The major element composition of the evaporation pond water at the Lucky Mc site is given in Table 2.1. A speciation analysis showed that 0.19 M of excess hydrogen (i.e., hydrogen not obtained from dissociation of water) was required to reproduce the measured pH. Acidity in the Lucky Mc pond water is provided predominately by sulfuric acid. Our neutralization calculation showed that each kilogram of the tailings solution could dissolve up to 23.5 grams of calcite and precipitate up to 31.2 grams of gypsum. The

neutralized pH was calculated to be 5.79. In a laboratory study, Sherwood and Serne (1983) experimentally determined that each liter of Lucky Mc leachate required 21.25 grams of calcite for neutralization to pH 7.3.

In contrast to the three sites discussed previously in this report, groundwater quality data were not available from a monitoring well network at the Lucky Mc site. Instead, the work of Erikson and Sherwood (1982) utilized soil samples obtained at different locations and depths under the pond. Sample characterization included pH measurements, x-ray diffraction analysis, and radioanalytical measurements.

Sediment samples were taken underneath the tailings pond at six locations. Sediments up to 60 cm below the bottom of the pond were sampled. An analysis of the soil properties and the calculated volume of solution neutralized led Erikson and Sherwood (1982) to conclude that leachate from the solution could have penetrated up to 11.4 m below the tailings pond. In contrast, low soil pH values (< 8) were limited to the upper 60 cm. Thus, an estimate of the neutralization length at the Lucky Mc site is 60 cm.

The saturated paste pH of a soil may be quite different from the pH of the solution in equilibrium with the soil. For example, in our neutralization calculation for the Lucky Mc leachate, the leachate in equilibrium with calcite and gypsum was at a pH of 5.79. The equilibrium pH of deionized water, calcite, and gypsum is calculated to be 9.14. Therefore, the neutralization length obtained from sediment analysis may be quite different from the neutralization length obtained from groundwater analyses.

SUMMARY

The four field sites examined in our review obviously do not represent a complete sampling of UMT disposal sites in the United States. We chose these sites for our review because of the availability of site characterization data and groundwater monitoring data. In summarizing the results of our review, we caution the reader to remember the small sample size and the

possibility of sample bias. In spite of these limitations, we feel that some important similarities among the sites merit discussion.

At all four sites, leachate had seeped into a shallow alluvial aquifer from a tailings disposal facility, as evidenced by elevated chloride concentrations found in monitoring wells and radionuclide levels in the soil at the Lucky Mc site. Leachates at the four sites were all acidic in character. The aquifer materials at all four sites contained carbonate minerals in various amounts. The major chemical interaction between leachates and aquifer materials at the sites we reviewed appears to be the dissolution of carbonate minerals and the precipitation of gypsum.

The ability of the leachate to consume soil buffering capacity was not found to be directly dependent on leachate pH. The buffering capacity consumption of the leachates were calculated using a geochemical speciation and mass transfer analysis, in which the leachate was allowed to equilibrate with calcite and gypsum. The Riverton leachate (pH 1.4) was found to be the most acid (consuming 88.7 gm of calcite/L), followed by the L-Bar leachate (pH 0.98, consuming 29.2 gm of calcite/L), the Lucky Mc leachate (pH 1.2, consuming 23.5 gm of calcite/L), and the FAP leachate (pH 2.16, consuming 5.26 gm of calcite/L).

In the generic model of Sheppard and Brown (1982), the manifestation of the neutralization of the leachate is the formation of a neutralization front that separates the acid zone from the transport zone. Only at the FAP site were these zones fully developed in the groundwater quality data. At the L-Bar and Riverton sites, in spite of the relatively high acidities of the leachates, the neutralization front was not detected in the monitoring network. The distance to the neutralization front at a given time must be a function of the leachate acidity, the soil buffering capacity, the porosity of the aquifer, and the flux of leachate entering the aquifer.

The other difference we found between the site data and the Sheppard and Brown (1982) model was elevated concentrations of uranium and sulfate beyond the neutralization zones. This effect was particularly apparent at the FAP

2.26

site, but was also present at the Riverton site. It appears from the water quality data we reviewed that the region outside the neutralization zone cannot be assumed to be uncontaminated by sulfate and uranium.

In the following chapters of this report, we discuss the use of a chemical transport model as an aid to identifying the geochemical processes that lead to the transport behavior we observed at the four field sites. We discuss the development and implementation of a generalized model for semi-quantitative calculations of leachate migration at UMT disposal sites. We offer this model as a supplement to the field observations and the qualitative treatment of Sheppard and Brown (1982).

3.0 DESCRIPTION OF REACTIVE TRANSPORT CODE

Understanding the temporal and spatial distribution of solutes dissolved in groundwater is an important component of analysis of contaminant hydrogeology. Prediction of solute migration requires a quantitative understanding of groundwater flow processes and chemical reactions. Developing such an understanding remains a challenging problem because of the complex nature both of subsurface geologic materials and of waste-disposal practices.

The one-dimensional advection-dispersion equation, including linear retardation, has been a common starting point for developing models to describe solute transport (Freeze and Cherry 1979). The importance of the classical description is partly because of the inclusion of three primary phenomena observed in a variety of field settings: the movement of solutes through groundwater systems, the dilution of chemical concentrations, and the differential velocities of solutes. In the advection-dispersion equation, these processes are described using three adjustable parameters, the average groundwater velocity, v, the coefficient of hydrodynamic dispersion, D, and the retardation factor, R. The importance of the advection-dispersion equation also derives from the availability of analytic solutions for a wide variety of initial and boundary conditions (van Genuchten and Alves 1982; Valocchi and Roberts 1983).

Although use of a constant retardation factor permits analytic solution of the transport equation in many cases, it has been recognized that retardation depends on a variety of solution and soil chemical properties, and that a constant retardation factor is inappropriate for describing solute transport in geologically complex systems (e.g., Reardon 1981; Serne and Muller 1987). Improvements to the classical description of solute transport have focused on providing more mechanistic treatments of chemical reaction processes. Ion-exchange, specific-ion adsorption, and precipitation-dissolution reactions are the primary mechanisms that have been invoked to account for chemical retardation and attenuation.

3.1

In one-step chemical transport models, the chemical and transport equations are combined into a set of coupled, nonlinear partial differential equations which are solved using numerical techniques. Rubin and James (1973), and Valocchi et al. (1981) replaced the constant retardation factor with ion-exchange equilibria to describe solute transport. The resulting set of coupled, nonlinear partial differential equations was solved numerically by the Galerkin finite element method in these investigations. Miller and Benson (1983) extended the treatment of ion-exchange equilibria by including aqueous complexation reactions and individual ion-activities in their model. Jennings et al. (1982) used a similar treatment while replacing the constant retardation factor with solute complexation and surface complexation equilibria. A general framework for including solute complexation, adsorption, and solubility equilibria in the transport equation was presented by Kirkner and Reeves (1988), and Reeves and Kirkner (1988) examined numerical solution techniques for a variety of cases involving aqueous complexation and adsorption.

In two-step chemical transport models, the solute movement calculation is separated from the chemical reaction calculation. Grove and Wood (1979) developed a model in which, for each time step, the transport equation (without retardation) was solved using a finite difference method for each solute, and the solutes were allowed to react through solute complexation, solubility, and ion-exchange equilibria calculated using a direct iteraction method. Walsh et al. (1982) employed a similar approach for solute movement, but relied on the Newton-Raphson method for calculation of solute complexation and solubility equilibria. Kirkner et al. (1984) and Cederberg et al. (1985) solved the transport equations using a finite element method, and solved solute complexation and surface complexation equilibria using the Newton-Raphson method. Narasimhan et al. (1986) simulated transport using an integrated finite difference method, and used the geochemical code PHREEQE (Parkhurst et al. 1980) as a module to solve solute complexation and solubility equilibria.

Kirkner and Reeves (1988) point out that although the methods currently employed to simulate solute transport are extendable to two- and three-

3.2

dimensional domains, the nature and size of the governing equations require extensive computational resources for a multicomponent/multidimensional solute transport simulation. Simulation of an ensemble of one-dimensional streamtubes (e.g., Hostetler et al. 1989) also requires extensive computational resources and neglects transverse dispersive phenomenon. Similarly, the simulation of solute transport under transient flow conditions is not adequately addressed in current models (Duffy et al. 1988).

STRUCTURE OF THE CTM CODE

A direct simulation method was chosen to calculate solute transport in the CTM code. Prior to a simulation, the transport pathline is divided into a number of arbitrarily shaped bins. A linear operator representing the solute movement processes is constructed, and the initial conditions in each bin (i.e., the aqueous, solid, and adsorbed masses of each chemical component) are specified. Finally, the geochemical reactions allowed to occur during the simulation are specified.

The two-step coupling algorithm was chosen to combine the transport and geochemical processes in the CTM code. During each time step in the simulation, the mobile constituents (i.e., solutes) are distributed along the one-dimensional pathline according to the advection, diffusion, and hydrodynamic dispersion properties of the porous media. This part of the calculation is the solute movement step. The geochemical step involves the reaction of the solution in each bin of the pathline with the immobile reactive soil constituents in that bin. Thus in each timestep during the calculation, the solute distribution is modified by both transport and geochemical processes.

MARKOV HYDROLOGIC MODEL

The solute movement processes represented in CTM are advection, diffusion, and hydrodynamic dispersion. Advection, the displacement of solutes because of bulk fluid displacement, and diffusion are described by

the fluid flow field and molecular diffusion coefficients, respectively. In CTM, hydrodynamic dispersion is modeled as a result of macroscopic variations in the flow field because of heterogeneities in the surrounding porous medium (Simmons 1982). This dispersion model contains the Fickian description as a special subcase.

For the purposes of illustration, consider a one-dimensional homogeneous streamtube with a uniform flow field. If a conservative tracer is injected as a pulse at time t, the solute will move downgradient and spread out. The resulting concentration distribution at a given later time is a probability density function (pdf) for distance traveled (Campbell et al. 1981). The mean of the pdf (mean distance traveled by the tracer) is given by:

$$E[c(x)] = v \ t \qquad\qquad (1)$$

where v is the pore-water velocity and t is the time since injection. In the Fickian model of dispersion, the pdf is normally distributed, with the variance of the concentration distribution given by:

$$Var[c(x)] = 2 \ D \ t \qquad\qquad (2)$$

where D is the coefficient of hydrodynamic dispersion:

$$D = \alpha_L \ v + D^* \qquad\qquad (3)$$

α_L is the dispersivity, and D^* is the effective molecular diffusion coefficient (Bear 1972). Non-Fickian pdfs lead to nonnormal solute concentration profiles (e.g., Simmons 1982; Gillham et al. 1984; Devary et al. 1984). The pdf concept is readily extended to two- and three-dimensions.

The Markov method, a direct simulation method, is used in CTM to implement the pdf-based description of solute movement. The simulation domain is discretized into a number of arbitrarily shaped bins. The number of elements and their geometries are chosen according to the domain symmetry

and the resolution required for the simulation. The total concentration of each solute is expressed as a state vector, with each entry in the vector representing the solute mass in a particular bin. At each timestep, the set of state vectors contains the entire information available about the solute mass distribution in the system.

A linear operator (the Markov transition matrix) is used to predict the evolution of the state vectors as a function of time. The Markov transition matrix is used to project the state vectors forward in time via:

$$S(t+1) = [T] S(t) \qquad (4)$$

where $S(t)$ is a state vector at time t, and $[T]$ is the Markov transition matrix. The elements of the transition matrix $[T]$ describe the transport of solute in the system. In particular, T_{ij} is the fraction of mass in bin i at time t that is transported to bin j at time t+1. The elements of the transition matrix can be expressed as a function of time if the fluid flow field is transient in nature.

The Markov transition matrix is constructed from the pdf defined for the system. The pdf is a spatially varying function depending on starting location (i.e., injection point) and time step length (Δt). The Markov transition matrix elements are obtained by integration of the pdf over bin volume:

$$T_{ij} = \int_{bin} pdf(x,i,\Delta t) \, dx \qquad (5)$$

For the homogeneous streamtube discussed above, use of the Fickian description of dispersion leads to a pdf that is independent of starting position:

$$pdf(x,\Delta t) = (4 \pi D \Delta t)^{-1/2} \exp[-(x - v \Delta t)^2 / (4 D \Delta t)] \qquad (6)$$

3.5

The mean and variance of the pdf are given by:

$$E[pdf(x)] = v \, \Delta t \tag{7}$$

and

$$Var[pdf(x)] = 2 \, D \, \Delta t \tag{8}$$

respectively. The matrix elements are simply:

$$T_{ij} = \{erf[(x_d - v \, \Delta t)/(4 \, D \, \Delta t)^{1/2}] \\ - erf[(x_u - v \, \Delta t)/(4 \, D \, \Delta t)^{1/2}]\} / 2 \tag{9}$$

where $erf(z)$ is the error function evaluated at z (Abramowitz and Stegun 1966), x_u is the x-coordinate of the upstream bin boundary, and x_d is the x-coordinate of the downstream bin boundary.

The lognormal pdf is similar to the normal pdf, however, the logarithm of the distance traveled is normally distributed:

$$pdf(x, \Delta t) = (4 \, \pi \, x \, D \, \Delta t)^{-1/2} \exp[-(\ln(x) - v \, \Delta t)^2 / (4 \, D \, \Delta t)] \tag{10}$$

The mean and variance of the lognormal distribution are also related to the time step length, mean groundwater velocity, and dispersion coefficient by Equations (7) and (8). The matrix elements for the lognormal pdf must be evaluated numerically.

The Markov method is most efficient for systems with a steady-state flow field. In this case, the transition matrix elements are independent of time and are evaluated prior to the transport simulation. During the transport simulation, solute movement is calculated by vector-matrix multiplication (equation 4), an efficient computational procedure. If the flow field changes with time, the matrix elements must be recalculated during each time step with consequent calculational overhead.

3.6

A conceptual model for solute movement contains the form of the pdf and the values for the controlling parameters. To develop a conceptual model for application to a laboratory experiment or field site, concentration distributions of a conservative tracer are required. The most direct method uses measurements of concentration as a function of distance at a fixed time. If several injection points are available, the variation in pdf with location can be investigated directly, otherwise the hypothesis of stationarity is usually invoked. The pdf and resulting matrix elements can be obtained directly from spatial integration of the concentration distributions. Alternatively, the form of the pdf can be chosen and parameters obtained through regression. A more indirect method of parameterization uses measurements of concentration as a function of time at a fixed location. In this method, the form of the pdf is chosen and the controlling parameters are obtained using regression analysis (e.g., Parker and van Genuchten 1984).

EQUILIBRIUM GEOCHEMISTRY MODEL

A focal point of chemical transport models is the use of specific geochemical mechanisms to describe attenuation. Chemical attenuation is a result of mass transfer from the aqueous phase to an immobile phase. The mass transfer reactions included in CTM are precipitation/dissolution and adsorption. Aqueous complexation reactions are used in CTM to calculate individual ion activities.

Molality is used as the concentration unit in the CTM code. The molality of the ith solute (m_i) is:

$$m_i = \omega\, n_i\, /\, n_w \tag{11}$$

where n_i is the number of moles of the ith solute, ω is equal to 1000 divided by the molecular weight of water, and the subscript w indicates the component water. The ionic strength (I) of the solution is given by a sum over all solutes:

$$I = 0.5\,(\Sigma\, m_i\, z_i^2) \tag{12}$$

where z_i is the charge of solute i. The Davies equation (Davies 1962) is used to calculate the individual ion activity coefficients (γ_i) of charged solutes:

$$\log \gamma_i = -A\, z_i^2 \left[\sqrt{I} / (1 + \sqrt{I}) - 0.3\, I \right] \tag{13}$$

where A is a constant (equal to 0.5092 at 25°C) related to the physical properties of water. For charge-neutral solutes, activity coefficients were approximated using:

$$\log \gamma_i = (0.1)\, I \tag{14}$$

(Felmy et al. 1984), and the activity of water by:

$$a_w = 1 - 0.017 \, \Sigma \, m_i \tag{15}$$

(Garrels and Christ 1965). The activity of specific adsorbates (m) is given by the Vanselow convention (Vanselow 1932):

$$a_m = n_m / (n_{js} + \Sigma n_m) \tag{16}$$

where a_m is the activity of the mth adsorbate, n_m is the number of moles of the mth adsorbate, and n_{js} is the number of moles of surface sites.

Each chemical component (basis species, indicated by the subscript j) is associated with a mass balance equation:

$$T_j = n_j + \Sigma \, \nu_{ij} \, n_i + \Sigma \, \nu_{lj} \, n_l + \Sigma \, \nu_{mj} \, n_m \tag{17}$$

where T_j is the total number of moles of component j, the subscript l indicates solids, m indicates adsorbates, and i indicates aqueous complexes.

Each derived species is represented by a mass action equation:

$$K_i = m_i \, \gamma_i \, / \, \prod_j (\gamma_j \, m_j)^{\nu_{ij}} \tag{18}$$

$$K_l = 1 \, / \, \prod_j (\gamma_j \, m_j)^{\nu_{lj}} \tag{19}$$

$$K_m = a_m \, / \, \prod_j (\gamma_j \, m_j)^{\nu_{mj}} \tag{20}$$

When the mass-action expressions are inserted into the mass balance equations, the result is a set of coupled, nonlinear, algebraic equations. The nonlinear equations are solved using Newton-Raphson iteration in a manner similar to Westall et al. (1976) and Felmy et al. (1984). Mass balance on all components (including water) is kept within a tolerance specified by the user.

The mass balance equations are normally solved for each bin at each timestep in the two-step algorithm. However, in CTM, advantage is taken of the fact that in some cases, the chemical composition of a number of bins may be identical and can be grouped together. An adaptive geochemical grid algorithm is used to group together bins having similar compositions (within a user-specified tolerance) so that only one chemical calculation is performed for the group of bins per time step. Significant time savings are obtained, particularly at time steps when the solute front has either not penetrated far into the domain, or has penetrated far enough that homogeneous chemical conditions are behind the front.

INPUT REQUIREMENTS FOR THE CTM CODE

The input data required to run the CTM code reside on 5 separate input files. These files are generated automatically in an interactive session with the CTM preprocessor code, PRE. The information specified in each of

3.9

the 5 files include the: 1) main run parameters, 2) geochemical model, 3) hydrologic model, 4) initial condition, and 5) boundary condition.

The main run parameter variables control the overall simulation. For any simulation, the user must define the type of geochemistry included in the calculation. The user has the choice of specifying either equilibrium speciation/solubility/adsorption geochemistry or constant Kd retardation geochemistry. The geochemistry input file contains the thermodynamic data for the chemical components, aqueous complexes, solid phases, adsorbates, adsorptive surfaces, and monitored species present in the geochemistry conceptual model. The file containing the hydrologic model contains the number of bins along the pathline and the Markov transition matrix. The Markov transition matrix is calculated using data input by the user pertaining to the timestep interval required, and average pore water velocity and dispersivity. The distribution of initial masses of the aqueous components, solid phases, and adsorbates stored on the initial condition file are input for each node at the initial conditions. The boundary conditions input file contains the aqueous masses of the components in the influent and are specified for each timestep.

OUTPUT FROM THE CTM CODE

The output from the CTM code is divided into a printed output file and a series of graphics files that are used with the CTM graphics postprocessor (POST) to plot solute profiles for a simulation. The printed output file for a speciation/solubility/adsorption simulation is divided into two sections and can be used to monitor the changes in the geochemistry of the mobile and immobile phases as aqueous solution migrates along the pathline. The first section echos the input data specified that gives the user a summary of the values of important geochemical and hydrological variables for the simulation. A listing of the geochemical conceptual model includes a description of the geochemistry used including the variables controlling the convergence of the geochemistry algorithm and the identity of all chemical components, complexes, solids, adsorbates, and monitored species in the simulation. The hydrologic conceptual model is listed next and includes the

3.10

row sum for the Markov traveling vector and the complete Markov transition matrix as a print option. The physical model listing includes the initial and boundary conditions, and lists the masses for each chemical component, solid, and adsorbate present in all bins at the initial condition, and the influent chemical composition used as the upstream boundary.

The second section of the printed output file lists the results of the coupled simulation as a function of space and time. This part of the output always lists the chemical composition of the influent solution (boundary condition), the masses of chemical components in the effluent, and the compositions of the mobile aqueous phase and immobile solid phase assemblage in all bins for each time step in the simulation. In addition, details of the aqueous speciation can be printed at the discretion of the user using several output print control options. Information provided for speciation calculations includes the identity of the phase assemblage at the specified bin and time step, the masses, concentrations, activity coefficients, and activities for the components and complexes as well as the masses and activities for the adsorbates and monitored species. Additional information about the aqueous solution includes the ionic strength, total cation and anion molality, and the charge imbalance.

Seven graphics output files are also prepared during each CTM simulation for the graphics post-processor (POST). The graphics files are read automatically when running the POST code. The types of graphs that can be plotted include: 1) a banner page that describes the model used, 2) the probability density function, 3) the influent component concentrations as a function of time, 4) the effluent component concentrations as a function of time, and 5) the concentrations of components, adsorbates, solids or the activities of monitored species as a function of distance along the pathline at any timestep. In Chapter 5, the results of the transport simulations made in this study are presented using plotted output from the CTM graphics postprocessor (POST).

4.0 GEOHYDROCHEMICAL CONCEPTUAL MODEL

Use of the chemical transport code CTM requires the development of a geohydrochemical conceptual model. A geohydrochemical conceptual model is divided into two parts; a hydrologic flow/transport model and a geochemistry model. The hydrologic model contains the mass transport information that includes the length of the one-dimensional pathline, and the average pore water velocity and dispersivity of a conservative tracer along the pathline. The geochemistry model requires a definition of the chemical state of the system at the initial condition and at the upstream boundary condition. The geochemistry model definition must include a list of the chemical components in the problem and their concentrations in the ambient pore water (initial condition) and in the leachate influent (boundary condition). Because mechanistic transport of reactive solutes involves mass transfer of solutes between the mobile aqueous phase and the immobile solid and adsorbed phases, the quantities of solids and adsorbates in the soil must also be specified at the initial condition. We have developed a generalized geohydrochemical conceptual model for UMT disposal sites based on our review of the four field sites discussed in Chapter 2.0 and on the generic model proposed by Sheppard and Brown (1982). The models developed in this study to be used in transport simulations are limited to applications of one-dimensional transport in a steady-state flow field in which all geochemical reactions are calculated using thermodynamic equilibrium constants.

TRANSPORT CONCEPTUAL MODEL

The four UMT disposal sites discussed in Chapter 2 are located in different groundwater flow systems and have been operating for different amounts of time. No single transport conceptual model can be made to fit all UMT disposal sites. However, we have developed a simplified one-dimensional transport conceptual model that can be used in conjunction with the chemical transport code CTM to identify coupled geohydrochemical transport processes at UMT disposal sites.

The transport processes of importance in groundwater systems are advection and dispersion (Freeze and Cherry 1979). Advection is the bulk movement of water in response to hydraulic head gradients. Dispersion is a miscible displacement process resulting from the mixing of fluid during advection. The consequence of advection is a displacement in the center of mass of a solute plume over time. The consequence of dispersion is spreading out of the solute plume over time.

The traditional description of transport in groundwater systems relies on the Fickian description of dispersion, which treats the dispersion process as a diffusion process about the center of mass. Advection is characterized by the mean pore water velocity and dispersion is characterized by the dispersivity. Consider an instantaneous injection of unit mass of a conservative tracer into a uniform flow field. After injection, the tracer concentration in the plume assumes a normal distribution with distance. During each time increment Δt, the center of mass of the plume is advected downstream by the amount $[v\,\Delta t]$, and the variance of the concentration distribution is equal to $[2\,\alpha\,v\,\Delta t]$ where α is the dispersivity. The two parameters controlling the concentration distribution are a function of the properties of the aquifer materials and the flow system.

Two dimensionless numbers guide the development of a transport conceptual model for use with CTM. The first is the displacement ratio R, which is equal to the mean distance traveled per time step relative to the column length. The second is the spreading ratio S which is equal to the standard deviation of the plume concentration after one time step divided by the mean distance traveled per time step. For the transport conceptual model used in the calculations discussed below, we chose R = 0.1 and S = 0.22. Therefore, during each time step in the simulation, the mean displacement of a conservative tracer is equal to one tenth of the total streamtube length and the standard deviation of the distribution grows by approximately one fifth of the displacement. The dimensionless numbers R and S were chosen for convenience in running the simulations and plotting the results.

Simulations performed with given R and S numbers can represent a variety of physical situations. For example, we chose to interpret our R and S numbers in terms of the values listed in Table 4.1, although other interpretations are equally valid. The groundwater velocity of 50 m/yr and the dispersivity of 2.4 m are typical of flow in coarse sediments over scale lengths of several thousand meters.

The spatial discretization was governed by the numerical resolution we desired for our calculations. Spatial discretization is characterized by two dimensionless numbers, the Courant number [$v \, \Delta t / \Delta x$] and the Peclet number [$\Delta x / \alpha$]. For our simulations, the Courant number was 5 and the Peclet number was 8.33. Peclet and Courant numbers in these ranges have been shown to provide adequate control of spatial discretization error with the Markov method (Hostetler and Erikson 1989).

TABLE 4.1. Definition of the Hydrologic Model

Pathline length = 1000 m

Number of bins = 50

Groundwater velocity = 50 m/yr

Dispersivity = 2.4 m

Time step length = 2 yr

GEOCHEMISTRY CONCEPTUAL MODEL

The geochemical model used in the calculations presented in this report was derived from the previous work for this project (Peterson et al. 1986) and from a brief review of the literature that pertains to the attenuation mechanisms of dissolved uranium. The majority of published information about the occurrence and mobility of uranium in the natural environment is focused on the geochemical conditions of formation and description of uranium ore deposits. Langmuir (1978a,b) presented critical reviews of the thermodynamic properties of dissolved uranium and the mineral-solution equilibria relevant to the formation of uranium ore deposits. Since 1978, other reviews by Krupka et al. (1983, 1985) and Tripathi (1984) have re-evaluated and compiled more recent thermodynamic data or have presented alternative viewpoints relevant to the aqueous behavior of U(IV) or U(VI).

Background

Uranium occurs in solids and in groundwaters in two primary oxidation states, U(IV) and U(VI). Thus, the redox conditions partly govern the form of dissolved uranium in groundwaters and the type of uranium solids formed. In addition, dissolved uranium concentrations are affected by the presence of complexing ligands such as OH^-, Cl^-, CO_3^{2-}, PO_4^{3-}, F^-, $H_4SiO_4^0$, SO_4^{2-} and organics such as fulvic and humic acids. Because of these complexation effects, the chemical composition of soil pore waters that mix with the UMT lixiviant also governs which uranium solid will be thermodynamically stable along a groundwater transport pathline.

The most common uranium ore minerals found in reduced environments are the U(IV) minerals which include uraninite (UO_2), coffinite [$U(SiO_4)_{1-x}(OH)_{4x}$], and (in some ore deposits in Japan that contain a source of phosphate), ningyoite [$(U,Ca,Ce)_2(PO_4)_2\cdot1-2H_2O$] (Muto 1965). U(IV) in solution exists as the uranous ion (U^{4+}) and is complexed in reduced groundwaters mainly in the form of several hydrolysis species, sulfate, chloride, phosphate, and by fluoride at pH values less than 4 (Langmuir 1978b). Between pH values of 5 and 8, the important U(IV) complexes include

4.4

the $U(OH)_4^0$ and $U(OH)_5^-$ hydrolysis species. At pH values less than 3, the U(IV) fluoride complexes are dominant.

Uranium minerals associated with ores from the Colorado Plateau also include the U(VI) minerals carnotite $[K_2(UO_2)_2(VO_4)_2]$, tyuyamunite $[Ca(UO_2)_2(VO_4)_2]$, and autunite $[Ca(UO_2)_2(PO_4)_2]$ (Langmuir 1978a). Dissolved U(VI) exists in solution as the uranyl ion (UO_2^{2+}), and forms dominant complexes with OH^-, CO_3^{2-}, F^-, PO_4^{3-}, SO_4^{2-} and organic ligands. The uranyl ion is complexed primarily by fluoride at pHs less than 4 and is strongly complexed by phosphate between pH values of 4 to 7.5 (Langmuir 1978a,b). At higher pH values, dissolved uranium can be present primarily as uranyl carbonate complexes. More recent work by Maya (1981) and Maya and Begun (1981) have shown evidence for additional hydroxocarbonato species that were not included in the calculations presented by Langmuir (1978a,b). The effects of the additional species on the U(VI) speciation scheme and on the adsorption of U(VI) were further evaluated by Tripathi (1984).

The proportion of the total dissolved uranium that is divided into U(IV) and U(VI) aqueous complexes and the effect of the speciation scheme on the relative stabilities of the U(IV) and U(VI) minerals will depend both on the redox potential and ligand concentrations in the soil pore water and UMT lixiviant. Because the uranium milling process uses a sulfuric acid leaching solution with sodium perchlorate added as an oxidant, the uranium dissolved in tailings solutions disposed of in ponds will be present as U(VI). Of the known complexing ligands affecting the concentrations of uranium in oxidized groundwater systems, the effects of dissolved carbonate and phosphate are considered the most important (Langmuir 1978a).

Attenuation Behavior of Uranium

The transport of uranium dissolved in acidic UMT lixiviants is affected by the aqueous speciation considerations mentioned above but also by other reactions between the lixiviant and the local soils and groundwaters. These reactions include precipitation of secondary uranium minerals, ion exchange of uranium on clay minerals, and specific-ion adsorption of uranium on

4.5

mineral surfaces. All three types of mass-transfer reactions could decrease the concentration of uranium in groundwaters migrating through a soil profile.

The precipitation of U(VI) minerals from an oxidized groundwater contaminated with UMT leachate is one possible mechanism that could attenuate the subsurface migration of uranium. The U(VI) minerals that may precipitate will depend on the pH and ligand concentrations in the groundwater. Some of the more common U(VI) minerals found in nature near uranium ore deposits include carnotite $[K_2(UO_2)_2(VO_4)_2]$, tyuyamunite $[Ca(UO_2)_2(VO_4)_2]$, autunite $[Ca(UO_2)_2(PO_4)_2]$, and uranophane $[Ca(UO_2)_2Si_2O_7 \cdot 6H_2O]$ (Langmuir 1978b). Of these U(VI) minerals, carnotite and tyuyamunite are the least soluble in groundwaters containing small quantities of dissolved vanadium. In the pH range of 5 to 8, either solid could limit the total concentration of dissolved uranium to levels less than 10^{-8} molar (~2 ppb U) at atmospheric pCO_2.

For groundwaters containing no vanadium but dissolved phosphate, autunite is the least soluble U(VI) mineral that could limit the concentration of uranium (Langmuir 1978b). The mineral uranophane is more soluble than any of the uranyl vanadate or phosphate minerals discussed above at expected vanadium and phosphorus concentrations in groundwaters (Langmuir 1978b). Therefore, should source-term concentrations of uranium in a UMT leachate enter a soil profile above the solubility limits of the U(VI) minerals discussed above, precipitation of these minerals could occur that would attenuate the concentrations of dissolved uranium along a pathline. The relative stabilities of these minerals will depend primarily on the concentrations of dissolved vanadium and phosphorus in the groundwater. The solubility-limited concentration of uranium transported through the soil profile will also depend on the groundwater pH, Eh, and carbonate concentration.

A second mechanism attenuating the transport of uranium through sediments is the adsorption of dissolved uranium on mineral surfaces, either by ion exchange or specific adsorption reactions. The adsorption of the

uranyl ion has been studied experimentally on a variety of mineral surfaces common in soils that include organic matter (peat), clay minerals, and ferric oxides and oxyhydroxides.

In a description of the mineralization of uranium ore deposits in Japan, Doi et al. (1975) suggested adsorption of uranium on organic matter was the most important factor in concentrating uranium on solid surfaces. Doi et al. (1975) reported that up to 100% adsorption of uranium occurred in suspensions of 1 g of peat per 100 ml uranyl perchloride acid solution (4 ppm U) between pH values of 3 and 8.5. Above pH 8.5, the uranium was desorbed because $NaHCO_3$ was used to adjust the pH of the solutions resulting in increased carbonate complexation of the uranyl ion.

Several experimental studies have been performed that have measured the affinity of the uranyl ion for different clay mineral surfaces commonly found in soils. Borovec (1981) measured the distribution coefficients (K_d) of uranium on kaolinite, illite, and montmorillonite in chloride solutions containing between 10^{-2} and 10^{-5} molar (2400-2 ppm) U(VI) at pH 6. For dissolved uranium concentrations less than 10^{-4} molar, the K_d values measured increased from 50 to about 1000 ml/g in the order kaolinite < illite < montmorillonite. Ames et al. (1983a) performed similar measurements for the same clay minerals at pH 7 in NaCl solutions and pH 8-9 in $NaHCO_3$ solutions. Maximum distribution coefficient values in the NaCl solutions were 500, 650, and 700 ml/g for illite, montmorillonite, and kaolinite, respectively. In the carbonate solutions, the cation exchange of uranyl ion on the clays was reduced because of aqueous complexation reactions forming uranyl carbonate species. As a result, the maximum distribution coefficients for illite and montmorillonite decreased to 110 and 2 which is consistent with the decreased affinity of clay mineral surfaces for the uranyl ion. Similar measurements by Ames et al. (1983b) were made for several mica minerals (biotite, phlogopite, muscovite) which are less prominent in weathered soils.

Perhaps the most important soil mineral surfaces with a strong affinity for adsorbing dissolved solutes are the surfaces of iron oxides and oxyhydroxides. Ames et al. (1983c) measured the adsorption of uranyl ion on

amorphous ferric hydroxide in NaCl solution at pH 7 and NaHCO$_3$ solution at pH 8.7. Calculations from the measurements suggest that the distribution coefficient for U(VI) is greater than 2 X 10^6 ml/g in NaCl solution and 3 X 10^4 ml/g in NaHCO$_3$ solution. More comprehensive studies of uranyl adsorption by iron oxides and oxyhydroxides have since been published by Hsi and Langmuir (1985) and Tripathi (1984). These studies discuss the adsorption of U(VI) over a wider range of pH values with and without dissolved carbonate present. For example, Hsi and Langmuir (1985) showed uranyl ion is strongly adsorbed at pH values greater than 5 to 6 by hematite, goethite, and amorphous ferric oxyhydroxide. Adsorption was greatest on the amorphous oxyhydroxide and least on hematite. At total uranium concentrations of 10^{-5} molar (24 ppm), essentially all U(VI) is adsorbed by 1 g/l of goethite and amorphous ferric oxyhydroxide above pH 5 in the carbonate free system. Hematite adsorbed only about 80% of the uranium over the same pH range. In the presence of dissolved carbonate at concentrations of 10^{-3}-10^{-2} molar (60-600 ppm), uranium adsorption is partially inhibited on all of the ferric oxide surfaces above pH 6.5.

The results of the adsorption studies of dissolved uranium on common mineral surfaces show that the iron oxides and oxyhydroxides have the strongest affinity for U(VI) adsorption. The affinity of these surfaces for the uranyl ion could reduce the dissolved uranium concentrations in groundwaters and thus retard the subsurface transport of uranium. The data also show that dissolved carbonate present at concentrations common in most groundwaters could inhibit the attenuation of dissolved uranium because of complexation effects. Thus, an accurate assessment of the potential for the attenuation of the subsurface transport of uranium requires site-specific field characterization data relevant to the groundwater chemistry and the types and quantities of minerals present in local subsurface soils.

The Thermodynamic Database

The database used by the CTM code is a modification of the database described by Krupka et al. (1988). The reactions in the database of Krupka et al. (1988) were in part taken from the MINTEQ code but were revised using

the thermodynamic data compilation of Wagman et al. (1982). Because the CTM database did not include data for uranium, we added thermodynamic data for U(VI) from the review of Tripathi (1984). This speciation scheme is similar to the one used by MINTEQ except for the addition of the aqueous species $(UO_2)_3(OH)_4^{+2}$, $(UO_2)_3(OH)_7^-$, $(UO_2)_4(OH)_7^+$, and $(UO_2)_2CO_3(OH)_3^-$ that are not in the MINTEQ database. The equilibrium constants for the solids schoepite and rutherfordine were also taken from the data compilation of Tripathi (1984).

The Conceptual Model

The geochemical model used in this study is largely based on the previous work for this project as summarized by Peterson et al. (1986). The model is based on the reaction of acidic tailings leachates with calcareous soils. The main attenuation mechanisms in this model include mineral precipitation reactions resulting from the neutralization of the acidic leachate by the dissolution of calcite present in the soil. In addition, specific-ion adsorption of selected trace metals onto the surface of amorphous hydrous ferric oxide (HFO) was also considered.

The chemical constituents in the model used in this study included those that are commonly found in groundwaters and uranium mill tailings leachates that could affect the transport behavior of uranium through complexation reactions or mass-transfer reactions. The list of chemical constituents in the geochemical model include H_2O, H, K, Ca, Mg, SO_4, CO_3, Cl, V(V), and U(VI). The inclusion of specific adsorption reactions in the model requires the addition of the immobile surface component to the list. We refer to the surface component for the adsorption of mobile species onto the surface of amorphous hydrous ferric oxide as HFO-. Table 4.2 lists the chemical components in the model and the chemical compositions of the system at the initial and boundary conditions.

Specific-ion adsorption reactions are also included in the thermodynamic adsorption database used by the CTM code for the adsorbing species in the model. The adsorption data are those discussed by Krupka et al. (1988) and

4.9

TABLE 4.2.   Definition of the Geochemical Model, Initial Condition, and Boundary Condition.

Chemical Components	Initial Condition molar	mg/L	Boundary Condition molar	mg/L
Ca^{+2}	$.14 \times 10^{-2}$	56	$.14 \times 10^{-1}$	548
Mg^{+2}	$.14 \times 10^{-2}$	34	$.65 \times 10^{-1}$	1580
K^{+}	$.57 \times 10^{-3}$	22	$.1 \times 10^{-2}$	40
UO_2^{+2}	$.10 \times 10^{-9}$	0.03 μg/L	$.30 \times 10^{-4}$	7
VO_2^{+}	$.10 \times 10^{-9}$	0.008 μg/L	$.21 \times 10^{-3}$	11
CO_3^{-2}	$.19 \times 10^{-2}$	114	$.10 \times 10^{-4}$	0.6
SO_4^{-2}	$.20 \times 10^{-2}$	192	$.83 \times 10^{-1}$	7920
Cl^{-}	$.35 \times 10^{-3}$	12	$.82 \times 10^{-2}$	290
HFO^{-}	$.11 \times 10^{-1}$	0.024 wt%	----	----
pH(units)	7.9		2.3	

Adsorbates

$HFO-H^{o}$	$.11 \times 10^{-2}$	
$HFO-H_2^{+}$	$.70 \times 10^{-6}$	
$HFO-Ca^{+}$	$.10 \times 10^{-2}$	
$HFO-UO_2OH^{o}$	$.56 \times 10^{-7}$	
$HFO-H_2SO_4$	$.15 \times 10^{-3}$	

Solids

Calcite	$.41 \times 10^{-1}$	0.024 wt%
Gypsum	0.0	
Schoepite	0.0	
Rutherfordine	0.0	
Tyuyamunite	0.0	
Carnotite	0.0	

4.10

include mass-action expressions for adsorption of the species H^+, Ca^{+2}, and SO_4^{-2}. The adsorption model used by the CTM code is a simple surface complexation site-binding model designed to calculate adsorption on the surface of amorphous hydrous ferric oxide (HFO). Adsorption of selected trace metals onto the surface of HFO was also included in the geochemical model described by Peterson et al. (1986). The immobile surface adsorbates formed by the above aqueous components and the surface site (HFO^-) include the surface protonation species $[HFO-H]^o$ and $[HFO-H_2]^+$, and the specific adsorption of the species $[HFO-Ca]^+$ and $[HFO-H_2SO_4]^-$. The procedure used to parameterize the mass-action expressions involved minimizing differences between model calculations and experimental adsorption data. The results of the parameterization procedure for the adsorbates listed above is discussed in detail in Krupka et al. (1988).

Because of the geochemical importance of the specific-ion adsorption of uranium in natural systems (Langmuir 1978a,b) and the strong adsorptive capacities of hydrous ferric oxide present in soils for the uranyl ion (Ames et al. 1983c; Hsi and Langmuir 1985), we also derived a mass-action expression for the adsorption of [U(VI)] onto hydrous ferric oxide. Using the parameterization procedure outlined in Krupka et al. (1988), the mass-action expression was optimized for [U(VI)] adsorption onto the surface of hydrous ferric oxide using the experimental data of Hsi and Langmuir (1985).

A comparison of the adsorption model predictions with the experimental measurements is illustrated in Figure 4.1. The adsorption reaction was parameterized for UO_2^{+2} adsorption in the carbonate-free system using one mass-action expression for the surface species $HFO-UO_2OH^o$. Once the adsorption behavior was verified for the carbonate-free system, the calculations were extended to the experimental conditions for the system with dissolved carbonate using the same equilibrium constant derived for the single adsorbate in the carbonate-free system. The model also reproduced reasonably well the desorption behavior that occurs in the system containing carbonate at pH values greater than 7. Because additional experimental data for U(VI) adsorption on HFO at different adsorbate/adsorbent ratios are not available, the adsorption behavior of U(VI) could not be verified further.
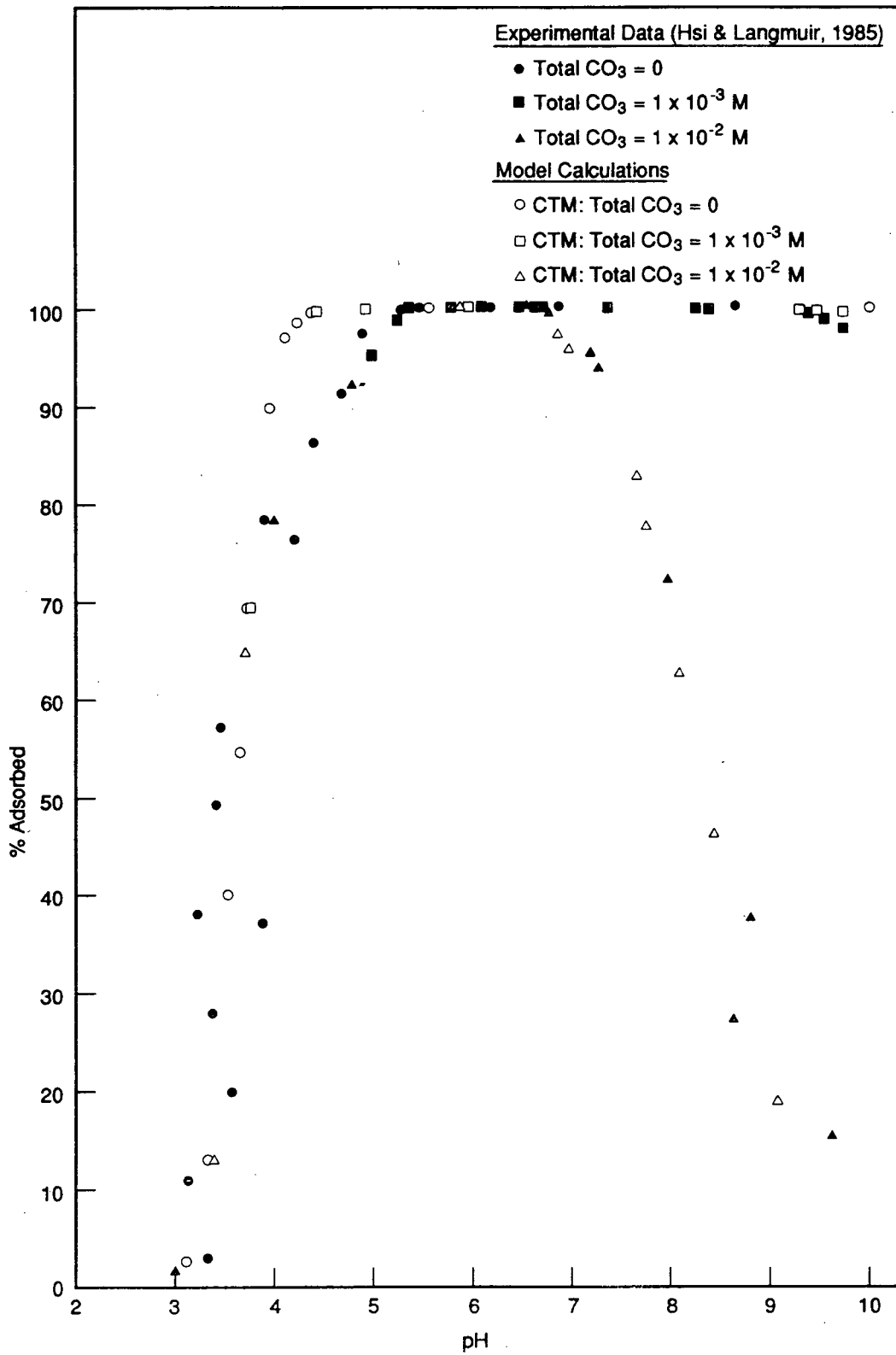
FIGURE 4.1. Adsorption of Uranyl Ion on the Surface of Hydrous Ferric Oxide.

The geochemistry conceptual model listed in Table 4.2 also includes a list of solids that are involved in solubility mass transfer reactions. Calcite was included in the model because it is present in calcareous soils and represents the soil acid buffering capacity. Gypsum, which was used as a solubility control in the work of Peterson et al. (1986), was also included in the current model. In addition, several U(VI) minerals were included in the model to show the effects of secondary U(VI) mineral precipitation on the transport behavior of uranium. The minerals included in the model include schoepite, carnotite, rutherfordine, and tyuyamunite.

Initial Conditions

The initial condition includes defining the chemical composition of the soil pore water, the soil acid buffering capacity, and the soil adsorption capacity at time t = 0. The composition of the ambient pore water is based on a measured groundwater from well TP1-D2 at the Federal American Partners site (Dames and Moore 1981). Using the measured groundwater composition and pH, the CTM code was used to obtain the distribution of aqueous species and to determine the proton condition of the groundwater. The results of the speciation calculation indicated that the groundwater was oversaturated with respect to calcite at the measured pH value of 7.9. Because the soil has a finite acid buffering capacity (wt % as $CaCO_3$) at the initial condition, the groundwater must be in equilibrium with calcite present in the soil. Therefore, a second CTM calculation was performed to obtain a groundwater composition in equilibrium with calcite at pH 7.9 by allowing calcite to precipitate from solution. The mass transfer calculation resulted in a lowering of the Ca and CO_3 concentrations from the measured values of 144 and 248 mg/L, to 56 and 114 mg/L, respectively (Table 4.2).

Definition of the initial condition also requires a specification of the soil chemistry. Because the conceptual model is designed to simulate the solubility/adsorption attenuation reactions that result from the neutralization of acidic leachate by a calcareous soil, the amounts of calcite and hydrous ferric oxide (HFO) present initially in the soil must be

4.13

specified. In choosing a value for the soil acid buffering capacity, a finite amount of calcite was selected such that, at some point during the simulation, the buffering capacity of the soil would become exhausted. This behavior has been observed at several UMT sites such as Federal American Partners (Dames and Moore 1981) and Lucky Mc Pathfinder (Erikson and Sherwood 1982) where over a period of years, the soil buffering capacity becomes exhausted and unneutralized leachate is transported beyond the disposal site. For the composition of the leachate used in this study (discussed below), it was determined that a soil acid buffering capacity of 0.024 wt % as $CaCO_3$ would be appropriate. In modeling an actual field site, the acid buffering capacity could be determined analytically using standard soils characterization techniques (Peterson et al. 1986). The amount of HFO in a soil can also be analytically determined using a hydroxylamine/hydrochloride extraction technique (e.g., Chou and Zhou 1983) that selectively removes HFO. Because we were unable to find analytic determinations of this parameter relevant to a UMT site, a concentration of HFO in the soil equal to the one used in the laboratory experiments for U(VI) adsorption (1 g/L) on HFO (Hsi and Langmuir 1985) was used. This concentration of HFO in the soil is identical to the one used to derive the adsorption behavior shown in Figure 4.1.

The concentrations of calcite and HFO measured analytically must be converted to a mole basis for the bulk soil per liter of pore water. Thus, the physical properties of the soil (bulk density, porosity) must also be known. For the simulations discussed in this study, we chose values that are consistent with sandy or silty soils. The bulk density and porsity used for the soil were 1.65 g/cm^3 and 0.40, respectively. Using the porosity and bulk density values, each liter of groundwater would contact 2500 cm^3 of soil or 4125 g of soil. Therefore, the values for a soil having 0.024 wt % calcite and 1 g/L HFO can be converted to 0.041 moles/L of calcite and 0.011 moles/L of HFO. A complete list of the initial condition is shown in Table 4.2.

The remaining solids (other than calcite) listed in Table 4.2 are included in the geochemistry model as potential solids. Potential solids are not present in the soil at the initial condition but are allowed to

4.14

precipitate should they become oversaturated during the simulation. The potential solubility controls allowed include gypsum, schoepite, rutherfordine, tyuyamunite, and carnotite. Gypsum has been identified as a precipitate at UMT sites where acidic leachate is neutralized by a calcareous soil (Erikson and Sherwood 1982) and was used as a solubility control in the previous work described by Peterson et al. (1986). The uranium solids listed in Table 4.2 have been identified by Langmuir (1978a,b) as being important solubility controls for U(VI) in low temperature groundwaters.

Boundary Conditions

The concentrations of the chemical components in the acidic leachate comprise the upstream boundary condition. The chemical composition used (Table 4.2) is based on a measured leachate composition from the Exxon Highland Mill (Sherwood and Serne 1983). The composition represents a UMT leachate generated from the sulfuric acid uranium leach process and contains about 7 mg/L total uranium and has a pH of 2.3. The measured redox potential for this leachate was +750 mV and all dissolved vanadium and uranium present in the leachate was assumed to be in their most oxidized state. The leachate influent composition used in the simulations was assumed to have a constant composition as a function of time.

A speciation calculation was performed for the Highland Mill leachate composition used in the transport simulations to determine its acidity relative to the leachates discussed in Chapter 2.0 for the L-Bar, Riverton, FAP, and Lucky Mc sites. We calculated that to neutralize 1 kg of the Highland Mill leachate required 1.26 grams of calcite and that 1.92 grams of gypsum would precipitate. The neutralized pH for the Highland Mill leachate was 6.85. Thus, the total acidity of the Highland Mill leachate is the smallest of the values calculated for any leachates from the field sites discussed in Chapter 2.0.

5.0 SIMULATION RESULTS

A series of CTM simulations were performed for the transport model summarized in Table 4.1 using the initial and boundary conditions listed in Table 4.2. Because the simulations are designed to examine the effects of the adsorption/solubility attenuation reactions involving dissolved U, a total of four CTM simulations were made that have different attenuation properties. Run 1 included adsorption attenuation only in which the soil acid buffering capacity (as wt% $CaCO_3$) was zero. Thus, any attenuation of reactive solutes occurred only by interactions between the solutes and the surface of HFO in a system in which the pH of the solution was unbuffered by calcite dissolution. Run 2 also included adsorption as the only attenuation mechanism for uranium except a finite amount of calcite equivalent to the acid buffering capacity was present in the soil. In run 3, solubility reactions were used to attenuate the concentrations of reactive solutes in a system having the finite acid buffering capacity listed in Table 4.2. Solubility reactions in the model included the dissolution of calcite, the precipitation of gypsum, and the precipitation of the most stable secondary uranium mineral in the list shown in Table 4.2. The final simulation (run 4) contained all of the attenuation mechanisms studied separately in runs 1-3. Thus, the attenuation mechanisms involve the competitive effects of solubility and specific-ion adsorption for reactive solutes.

We compare the results of our simulations to the generic model of Sheppard and Brown (1982) and to the field observations summarized in Chapter 2.0. From the simulation results, the frontal velocities representing the migration of the breakthrough fronts of chloride, pH, sulfate, and total U were calculated. In our simulations, chloride migrates as a conservative tracer and its transport is dependent only on the advection and dispersion processes represented in the transport model. The migration of H^+, SO_4^{2-}, and UO_2^{2+} depend also on the geochemical attenuation mechanisms included in the geochemical conceptual model. The relative frontal velocities of the reactive constituents can be used to delineate the relationship between the solute profiles and the locations of the acid, neutralization, and transport zones.

5.1

RUN 1: ATTENUATION BY ADSORPTION WITH ZERO SOIL ACID BUFFERING CAPACITY

In the first simulation, the attenuation of solutes is the result only of specific-ion adsorption mechanisms on the surface of amorphous hydrous ferric oxide (HFO). For run 1, the soil acid buffering capacity was set equal to zero by specifying that the soil present at the initial conditions contained no calcite. The concentrations of chemical species used for the initial and boundary conditions are those listed in Table 4.2. Note in Table 4.2 that our model includes competitive adsorption thus UO_2^{2+} must compete with other adsorbing solutes (H^+, Ca^{2+}, and SO_4^{2-}) for surface sites on the hydrous oxide. The transport characteristics used for all subsequent simulations included a groundwater velocity of 50 m/yr and dispersivity of 2.4 m for a transport pathway 1000 m long. The length of each timestep in all simulations is equivalent to 2 yr.

Interpreting the results of a coupled geohydrochemical simulation first requires an understanding of the transport of a conservative tracer. In the case of all of the subsequent examples, chloride (Cl^-) is a conservative tracer because no mass-transfer reactions occur between aqueous chloride and the immobile phases (solids or adsorbates) in the system. Figure 5.1 shows the distribution of chloride after 10 years (timestep 5) in this simulation. Total dissolved chloride enters the pathway at the leachate boundary concentration of 290 mg/L (log mol=-2.1) as shown in Figure 5.1. After 10 years of transport, the average distance traveled at a velocity of 50 m/yr for the conservative tracer is 500 m which is at the center of mass of the advection/dispersion front (breakthrough distance) shown in Figure 5.1. Because of advective/dispersive processes alone, the Cl^- concentration decreases along the advection/dispersion front from the value at the leachate boundary to that of the initial condition (12 mg/L or log mol = -3.5) that represents the Cl^- concentration in the uncontaminated groundwater. Because the same transport model was used in all the simulations, Figure 5.1 also represents the distribution of chloride after 10 years in all subsequent simulations. These results for chloride are consistent with the features of the generic contaminant plume model of Sheppard and Brown (1982).

5.2

Figure 5.2 shows the advance of the pH front after 10 yr that shows the increase in pH values from the leachate boundary value (2.3) to the pH of the uncontaminated groundwater (7.9) present at the initial conditions. In contrast to the transport of Cl⁻ shown in Figure 5.1, note that the pH breakthrough front has traveled a distance of only 440 m after 10 yr. Thus, the average local velocity of the pH breakthrough front (44 m/yr) is retarded relative to chloride (50 m/yr). In this example, the retardation is the result of the strong affinity of H^+ for the surface of HFO through specific adsorption reactions. The three zones (acid zone, neutralization zone, transport zone) described in the model of Sheppard and Brown (1982) also are apparent in Figure 5.2. However, in this particular case, the pH distribution into 3 distinct zones is not the result of the neutralization of leachate by calcareous soils because the soil in this example has a zero acid buffering capacity. This example shows that, in addition to neutralization of acidic leachate by carbonate minerals, the appearance of the pH front to be divided into 3 distinct zones can also be the result of simple advective/dispersive mixing of a leachate having a low pH with an ambient groundwater having a higher pH.

The pH distribution after 20 years for run 1 is shown in Figure 5.3. At this time in the simulation, the pH breakthrough front has migrated an average distance of 860 m relative to the Cl⁻ breakthrough front which has migrated 1000 m. Thus, the average local velocity of the pH front is 43 m/yr. The difference in the local velocities calculated for the pH front at 10 and 20 years shows that the retardation involving the pH is nonlinear. The nonlinearity in the transport behavior is the result of the adsorption behavior of H^+ which also is nonlinear with respect to groundwater composition. Constant retardation (K_d) transport models are not capable of producing nonlinear transport behavior because the retardation factor is independent of groundwater composition.

FIGURE 5.1. Calculated Distribution of Chloride after 10 Years for the System Having Specific-Ion Adsorption Attenuation and Zero Soil Acid Buffering Capacity.

FIGURE 5.2. Calculated Distribution of pH after 10 Years for the System Having Specific-Ion Adsorption Attenuation and Zero Soil Acid Buffering Capacity.

FIGURE 5.3. Calculated Distribution of pH after 20 Years for the System Having Specific-Ion Adsorption Attenuation and Zero Soil Acid Buffering Capacity.

Figure 5.4 shows the distribution of the total sulfate concentration as a function of distance after 10 years. The solute profile shows the elevated concentration of SO_4^{2-} in the acid zone near the influent boundary (7920 mg/L or log mol = -1.1), and the concentration decreasing along the advection/dispersion front to the value in the uncontaminated groundwater (192 mg/L or log mol = -2.7). Any attenuation of SO_4^{2-} in this example is the result only of the specific adsorption of sulfate on the surface of HFO. The simulation showed that the breakthrough distance after 10 years for SO_4^{2-} in the plume is 500 m and thus the behavior of sulfate approximates that of a conservative tracer. Sulfate is not actually a conservative tracer because small amounts of sulfate are being adsorbed on HFO along the transport pathline. However, the mass of sulfate adsorbed is very small relative to the amount of aqueous sulfate. From the concentrations of dissolved and adsorbed sulfate in each bin of the pathline, we calculated values for the local K_d of sulfate. The dimensionless K_ds for sulfate along the pathway varied from about 0.03 near the influent boundary to about 0.07 beyond the advection/dispersion front indicating that sulfate is not strongly retarded by adsorption alone. In this particular case, SO_4^{2-} is not strongly adsorbed relative to H^+. In Figure 5.4, sulfate appears to travel as a conservative tracer with a local average velocity of 50 m/yr only within the spatial resolution of the bin width (20 m). Therefore, a much smaller bin width must be used to distinguish the behavior of a reactive solute having a small retardation from the transport behavior of a conservative tracer. This example also shows that sulfate concentrations may not always decrease as rapidly with distance relative to chloride as shown in the generic model of Sheppard and Brown (1982).

The transport of uranyl ion (UO_2^{2+}) is attenuated only by specific-ion adsorption on the surface of HFO in run 1. Figure 5.5 shows the solute profile for UO_2^{2+} after 10 years. In the acid zone near the leachate boundary, the UO_2^{2+} concentration is equivalent to that of the leachate (7 mg/L or log mol = -4.5) because the pH in this region is less than 3.0 and the adsorption of the uranyl ion at low pH values is near zero (Figure 4.1). Therefore, dimensionless K_d values for uranium calculated from the data at 10 years for the acid region are nearly zero. As the pH front migrates outward
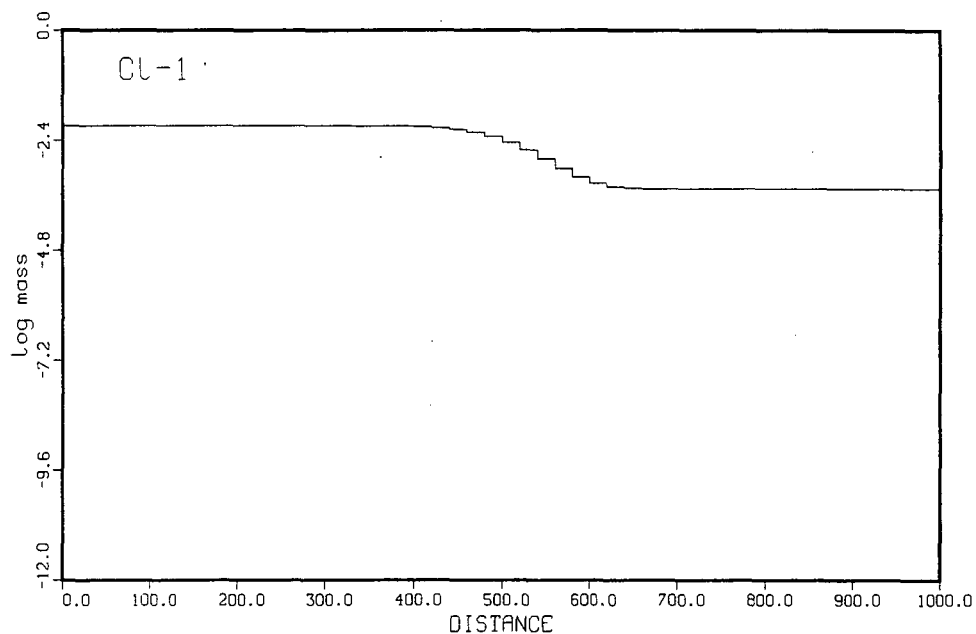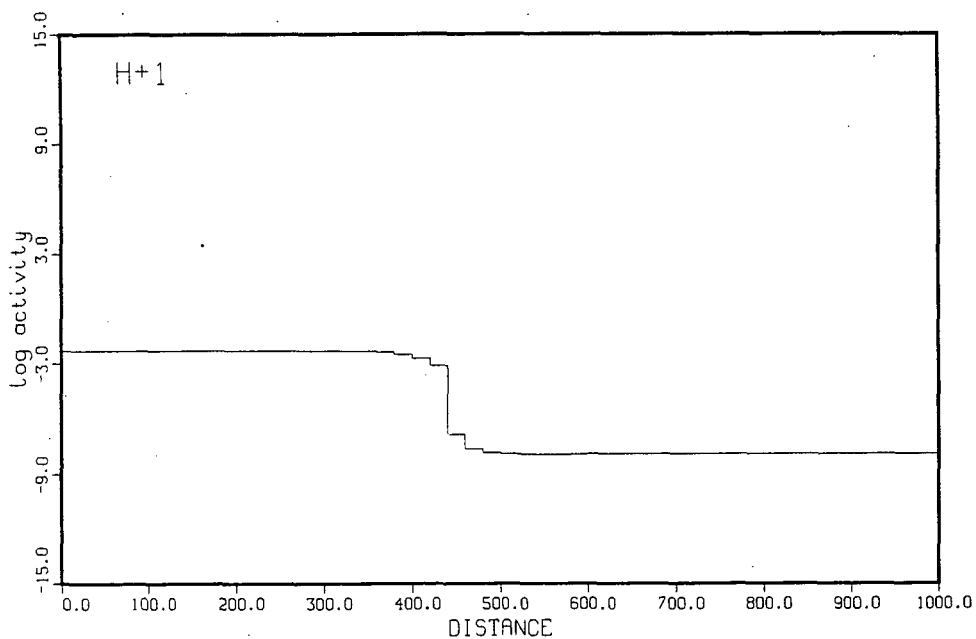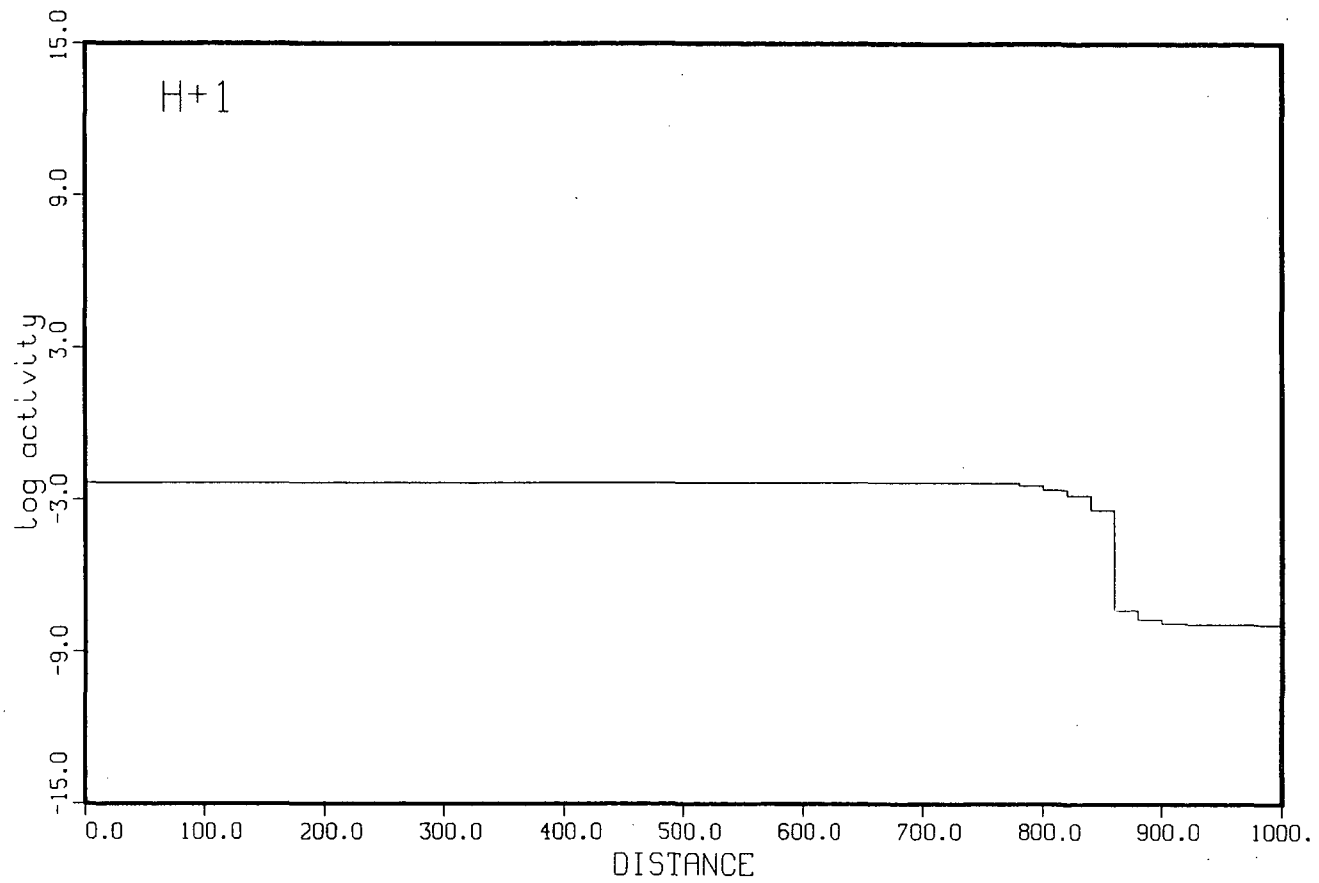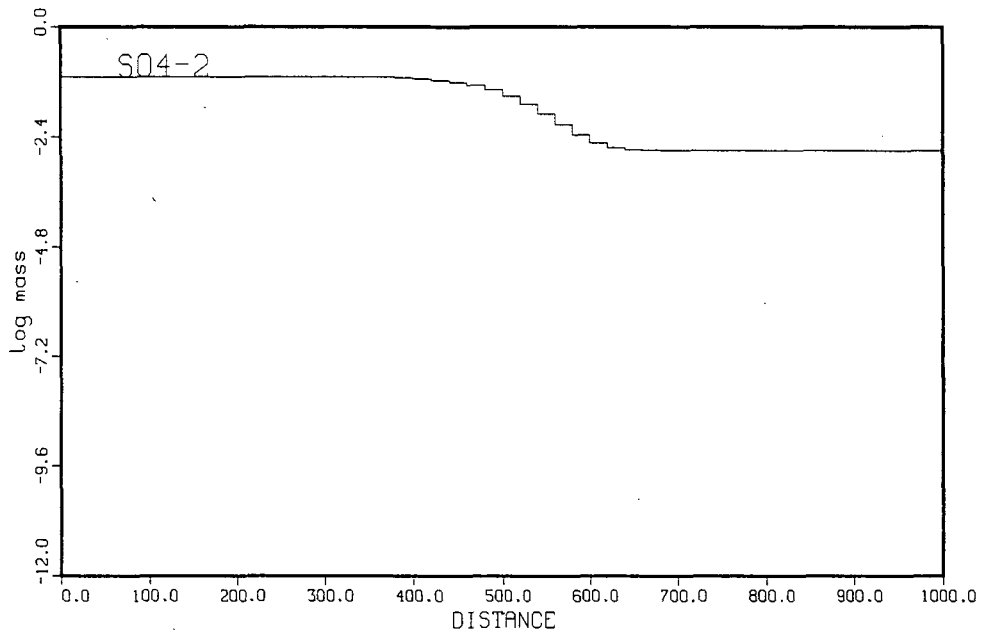
FIGURE 5.4. Calculated Distribution of Sulfate after 10 Years for the System Having Specific-Ion Adsorption Attenuation and Zero Soil Acid Buffering Capacity.

FIGURE 5.5. Calculated Distribution of Uranyl after 10 Years for the System Having Specific-Ion Adsorption Attenuation and Zero Soil Acid Buffering Capacity.

5.7

from the evaporation pond as a function of time, uranium that had been previously adsorbed on the upgradient sediments at earlier times is continuously remobilized (desorbed) because the low pH leachate is advancing downgradient. The remobilized aqueous uranium is advected and dispersed with the groundwater and results in the increase in total U concentrations along the trailing (upgradient) edge of the advection/dispersion front (350-450 m). At this distance from the evaporation pond, the uranium concentrations in the groundwater are actually greater than those in the leachate. At a distance of about 450 m, the pH increases from near 3 to about 7 and uranium is strongly adsorbed. This behavior is reflected as the sharp decrease in aqueous uranium concentrations in Figure 5.5. Local dimensionless K_{ds} in this region calculated from the amounts of uranium adsorbed and dissolved increase to values of about 900. Downgradient of the advection/dispersion front, the concentration of aqueous uranium is regulated by specific-ion adsorption and eventually decreases to the value at the initial conditions (0.03 μg/L or log mol = -10.0). In this region, the local dimensionless K_d for uranium is about 560. For this particular example, the uranium breakthrough front has traveled an average distance of 440 m in 10 yr. The specific-ion adsorption of uranium thus has retarded the local velocity of uranium to about 44 m/yr in comparison to the 50 m/yr for the chloride conservative tracer.

RUN 2: ATTENUATION BY ADSORPTION WITH FINITE SOIL ACID BUFFERING CAPACITY

Run 2 contains the same specific-ion adsorption attenuation mechanisms as run 1 except that a finite quantity of calcite is present that represents the acid buffering capacity of the soil. The hydrology model (see Table 4.1) and geochemical initial and boundary conditions (see Table 4.2) are both identical to run 1.

After 10 years of contact with the migrating leachate, the buffering capacity of the soil is exhausted out to a distance of about 80 m from the evaporation pond (Figure 5.6) because of calcite dissolution by the acidic leachate. Calcite is still present in the soil beyond 80 m and is available to buffer the pH of the migrating leachate. Figure 5.7 shows the resulting

FIGURE 5.6. Calcite Dissolution Front after 10 Years for the System Having Specific-Ion Adsorption Attenuation and a Finite Soil Acid Buffering Capacity.
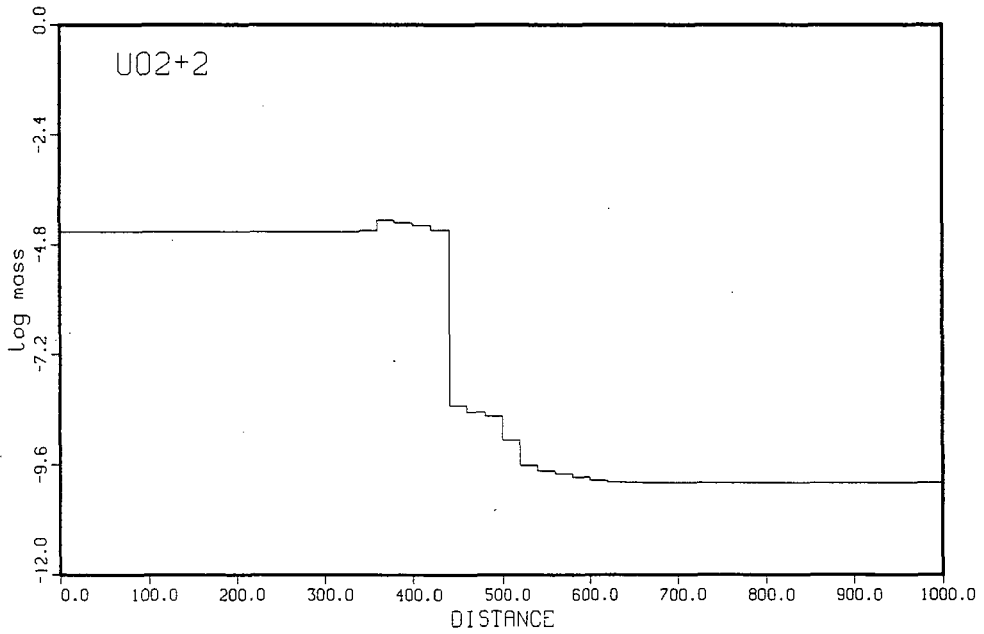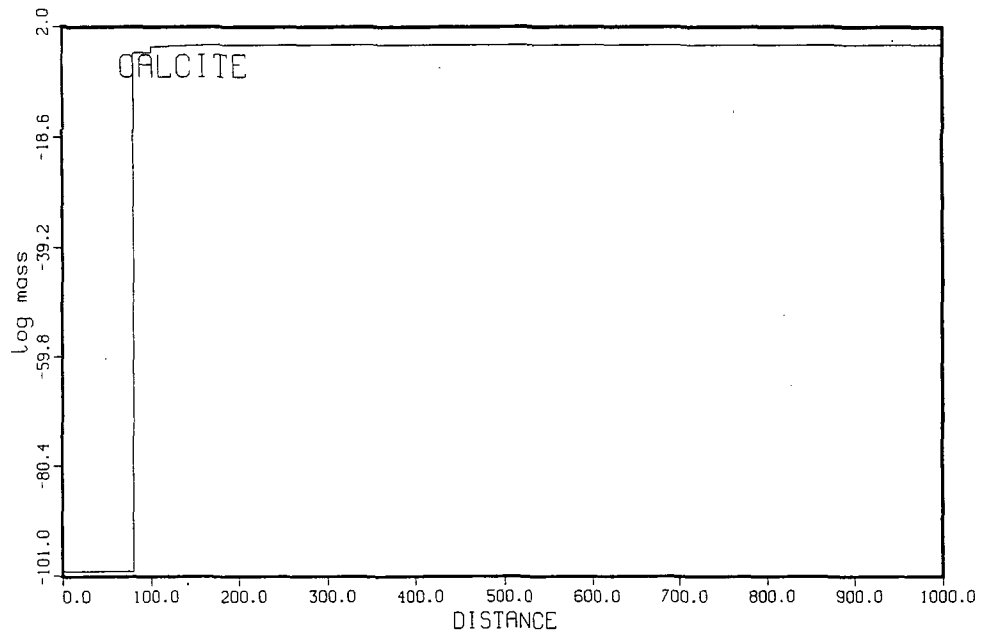

FIGURE 5.7. Calculated Distribution of pH after 10 Years for the System Having Specific-Ion Adsorption Attenuation and a Finite Soil Acid Buffering Capacity.

5.9

pH profile after 10 years for the system with a finite soil acid buffering capacity. In the region where all calcite has dissolved, the pH of the groundwater is equivalent to that of the leachate (2.3). At about 80 m from the pond where calcite is still present in the soil the pH rises abruptly to about 6.5. At all distances downgradient of 80 m, calcite is in equilibrium with the groundwater. The pH increases slightly along the advection/ dispersion front (350-550 m) until the pH of the initial conditions (7.9) is reached. Calcite is in equilibrium with solution at a lower pH on the upgradient side of the advection/dispersion front because of differences in the proton condition of the modified leachate composition relative to the initial condition.

The pH breakthrough front for run 2 has migrated to 80 m in 10 years as compared to the breakthrough distance for a conservative tracer (500 m). The local pH front velocity is about 8 m/yr, in contrast to the average groundwater velocity of 50 m/yr. This local velocity for the pH front is considerably less than the local velocity in run 1 (44 m/yr) in which the soil had a zero acid buffering capacity. Thus, the acid buffering capacity of the soil can greatly retard the velocity of the migrating pH front. This simulation emphasizes the importance of quantifying the soil acid buffering capacity at field sites in order to accurately calculate the advance of the pH front because the attenuation behavior (either by adsorption or solubility) of many solutes is strongly pH dependent.

The quantity of SO_4^{2-} adsorbed on the surface of HFO was small relative to the aqueous SO_4^{2-} concentration between the pH values of the leachate boundary condition (2.3) and the initial conditions (7.9). The solute profile for sulfate after 10 years in run 2 was virtually identical to the profile calculated in run 1 (Figure 5.4). In these two cases, the differences in the advances of the pH fronts did not influence the adsorption behavior of SO_4^{2-}. At the lowest pH values in the acid zone, the adsorption affinity of SO_4^{2-} is small compared to the affinity of H^+ for the surface of HFO. At the higher pH values, the amount adsorbed approaches zero because of the anionic adsorption behavior of SO_4^{2-}. These two examples point out that the distribution of SO_4^{2-} may not always follow the transport behavior

5.10

outlined in the generic model of Sheppard and Brown (1982) when the only attenuation mechanism for SO_4^{2-} is specific-ion adsorption.

Because of the dependence of the adsorption of UO_2^{2+} on pH and carbonate complexation (Figure 4.1), the solute profile for total dissolved uranium is considerably different for the system with a finite soil acid buffering capacity (Figure 5.8). In the region out to 80 m where the buffering capacity of the soil has been exhausted, the concentration of dissolved UO_2^{2+} exceeds that of the influent because of the desorption of UO_2^{2+} at low pH. Beyond 80 m the increase in pH from 6.5 to 7.9 increases the amount of UO_2^{2+} adsorbed and the total aqueous U concentration decreases rapidly to the value at the initial conditions.

The breakthrough distance for the UO_2^{2+} front is 260 m after 10 years which is equivalent to an average local velocity of 26 m/yr. This value is nearly half the local velocity for the advance of the uranium front in the system with a zero acid buffering capacity (Figure 5.5). The difference in frontal velocities is primarily the result of increased adsorption occurring in the system where calcite buffers the pH over most of the transport pathway. Local dimensionless K_ds calculated from the amounts of dissolved and adsorbed uranium are similar to those calculated for the system having a zero acid buffering capacity. Local dimensionless K_ds in run 2 varied from about 1 in the acid zone to about 560 in the neutralization and transport zones where the pH is above 6.5. However, because calcite buffered the pH of the groundwater over long distances along the pathway in run 2, the dimensionless K_d averaged over the entire transport pathway (global K_d) was about 0.5. In contrast, the global K_d was about 0.05 in run 1 where calcite was not present to buffer the pH.

RUN 3: ATTENUATION USING SOLUBILITY CONSTRAINTS

A second important attenuation mechanism involves the effects of solubility (precipitation/dissolution) equilibria on calculated profiles of reactive solutes. We examined the transport behavior involving solubility constraints in run 3. In this simulation, the boundary conditions (Table 4.
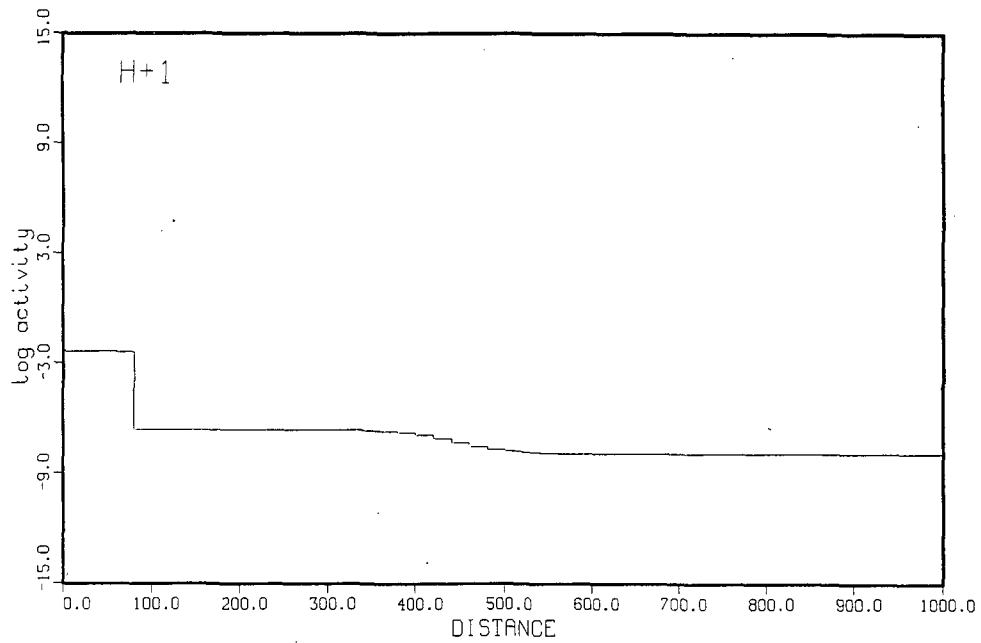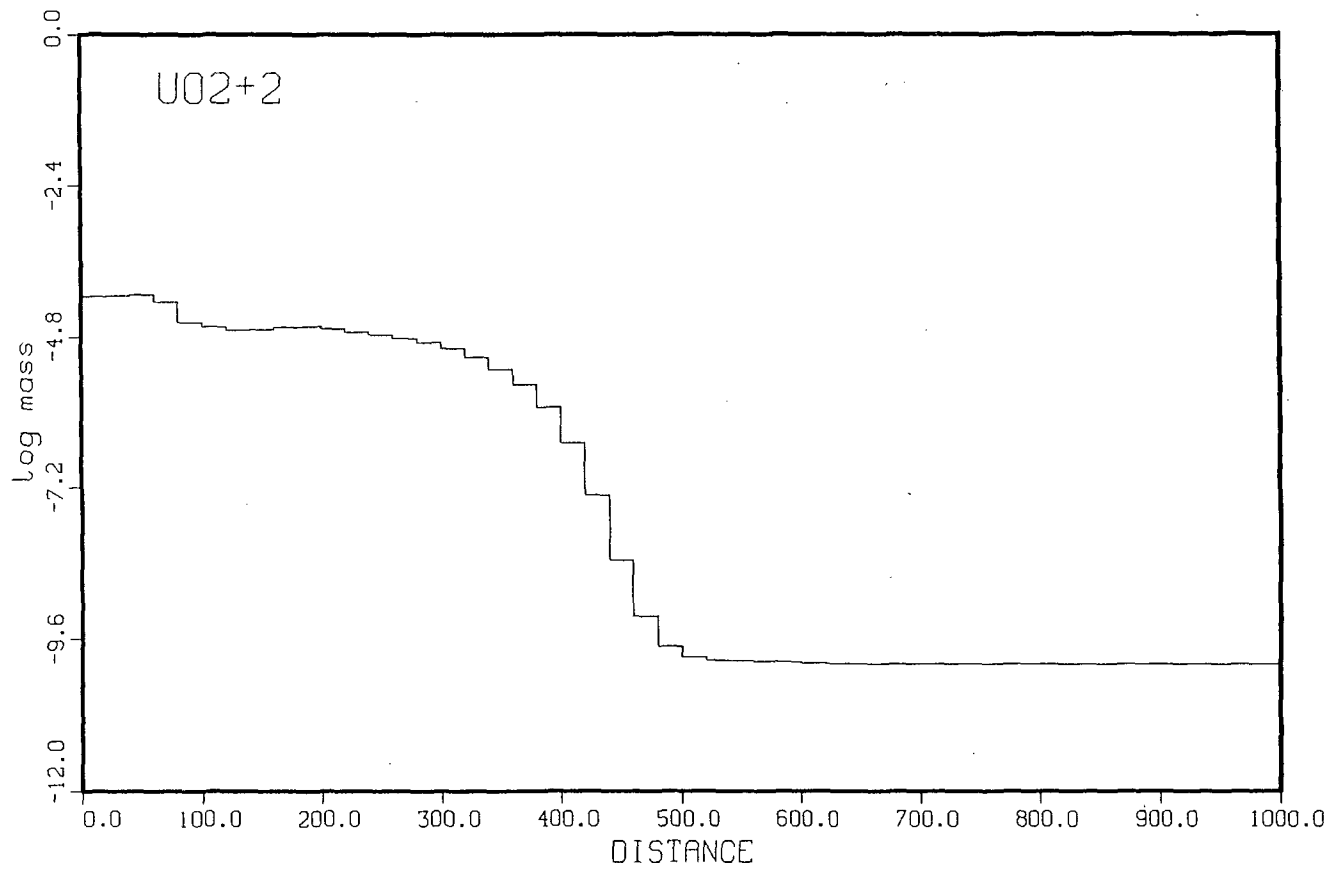
FIGURE 5.8. Calculated Distribution of Uranyl after 10 Years for the System Having Specific-Ion Adsorption Attenuation and a Finite Soil Acid Buffering Capacity.

2) and hydrologic model (Table 4.1) were the same as in the previous two simulations. However in run 3, adsorption of solutes on the surface of HFO was not allowed and several solubility controls were introduced to regulate the concentrations of selected solutes. Run 3 used the same quantity of calcite present in the soil at the initial conditions as run 2 to buffer the pH of the leachate interactions with the soil. In addition, several potential solids were specified that are not present in the soil initially but were allowed to precipitate/redissolve during the simulation should they become oversaturated in the aqueous phase. The potential solids are those listed in Table 4.2 with zero mass at the initial conditions and include gypsum, schoepite, rutherfordine, tyuyamunite, and carnotite. Gypsum is an important precipitate in soils contacted with acidic UMT leachates (Erikson and Sherwood 1982; Peterson et al. 1986) and was included in the geochemical conceptual model to control sulfate concentrations. The remaining four minerals are all potential solubility controls for U(VI). The relative stabilities and occurrence of these minerals are discussed in detail in Langmuir (1978a,b) and Krupka et al. (1985). Of the potential U(VI) minerals listed in Table 4.2, only the most stable one (least soluble) will precipitate from solution at any bin or timestep in the simulation.

Figures 5.9, 5.10, and 5.11 show the mineral profiles for the solubility run that illustrate the calcite dissolution front, and the precipitation fronts of gypsum and tyuyamunite, respectively. In this example, there is sufficient sulfate in the leachate and calcium dissolved from calcite dissolution to precipitate gypsum along the transport pathway. Because of the quantity of vanadate being advected and dispersed from the leachate, tyuyamunite is the least soluble of the potential U(VI) solubility controls and thus it also precipitates in the higher pH regions of the transport pathway.

The calcite buffering capacity of the soil in run 3 after 10 years has been exhausted out to 100 m (Figure 5.9) in contrast to the calcite dissolution front migrating 80 m in adsorption run number 2 (Figure 5.6). Thus, the acid zone of low pH values also extends out to about 100 m (Figure 5.12). The calcite dissolution front has advanced further in run 3 for the

FIGURE 5.9. Calcite Dissolution Front after 10 Years for the System Having Solubility Constraints Only.

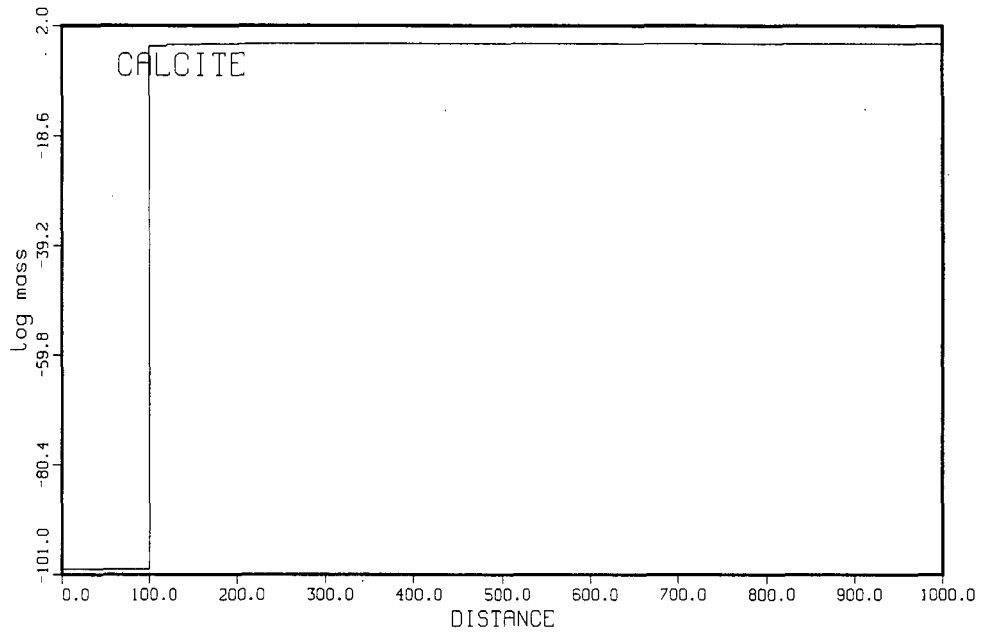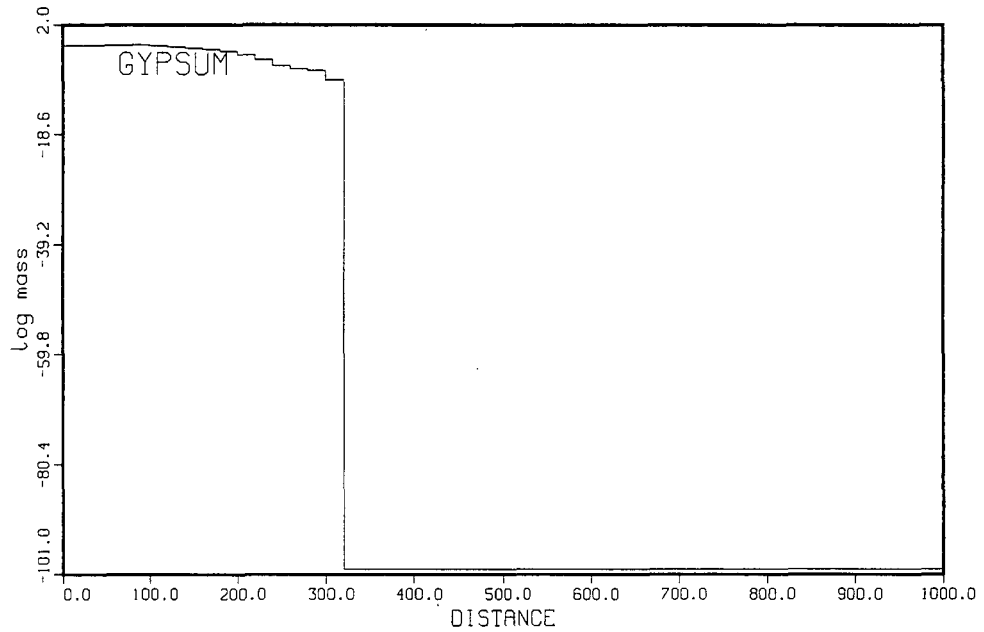FIGURE 5.10. Gypsum Precipitation Front after 10 Years for the System Having Solubility Constraints Only.
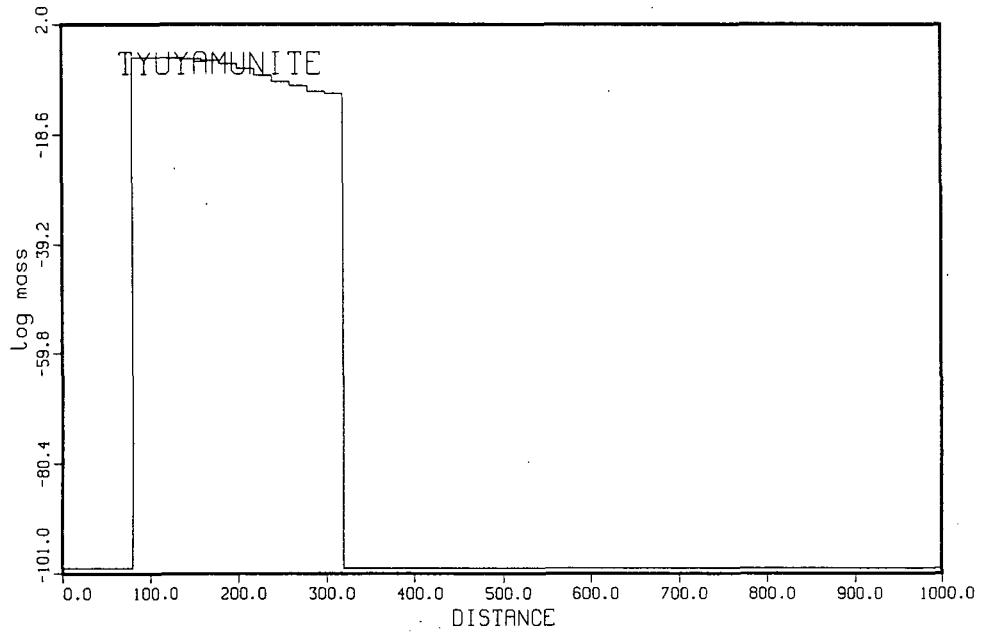
FIGURE 5.11. Tyuyamunite Precipitation Front after 10 Years for the System
Having Solubility Constraints Only.
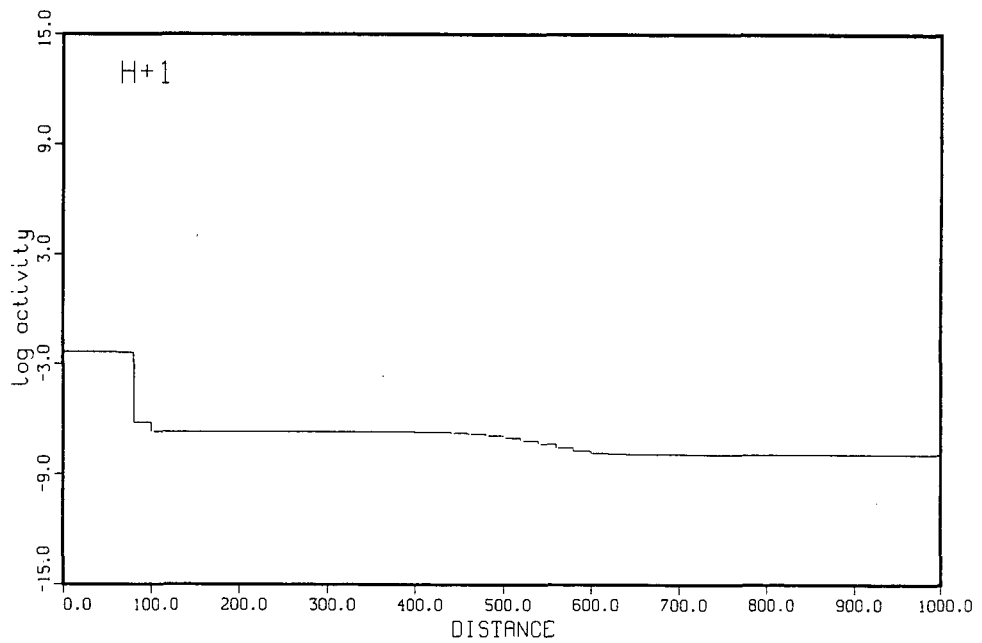
FIGURE 5.12. Calculated Distribution of pH after 10 Years for the System
Having Solubility Constraints Only.

5.15

same time period because of the additional solubility constraint involving gypsum precipitation and its effect on the Ca^{2+} activity.

The neutralization of the acidic leachate by the calcite soil buffering capacity results in the gypsum precipitation front shown in Figure 5.10. The precipitation front for gypsum begins at the pond boundary even though the pH in this acid region is that of the leachate (2.3). The gypsum present at these distances was precipitated here during earlier times when the pH in this region was still buffered by the soil calcite buffering capacity. Because gypsum is stable at these low pH values it does not completely redissolve as the acid zone migrates downgradient. This behavior can be contrasted to the migration front of tyuyamunite (Figure 5.11) which is not stable at low pH values and thus redissolves as the acid front migrates downgradient with time. The gypsum precipitation front extends out to 320 m beyond which gypsum does not precipitate because the solubility product involving the individual ion activities of Ca^{2+} and SO_4^{2-} is not satisfied.

The pH breakthrough front has migrated 80 m after 10 years for run 3 (Figure 5.12), the same distance as in run 2. Thus, the average local velocity of the pH breakthrough front for the solubility and adsorption simulations having a finite calcite buffering capacity is 8 m/yr. Although gypsum is a solubility control for sulfate, not enough gypsum precipitated to alter the solute profile for sulfate and it is nearly identical to the profiles from runs 1 and 2 in which the attenuation mechanisms were specific-ion adsorption (Figure 5.4).

The effects of controlling the concentration of dissolved uranium using solubility equilibrium with tyuyamunite instead of specific-ion adsorption on the surface of HFO greatly affected the transport behavior of uranium. Figure 5.13 illustrates the solute profile for UO_2^{2+} after 10 years for run 3. In the acid zone up to a distance of 60 m where the pH is 2.3, the UO_2^{2+} concentration is equivalent to that of the leachate (7 mg/L, log mol = -4.5). After 10 years of contact with the leachate, all of the tyuyamunite precipitated in the previous timesteps has been redissolved up to 80 m away from the pond boundary (Figure 5.11). The dissolution of tyuyamunite coupled with

5.16
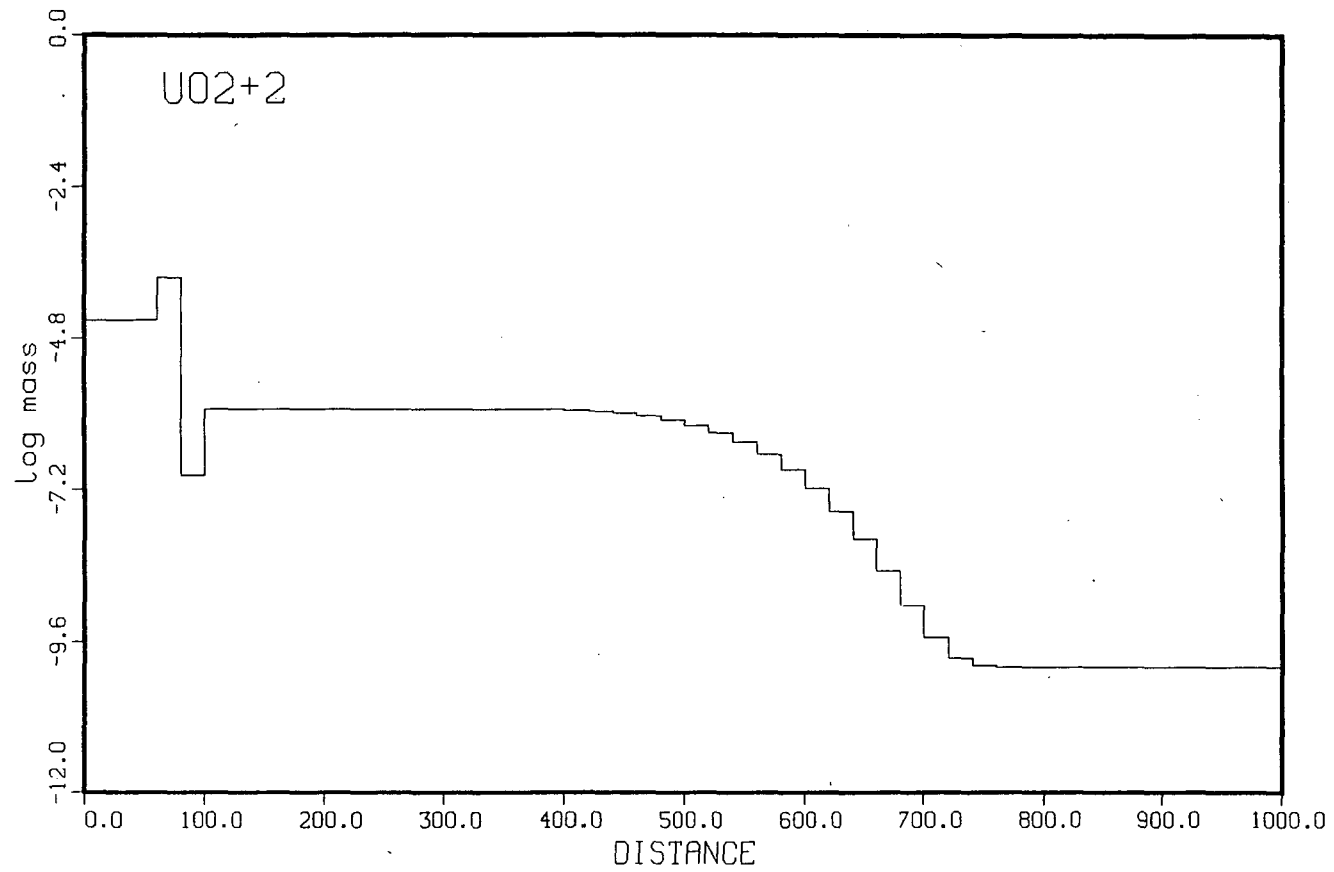
<u>FIGURE 5.13.</u> Calculated Distribution of Uranyl after 10 Years for the System Having Solubility Constraints Only.

downgradient advection and dispersion results in the increase in dissolved uranium concentrations between 60 and 80 m. At 80 m, the pH increases rapidly to between 7 and 8 and the precipitation of tyuyamunite lowers the uranium concentration at distances between 80 and 100 m from the pond boundary to a value of about 10^{-7} molal (24 μg/L). The stable solid phase assemblage between 80 and 100 m consists of gypsum and tyuyamunite. At 100 m, calcite reenters the stable solid phase assemblage and results in the increase of dissolved uranium because of the additional constraint on the activity of Ca^{2+} and the strong complexation of the uranyl ion by dissolved carbonate. At distances between 100 and 320 m, the solid phase assemblage consisting of calcite, gypsum, and tyuyamunite regulates the uranium concentrations at about 10^{-6} molal (240 μg/L). At greater distances, the uranium concentrations decrease along the advection/dispersion front reaching the concentration at the initial conditions (10^{-10} molal) at a distance of about 750 m from the pond boundary.

The average local velocity of the uranium breakthrough front in run 3 is 8 m/yr, a value considerably smaller than the average velocities for run 1 (44 m/yr), or run 2 (26 m/yr). Therefore, the highest retardation for the transport of uranium for the first three simulations occurred in the system where dissolved uranium was solubility-controlled by tyuyamunite and calcite was present to buffer the pH of the migrating acidic leachate. The differences in retardation behavior are reflected in the local dimensionless K_ds calculated for run 3 as compared to the values from the previous simulations that used specific-ion adsorption as the only attenuation mechanism. In run 3 after 10 years, the local dimensionless K_d values for uranium ranged from zero along most of the pathline (in the acid and transport zones where tyuyamunite had not precipitated) to values as large as 650 in regions where tyuyamunite was a solubility control. The global K_d averaged over the entire length of the pathline was about 2 in run 3. The global K_d for uranium in run 3 is larger than the values calculated for run 1 (0.05) or for run 2 (0.5). In these simulations, the insolubility of tyuyamunite appears to retard the migration of uranium to a greater extent than specific-ion adsorption of uranyl on the surface of HFO.

RUN 4: ATTENUATION USING BOTH SOLUBILITY AND ADSORPTION CONSTRAINTS

The final simulation performed combines the adsorption and solubility attenuation mechanisms that were examined separately in runs 2 and 3 into one simulation. The hydrologic model and the initial and boundary conditions used are those listed in Tables 4.1 and 4.2, respectively. In this case, the combined effects of adsorption and solubility on solute migration can be compared directly to the previous simulations that examined the independent effects of these attenuation mechanisms.

The dissolution/precipitation fronts for the solid phases in run 4 have similar characteristics to the profiles previously discussed for runs 2 and 3. The calcite dissolution front in run 4 after 10 years is nearly the same as in run 2 (Figure 5.6) in that the buffering capacity of the soil has been exhausted out to 80 m from the pond boundary. Consequently, the pH profile also is nearly the same as in run 2 (Figure 5.7); the pH out to 80 m where all of the calcite has dissolved is equal to 2.3 and then rapidly increases to near 7 at 80 m. Beyond 80 m, the pH is buffered by equilibrium with calcite and gradually increases to the value at the initial conditions (7.9). The precipitation front of gypsum for run 4 (Figure 5.14) has the same characteristics as the solubility-only simulation (run 3) with the exception that the front extends out to 240 m from the pond instead of 320 m from the pond (Figure 5.10). The gypsum precipitation front has not migrated as far in run 4 because of the additional mass of SO_4^{2-} immobilized by adsorption reactions. Similar behavior is evident for the precipitation front of tyuyamunite (Figure 5.15) when compared to the results obtained in run 3 (Figure 5.11).

The average local velocities of the transported solutes are not very different in run 4 compared to runs 2 and 3. The average local velocity of the migration of the pH front is the same (8 m/yr) as in the previous runs (2 and 3) containing calcite in the soil. The local velocity for uranium (8 m/yr) is also the same as in the previous run that used to solubility of tyuyamunite as the only constraint on the concentrations of dissolved uranium. However, the combined effects of solubility and adsorption slightly
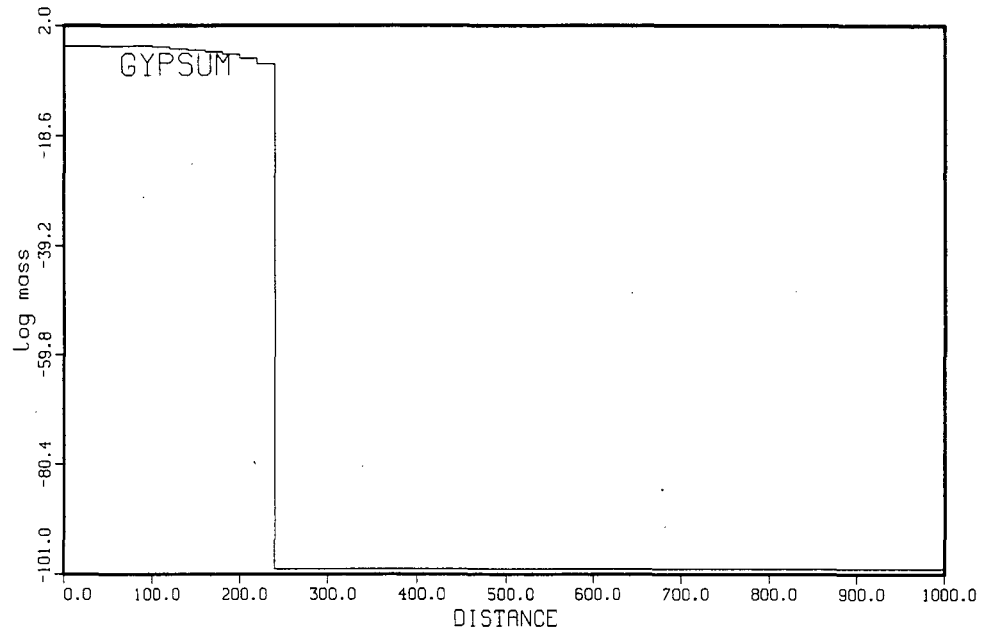
FIGURE 5.14. Gypsum Precipitation Front after 10 Years for the System Having Both Specific-Ion Adsorption and Solubility Attenuation with a Finite Soil Acid Buffering Capacity.
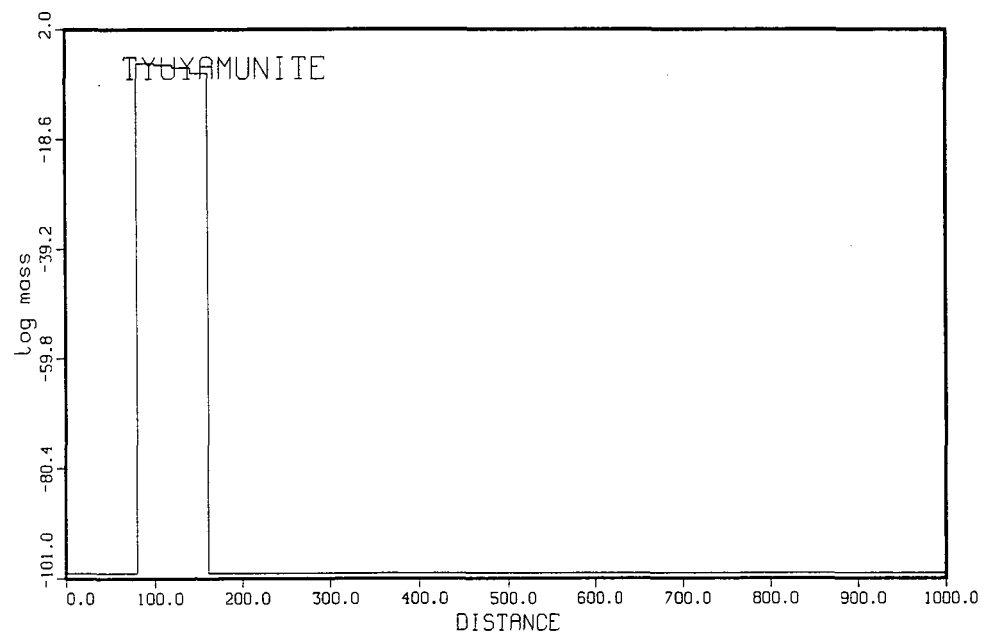

FIGURE 5.15. Tyuyamunite Precipitation Front after 10 Years for the System Having Both Specific-Ion Adsorption and Solubility Attenuation with a Finite Soil Acid Buffering Capacity.

retarded the migration of sulfate. The calculated local velocity for sulfate in run 4 was 48 m/yr as compared to 50 m/yr in runs 2 and 3.

Even though the calculated local velocity for the migration of the uranium front in runs 3 and 4 were the same, there are considerable differences in the transport behavior of uranium for the combined effects of solubility and adsorption equilibria. Figure 5.16 shows the solute profile for uranium using both adsorption and solubility mechanisms to attenuate the transport of uranium. In the acid zone near the pond boundary where the pH is 2.3, the uranium concentration is higher than the leachate value (log mol = -4.5) because of the combined desorption and redissolution of uranium that was immobilized from the previous timesteps. At 80 m where the solution is buffered by calcite, the pH increase causes uranium to precipitate from solution as tyuyamunite and to be adsorbed on the surface of HFO. At distances greater than 80 m, note that any given concentration of uranium above the value of the initial conditions (10^{-10} molal) appears to have migrated further after 10 years for the solubility-only run (Figure 5.13) than for run 4 in which dissolved uranium is immobilized by both adsorption and precipitation. The same behavior is evident in comparing Figure 5.13 (solubility-only) and Figure 5.8 (adsorption-only). The immobilization of uranium for the solubility constraint requires the solution to be saturated with respect to tyuyamunite which, at any time during the simulation, occurs over a short distance of the pathline. On the other hand, the adsorption of uranium from solution occurs continuously along the pathline.

In the previous simulations, we used the results of a coupled geohydrochemical transport model to compare relative velocities of breakthrough fronts for conservative and nonconservative solutes. The results showed the importance of soil acid buffering capacity in retarding the breakthrough fronts involving the pH and dissolved uranium. The simulation in which calcite was not present in the soil to neutralize the acidic leachate (run 1) had the furthest distance to breakthrough (440 m) for both the pH and uranium fronts after 10 years. For the runs having a finite quantity of calcite present to buffer the pH of the migrating leachate, the distance to breakthrough for the pH front after 10 years was the same for all
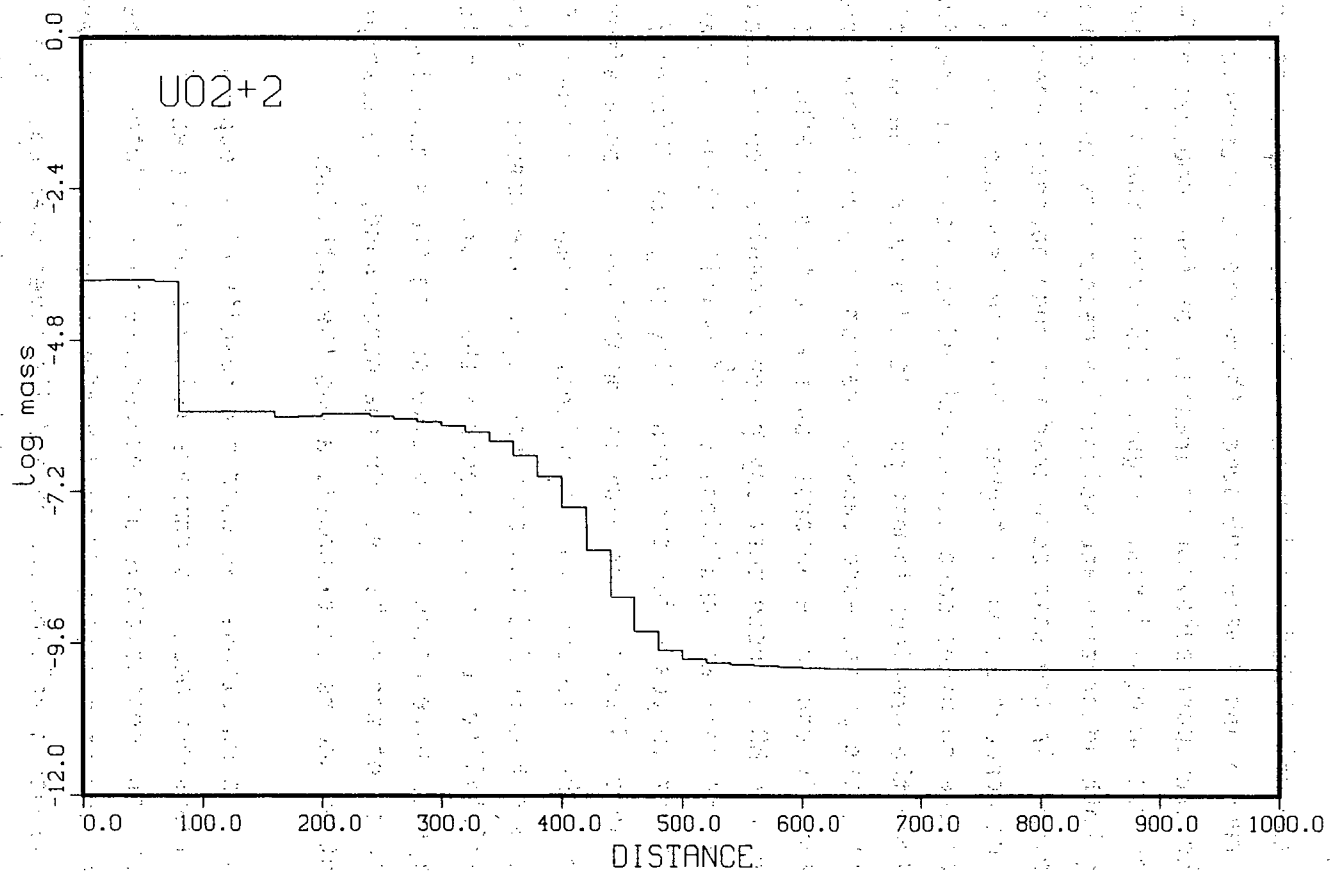
FIGURE 5.16. Calculated Distribution of Uranyl after 10 Years for the System Having Both Specific-Ion Adsorption and Solubility Attenuation with a Finite Soil Acid Buffering Capacity.

runs (80 m) and was independent of whether the attenuation was the result of specific-ion adsorption, solubility, or both. This is not the case for uranium which showed a breakthrough distance of 260 m in 10 years for the adsorption-only simulation (run 2), and a breakthrough distance of only 80 m for the solubility (run 3) and solubility/adsorption (run 4) simulations. The shorter distances to breakthrough for the simulations involving solubility equilibria show that the precipitation of insoluble U(VI) minerals such as tyuyamunite are capable of immobilizing large quantities of uranium in the neutralization zone and that precipitation is an efficient mechanism retarding the breakthrough velocity of the uranium front.

Although the identification of the location of the acid and neutralization zones is facilitated by simply examining pH profiles, there are more subtle differences evident in the profiles for dissolved uranium in the region beyond the neutralization zone. These differences are caused by the attenuation behavior of uranium and depend on whether solubility constraints or specific-ion adsorption reactions (or both) were used to regulate the concentrations. Figures 5.8, 5.13, and 5.16 illustrate the differences for the simulations involving adsorption-only (run 2), solubility-only (run 3), and solubility plus adsorption (run 4), respectively. The two simulations including adsorption as an attenuation mechanism are characterized as having a lower concentration at some arbitrary distance from the pond boundary within the transport zone. The differences in attenuation behavior can be quantified if we first assume an arbitrary reference concentration of interest, rather than the concentration at breakthrough ($C/C_0=0.5$). The calculation focuses on identifying at what distance (for a particular time) will the reference concentration be exceeded. This approach may perhaps be a more meaningful measure of the environmental impact of UMT operations on groundwater quality if the arbitrary reference concentrations were replaced by maximum allowable concentration limits. In this case, we chose a reference concentration for uranium of 75 μg/L (log mol = -6.5).

The breakthrough distances for uranium after 10 years are 260 m for adsorption alone, and 80 m for solubility and combined solubility and

5.23

adsorption. However, the distances at which the reference level for uranium of 75 μg/L was exceeded were 420 m for adsorption alone, 560 m for solubility alone, and 360 m for combined adsorption and solubility. Typical environmental regulations focus on the latter measure (i.e., the contaminated zone is the region in which the reference concentration is exceeded). This observation points out the importance of the relationship between the solubility limit and the reference concentration. If the reference limit is below the solubility limit, once precipitation has reduced the aqueous concentration to the solubility limit, in the absence of changes in solution pH or major element chemistry, no mechanism exists to further attenuate the contaminant concentration. Adsorption, in contrast, acts continuously along the pathline to attenuate solute concentrations, and will eventually reduce concentrations below any reference level. The zone of contamination at a given site thus depends not only on the geochemical mechanisms operating at the site but also on the reference level used to define the contamination.

6.0 SUMMARY AND CONCLUSIONS

A chemical transport code was used to qualitatively describe the effects of geochemical processes on the transport of uranium from UMT disposal sites. The geochemical mechanisms responsible for uranium transport behavior were inferred from field observations of contaminant plumes, and from information gathered from laboratory experiments and geochemical modeling calculations. These observations were recast in terms of transport and geochemical conceptual models and were used to calculate the attenuation behavior of uranium resulting from adsorption or solubility processes, or both.

FIELD OBSERVATIONS

We reviewed site characterization data, groundwater monitoring data, and sediment radioanalytical data for the following four UMT disposal sites; Sohio L-Bar, Riverton, Federal American Partners, and Lucky Mc. The waste disposal facilities at these sites included both tailings impoundments and evaporation ponds. At all four sites, leachate had seeped from the disposal facility into a shallow aquifer in alluvial material, as evidenced by the measurement of elevated concentrations of chloride, sulfate, and uranium or elevated pH levels in monitoring wells, and radionuclide concentrations found in contaminated sediments.

The geochemical interactions between acidic UMT leachates and the calcareous sediments found at many sites are dominated by acid/base reactions. The primary reactions are the dissolution of calcite and the precipitation of gypsum. As leachate migrates into the aquifer, a neutralization front appears that separates the low pH region in which calcite is absent (on the side close to the facility) from the higher pH region in which calcite is present. Total uranium and sulfate concentrations were found to be high inside the neutralization front, and variable beyond the neutralization front.

The leachates at the four sites all exhibited an acidic character. Speciation calculations showed acidity in the leachates has two sources:

sulfuric acid from the processing solution, and elevated aluminum and iron concentrations. We developed a quantitative calculation for determining the ability of UMT leachates to consume soil buffering capacity. In our calculation, the leachate is allowed to dissolve calcite and precipitate gypsum until both solid phases are in equilibrium. This calculation was used to represent the neutralization of the leachate by the soil materials.

The pH of the leachate was not found to be a complete measure of its ability to consume the soil buffering capacity. For example, the measured pH of the L-Bar leachate (0.98) is lower than the measured pH of the Riverton leachate (1.4). However, because of the elevated concentrations of aluminum and iron in the Riverton leachate, it was capable of consuming 89 g of calcite per liter of leachate, more than three times the amount consumed by the L-Bar leachate. Because of the strong dependence of the attenuation of uranium, sulfate, and trace metals on the pH, knowledge of the aqueous acid/base chemistry and the soil acid buffering capacity is essential in understanding the transport of reactive contaminants from UMT leachate impoundments.

INTERPRETATION OF FIELD DATA

We used the generic model of Sheppard and Brown (1982) as a starting point to interpret the soil and water quality data. The generic model divides a contaminated field site into three zones; the acid zone, the neutralization zone, and the transport zone. The acid zone is closest to the impoundment and is characterized by having pH values similar to the leachate because the acid buffering capacity of the soil has been consumed. The concentrations of chloride, sulfate, and trace metals are high in the acid zone. The second zone out from the impoundment is the neutralization zone which is characterized by an increase in the pH from the acidic influent values to near neutral pH values. There is a decrease in the concentrations of sulfate, trace metal, and radionuclide concentrations in the neutralization zone. In the third zone, the transport zone, the pH increases from neutral to alkaline values and the buffering capacity of the soil is unaffected by the leachate. The transport zone is dominated by advective/dispersive processes.

We found that in only one site (the Federal American Partners site) were all of the three zones of the generic model readily apparent. In the other three sites, either the inner two zones did not exist or they were not detected by the monitoring methods because observation wells were located too far downgradient from the leachate source. An additional complication is the variability of sulfate and uranium concentrations beyond the neutralization front. We found that uranium and sulfate mobility is not always limited to the region inside the neutralization zone as suggested by the model of Sheppard and Brown (1982). A series of coupled geohydrochemical simulations were performed to investigate the effects of different attenuation mechanisms on the transport of reactive solutes. The results are compared to the observations at the four field sites studied and the generic model of Sheppard and Brown (1982).

RESULTS OF COUPLED TRANSPORT SIMULATIONS

The use of the chemical transport code CTM requires the development of a geohydrochemical conceptual model which is divided into two parts; a hydrologic flow/transport model and a geochemistry model. The mechanisms included in the transport and geochemical conceptual models were based on the observations of contaminant plumes in the field and the generic model of Sheppard and Brown (1982). However, the conceptual models used were not specific to any one site because not enough field data existed for any of the sites to derive a set of comprehensive site-specific initial and boundary conditions. Instead, we developed conceptual models to investigate the attenuation behavior of reactive solutes that are involved in adsorption and solubility mass-transfer reactions.

The transport model used included advection and dispersion processes and values used for the average groundwater velocity and dispersivity were typical of sandy or silty soils. The geochemistry model was formulated from data generated previously on this project and from the review of leachate and soil properties typical of UMT disposal sites. The soil chemical properties included in the model were the soil acid buffering capacity and specific-ion

adsorption capacity. The acid buffering capacity refers to the quantity of calcite present in the soil which will control the neutralization of the leachate because of calcite dissolution. Thus, the acid buffering capacity will control the advance of the pH front. The adsorption capacity refers to the ability of the soil to specifically adsorb reactive solutes. The adsorption model included in the simulations refers to the adsorption of reactive solutes on the surface of hydrous ferric oxide.

The simulations performed examined the effects of solubility and/or adsorption attenuation mechanisms on the transport of reactive solutes. A total of four simulations were performed: 1) adsorption attenuation only without calcite buffering capacity, 2) adsorption attenuation only with a finite calcite buffering capacity, 3) solubility only with a finite calcite buffering capacity, and 4) both solubility and adsorption attenuation with a finite calcite buffering capacity. The adsorption mechanisms in the simulations included the competitive adsorption of H^+, SO_4^{2+}, and UO_2^{2+} for the free sites on the hydrous ferric oxide surface. The solubility mechanisms included the dissolution of calcite, precipitation of gypsum, and the precipitation of the most stable U(VI) mineral from a list of potential solids that included schoepite, rutherfordine, carnotite, and tyuyamunite. A background well water composition measured at the Federal American Partners site was used for the initial conditions, and the boundary condition used was based on a measured UMT leachate composition from the Exxon Highland Mill site.

The results of the simulations showed that the location of the neutralization front is governed by the flux of leachate entering the aquifer, the buffering capacity of aquifer materials, and the ability of the leachate to consume buffering capacity. The velocity of the neutralization front (as measured by the pH breakthrough front) was several times slower than the chloride breakthrough velocity in simulations where H^+ was immobilized either by specific-ion adsorption or the dissolution of calcite. In addition, the pH breakthrough front had the highest retardation in simulations that had a finite acid buffering capacity.

6.4

The velocities of the uranium and sulfate breakthrough fronts are governed by both solubility and adsorption reactions. The uranium front had the highest retardation in simulations in which aqueous uranium was controlled by the solubility of tyuyamunite because this solubility mechanism is capable of immobilizing large quantities of uranium in the neutralization zone. The inclusion of the adsorption of uranium in addition to the solubility mechanism did not significantly affect the retardation of uranium. Depending on the source strength, the solubility of the controlling solid phase, and the ability to compete for adsorption sites, uranium and sulfate mobility may be greater than pH mobility.

The amounts of mobile and immobile (either by adsorption or solubility constraints) reactive constituents that were calculated in the simulations were used to compute local dimensionless K_d values along the transport pathline. These computations showed that K_d values for either sulfate or uranium at different locations in the streamtube may be greater than or less than unity for competitive adsorption attenuation. For solubility attenuation, the K_d values can range from several hundred in zones of mineral precipitation to zero in zones where precipitation is inhibited. Therefore, these simulations show that the retardation behavior of reactive solutes can be highly nonlinear when mechanistic mass-transfer reactions are included in a transport model. Thus, these calculations point out the inability of a constant K_d retardation transport model to successfully reproduce the nonlinear contaminant distributions that occur in heterogeneous geochemical systems.

RECOMMENDATIONS

We have shown that the chemical reaction transport modeling approach can be used in conjunction with field observations to identify geochemical reactions of importance at UMT disposal sites. In order to provide quantitative assessments of contaminant mobility at a specific site, further characterization data for waste type and environmental setting must be made available. In particular, more specific data needs to be recorded with respect to site-specific initial and boundary conditions.

The lack of site-specific data needed to derive the initial conditions is mostly the result of an insufficient number and poor placement of the monitoring wells, and not conducting the measurements needed for the soil and groundwater chemical properties. An insufficient number of wells directly limits the ability to characterize the flow field, identify important heterogeneities in the subsurface soils, and precludes obtaining sufficient soil and groundwater samples for chemical analysis. Poor placement of the wells results in the inability to characterize the extent of contamination at a particular time. For example, in three of the four sites studied, the location of the acid and neutralization zones could not be delineated in the field because wells were placed too far downgradient of the acidic leachate source.

Measurements need to be performed to characterize the hydrologic and chemical properties of the subsurface media. Within the context of the one-dimensional transport calculations presented in this study, the variation in the average groundwater velocities and dispersivities of the subsurface soils need to be defined. The chemical properties needed in the simulations include estimates of the calcite content of the soils to calculate the acid buffering capacity and a measure of the hydrous ferric oxide content to calculate the soil adsorptive capacity. Analysis of the leachate chemistry, particularly as a function of time, is also required to better define the boundary condition.

We have shown that in the absence of detailed site characterization data a generalized model can be developed to qualitatively calculate the transport of solutes at UMT disposal sites. Because of the lack of site-specific data, we combined observations from a number of UMT disposal sites with the observations of Sheppard and Brown (1982). The generalized model is useful for estimating the velocities of the pH and uranium contamination fronts, and for screening sites to estimate the relative potential for migration. However, the generalized model should not be viewed as a performance assessement tool for UMT disposal sites in the absence of detailed site characterization data.

7.0 REFERENCES

Abramowitz, M., and I. A. Stegun. 1966. "Handbook of Mathematical Functions with Formulas, Graphs, and Mathematical Tables." Applied Mathematics Series No. 55. U.S. Department of Commerce, National Bureau of Standards, Washington D.C.

Ames L. L., J. E. McGarrah, and B. A. Walker. 1983a. "Sorption of Trace Constituents from Aqueous Solutions onto Secondary Minerals. I. Uranium." Clays Clay Miner. 31:321-334.

Ames L. L., J. E. McGarrah, and B. A. Walker. 1983b. "Sorption of Uranium and Radium by Biotite, Muscovite, and Phlogopite." Clays Clay Miner. 31:343-351.

Ames L. L., J. E. McGarrah, B. A. Walker, and P. F. Salter. 1983c. "Uranium and Radium Sorption on Amorphous Ferric Oxyhydroxide." Chem. Geol. 40:135-148.

Bear, J. 1972. Dynamics of Fluids in Porous Media. Elsevier, New York. 764 pp.

Borovec, Z. 1981. "The Adsorption of Uranyl Species by Fine Clay." Chem. Geol. 32:45-58.

Campbell, J. E., D. E. Longsine, and M. Reeves. 1981. "Distributed Velocity Method of Solving the Convective-Dispersion Equation: 1. Introduction, Mathematical Theory, and Numerical Implementation." Adv. Water Resour. 4:102-108.

Cederberg, G. A., R. L. Street, and J. O. Leckie. 1985. "A Groundwater Mass Transport and Equilibrium Chemistry Model for Multicomponent Systems." Water Resour. Res. 21:1095-1104.

Chou, T. T., and L. Zhou. 1983. "Extraction Techniques for Selective Dissolution of Amorphous Iron Oxides from Soils and Sediments." Soil Sci. Soc. Am. J. 47:225-232.

Dames and Moore. 1981. Detailed Seepage Investigation of Mill Waste Disposal Alternatives West Gas Hills, Wyoming for Federal American Partners Volume 1. Dames and Moore Job 10500-004-06, Salt Lake City, Utah.

Davies, C. W. 1962. Ion Association. Butterworths Publishers, Washington, D.C. 190 pp.

Devary, J. L., C. S. Simmons, and R. W. Nelson. 1984. Groundwater Model Parameter Estimation Using a Stochastic-Convective Approach. CS-3629, Electric Power Research Institute, Palo Alto, California.

Doi K., S. Hirono, and Y. Sakamaki. 1975. "Uranium Mineralization by Ground Water in Sedimentary Rocks, Japan." Econ. Geol. 70:628-646.

Duffy, C. J., C. T. Kincaid, and P. S. Huyakorn. 1988. "A Review of Groundwater Models for Assessment, Prediction, and Control of Nonpoint Source Pollution." Presented at the International Symposium on Water Quality Modeling of Agricultural Non-Point Sources, Utah State University, Logan, Utah.

Erikson, R. L., and C. J. Hostetler. 1989. "Coupling of Speciation and Transport Models." Presented at the Workshop on Metal Speciation and Transport in Groundwaters, U.S. Environmental Protection Agency, Jekyll Island, Georgia.

Erikson, R. L. and D. R. Sherwood. 1982. "Interaction of Acidic Leachate with Soil Materials at Lucky Mc Pathfinder Mill, Gas Hills, Wyoming." In Symposium on Uranium Mill Tailings Management, Fort Collins, Colorado, p. 335-351.

Felmy, A. R., D. C. Girvin, and E. A. Jenne. 1984. MINTEQ-A Computer Program for Calculating Aqueous Geochemical Equilibria. EPA-600/3-84-032, National Technical Information Service PB84-157148, Springfield, Virginia.

Freeze, R. A., and J. A. Cherry. 1979. Groundwater. Prentice-Hall Inc., Englewood Cliffs, New Jersey. 604 pp.

Garrels, R. M., and C. L. Christ. 1965. Minerals, Solutions, and Equilibria, Harper and Row, New York, 450 pp.

Gillham, R. W., E. A. Sudicky, J. A. Cherry, and E. O. Frind. 1984. "An Advection-Diffusion Concept for Solute Transport in Heterogeneous Unconsolidated Geological Deposits." Water Resour. Res. 20:369-378.

Grove, D. B. and W. W. Wood. 1979. "Prediction and Field Verification of Subsurface-Water Quality Changes During Artificial Recharge, Lubbock, Texas." Ground Water 17:250:257.

Hostetler, C. J., and R. L. Erikson. 1989. FASTCHEM™ Package: User's Guide to EICM, the Coupled Geohydrochemical Transport Code. EPRI EA-5870-CCM Volume 5, Electric Power Research Institute, Palo Alto California.

Hostetler, C. J., R. L. Erikson, J. S. Fruchter, and C. T. Kincaid. 1988. Overview of the FASTCHEM™ Package: Application to Chemical Transport Problems. EPRI EA-5870-CCM Volume 1, Electric Power Research Institute, Palo Alto California.

Hostetler, C. J., and B. E. Optiz. 1985. "Simulation of Solute Transport: A Markov Model." In Practical Applications of Ground Water Models, pp. 338-352.

Hsi C-K. D., and D. Langmuir. 1985. "Adsorption of Uranyl onto Ferric Oxyhydroxides: Application of the Surface Complexation Site-Binding Model." Geochim. Cosmochim. Acta. 49:1931-1941.

Jennings, A. A., D. J. Kirkner, and T. L. Theis. 1982. "Multicomponent Equilibrium Chemistry in Groundwater Quality Models." Water Resour. Res. 18:1089-1096.

Kirkner, D. J., T. L. Theis, and A. A. Jennings. 1984. "Multicomponent Solute Transport with Sorption and Soluble Complexation." Adv. Water Resour. 7:120-125.

Kirkner, D. J., and H. Reeves. 1988. "Multicomponent Mass Transport with Homogeneous and Heterogeneous Chemical Reactions: Effect of the Chemistry on the Choice of Numerical Algorithm 1. Theory." Water Resour. Res. 24:1719-1729.

Krupka, K. M., R. L. Erikson, S. V. Mattigod, J. A. Schramke, C. E. Cowan, L. E. Eary, J. R. Morrey, R. L. Schmidt, and J. M. Zachara. 1988. Thermochemical Data Used by the FASTCHEM™ Package. EPRI EA-5872-CCM, Electric Power Research Institute, Palo Alto California.

Krupka K. M., E. A. Jenne, and W. J. Deutsch. 1983. Validation of the WATEQ4 Geochemical Model for Uranium. PNL-4333, Pacific Northwest Laboratory, Richland, WA.

Krupka K. M., D. Rai, R. W. Fulton, and R. G. Strickert. 1985. "Solubility Data for U(VI) Hydroxide and Np(IV) Hydrous Oxide: Application of MCC-3 Methodology." Mat. Res. Soc. Symp. Proc. 44:753-760.

Langmuir D. 1978a. "Uranium Solution-Mineral Equilibria at Low Temperatures with Applications to Sedimentary Ore Deposits." Geochim. Cosmochim. Acta 42:547-569.

Langmuir D. 1978b. "Uranium Solution-Mineral Equilibria at Low Temperatures with Applications to Sedimentary Ore Deposits. In Uranium Deposits, Their Mineralogy and Origin, pp. 17-56. Mineralogical Association of Canada, Short Course Handbook 3, Univ. Toronto Press, Toronto, Canada.

Longmire, P., and D. Brookins. 1982. "Trace Metal, Major Element, and Radionuclide Migration in Groundwater from and Acid Leaching Uranium Tailings in the Grants Mineral Belt, New Mexico." In Symposium on Uranium Mill Tailings Management, pp. 315-333. Fort Collins, Colorado.

Matthews, M. L. 1985. "The Current Status of the Uranium Mill Tailings Remedial Actions Project." In Symposium on Management of Uranium Mill Tailings, Low-Level Waste and Hazardous Waste, pp. 125-130. Fort Collins, Colorado.

Maya L. 1981. "Hydrolysis and Carbonate Complexation of Dioxouranium(VI) in the Neutral-pH Range at 25°C." Inorg. Chem. 21:2895-2898.

Maya L., and G. M. Begun. 1981. "A Raman Spectroscopy Study of Hydroxo and Carbonato Species of the Uranyl(VI) Ion." J. Inorg. Nucl. Chem. 43:2827-2832.

Miller, C. W., and L. V. Benson. 1983. "Simulation of Solute Transport in a Chemically Reactive Heterogenous System: Model Development and Application." Water Resour. Res. 19:381-391.

Muto T. 1965. "Thermochemical Stability of Ningyoite." Min. Jour. 4:245-274.

Narasimhan, T. N., A. F. White, and T. Tokunaga. 1986. "Groundwater Contamination from an Inactive Uranium Mill Tailings Pile, 2. Application of a Dynamic Mixing Model." Water Resour. Res. 22:1820-1834.

Parker, J. C., and M. Th. van Genuchten. 1984. Determining Transport Parameters from Laboratory and Field Tracer Experiments. Bulletin 84-3. Virginia Agricultural Experimental Station, Blacksburg, Virginia.

Parkhurst, D. L., D. C. Thorstenson, and L. N. Plummer. 1980. PRHEEQE - A Computer Program for Geochemical Calculations. U.S. Geological Survey, Water Resources Investigations 80-96, 210 pp.

Peterson, S. R., W. J. Martin, and R. J. Serne. 1986. Predictive Geochemical Modeling of Contaminant Concentrations in Laboratory Columns and in Plumes Migrating from Uranium Mill Tailings Waste Impoundments. NUREG/CR-4520 (PNL-5788), U.S. Nuclear Regulatory Commission, Washington D.C.

Reardon, E. J. 1981. "Kd's - Can They be Used to Describe Reversible Ion Sorption Reaction in Contaminant Migration?" Ground Water 19:279-286.

Reeves, H., and D. J. Kirkner. 1988. "Multicomponent Mass Transport with Homogeneous and Heterogeneous Chemical Reactions: Effect of the Chemistry on the Choice of Numerical Algorithm 2. Numerical Results." Water Resour. Res. 24:1730-1739.

Rubin, J., and R. V. James. 1973. "Dispersion-Affected Transport of Reacting Solutes in Saturated Porous Media: Galerkin Method Applied to Equilibrium-Controlled Exchanges in Unidirectional Water Flow." Water Resour. Res. 9:1332-1356.

Schindler, P. W., B. Furst, R. Dick, and P. U. Wolf. 1976. "Ligand Properties of Surface Silanol Groups." J. Colloid Interface Sci. 55:469-475.

Serne, R. J., and A. B. Muller. 1987. "A Perspective on Adsorption of Radionuclides onto Geologic Media." In The Geological Disposal of High Level Radioactive Wastes, ed. D. G. Brookins, pp. 407-443. Theophrastus Publications, Athens, Greece.

Sheppard, T. A. and S. E. Brown. 1982. "A Generic Model of Contaminant Migration from Uranium Tailings Impoundments." Symposium on Uranium Mill Tailings Management, Fort Collins, Colorado, p. 241-257.

Sherwood, D. R., and R. J. Serne. 1983. Evaluation of Selected Neutralizing Agents for the Treatment of Uranium Tailings Leachates. NUREG/CR-3030 (PNL-4524), U.S. Nuclear Regulatory Commission, Washington, D.C.

Simmons, C. S. 1982. "A Stochastic-Convective Transport Representation of Dispersion in One-Dimensional Porous Media Systems." Water Resour. Res. 18:1194-1214.

Theis, T. L., D. J. Kirkner and A. A. Jennings. 1982. Multi-Solute Subsurface Modeling for Energy Solid Wastes. C00-10253-3, Department of Civil Engineering, University of Notre Dame, Notre Dame, Indiana.

Tripathi V. S. 1984. Uranium (VI) Transport Modeling: Geochemical Data and Submodels. PhD. Dissertation, Stanford University, Palo Alto, California.

U.S. Environmental Protection Agency. 1988. Code of Federal Regulations, Title 40, Part 192, Office of the Federal Register.

U.S. Nuclear Regulatory Commission. 1984. Code of Federal Regulations, Title 10, Part 40, Appendix A, Office of the Federal Register.

Valocchi, A. J., R. L. Street, and P. V. Roberts. 1981. "Transport of Ion-Exchanging Solutes in Groundwater: Chromatographic Theory and Field Simulation." Water Resour. Res. 17:1517-1527.

Valocchi, A. J., and P. V. Roberts. 1983. "Attenuation of Groundwater Contaminant Pulses." J. Hydraulic Eng. 109:1665-1682.

van Genuchten, M. Th., and W. J. Alves. 1982. Analytical Solutions of the One-Dimensional Convective Dispersive Solute Transport Equation. U.S. Department of Agriculture, Technical Bulletin No. 1661. 151 pp.

Vanselow, A. P. 1932. "Equilibria of the Base-Exchange Reactions of Bentonites, Permutites, Soil Colloids and Zeolites." Soil Sci. 33:95-113.

Wagman, D. D., W. H. Evans, V. B. Parker, R. H. Shumm, I. Halow, S. M. Bailey, K. L. Churney, and R. L. Nuttall. 1982. The NBS Tables of Chemical Thermodynamic Properties. Selected Values for Inorganic and C1 and C2 Organic Substances in SI Units. Vol. II, Supplement, American Chemical Society, New York.

Walsh, M. P., L. W. Lake, and R. S. Schecter. 1982. "A Description of Chemical Precipitation Mechanisms and their Role in Formation Damage During Stimulation by Hydrofluoric Acid." Symposium on Oilfield and Geothermal Chemistry. Society of Petroleum Engineers, Dallas, Texas.

Westall, J. C., J. L. Zachary, and F. M. M. Morel. 1976. _MINEQL, A Computer Program for the Calculation of Chemical Equilibrium Composition of Aqueous Systems_. Tech. Note 18, Dept. Civil Eng., Massachusetts Institute of Technology, Cambridge, Massachusetts.

White, A. F., J. M. Delany, T. N. Narasimhan, and A. Smith. 1984. "Groundwater Contamination from an Inactive Uranium Mill Tailings Pile 1. Application of a Chemical Mixing Model." _Water Resour. Res._ 20:1743-1752.

Wright, W. and A. K. Turner. 1987. "A Combined Modeling Program for Evaluating the Cover Design at a Uranium Mill Tailings Disposal Site." In _Solving Ground Water Problems with Models_, pp. 853-869. National Water Well Association, Denver, Colorado.

DISTRIBUTION

No. of
Copies

No. of
Copies

OFFSITE

U.S. Nuclear Regulatory
Commission
Division of Technical
Document Control
7920 Norfolk Avenue
Bethesda, MD 20014

F. W. Ross
U.S. Nuclear Regulatory
Commission
Office of Nuclear Material
Safety and Safeguards
55111 Rockville Pike
Rockville, MD 20852

10 Lynn Deering
U.S. Nuclear Regulatory
Commission
Office of Nuclear Material
Safety and Safeguards
55111 Rockville Pike
Rockville, MD 20852

P. H. Lohaus
U.S. Nuclear Regulatory
Commission
Office of Nuclear Material
Safety and Safeguards
55111 Rockville Pike
Rockville, MD 20852

10 R. J. Starmer
U.S. Nuclear Regulatory
Commission
Office of Nuclear Material
Safety and Safeguards
55111 Rockville Pike
Rockville, MD 20852

T. Nicholson
U.S. Nuclear Regulatory
Commission
Waste Management Branch
55111 Rockville Pike
Rockville, MD 20852

R.L. Bangart
U.S. Nuclear Regulatory
Commission
Office of Nuclear Material
Safety and Safeguards
55111 Rockville Pike
Rockville, MD 20852

George F. Birchard
U.S. Nuclear Regulatory
Commission
Office of Nuclear
Regulatory Research
55111 Rockville Pike
Rockville, MD 20852

J.J. Surmeier
U.S. Nuclear Regulatory
Commission
Office of Nuclear Material
Safety and Safeguards
55111 Rockville Pike
Rockville, MD 20852

Edward J. O'Donnell
U.S. Nuclear Regulatory
Commission
Office of Nuclear
Regulatory Branch
55111 Rockville Pike
Rockville, MD 20852

Myron Fliegel
U.S. Nuclear Regulatory
Commission
Office of Nuclear Material
Safety and Safeguards
55111 Rockville Pike
Rockville, MD 20852

Sandra Wastler
U.S. Nuclear Regulatory
Commission
Office of Nuclear Material
Safety and Safeguards
55111 Rockville Pike
Rockville, MD 20852

Daniel Gillen
U.S. Nuclear Regulatory
  Commission
Office of Nuclear Material
  Safety and Safeguards
55111 Rockville Pike
Rockville, MD 20852

Mark Thaggard
U.S. Nuclear Regulatory
  Commission
Office of Nuclear Material
  Safety and Safeguards
55111 Rockville Pike
Rockville, MD 20852

Timothy McCartin
U.S. Nuclear Regulatory
  Commission
Office of Research
55111 Rockville Pike
Rockville, MD 20852

Giorgio Gnugnoli
U.S. Nuclear Regulatory
  Commission
Office of Nuclear Material
  Safety and Safeguards
55111 Rockville Pike
Rockville, MD 20852

Jack Parrott
U.S. Nuclear Regulatory
  Commission
Office of Nuclear Material
  Safety and Safeguards
55111 Rockville Pike
Rockville, MD 20852

No. of
Copies

ONSITE

48   Pacific Northwest Laboratory

R. C. Arthur
M. P. Bergeron
L. J. Criscenti
L. E. Eary
R. L. Erikson (10)
J. W. Falco
J. S. Fruchter
J. M. Hales
P. C. Hays
C. J. Hostetler (10)
M. L. Kemner (5)
C. T. Kincaid
K. M. Krupka
W. T. Pennell
R. G. Riley
L. E. Rogers
J. A. Schramke
R. J. Serne
R. L. Skaggs
J. M. Zachara
Publishing Coordination
Technical Information (5)

U.S. NUCLEAR REGULATORY COMMISSION

BIBLIOGRAPHIC DATA SHEET

(See instructions on the reverse)

2. TITLE AND SUBTITLE

Mobilization and Transport of Uranium at Uranium Mill Tailings Disposal Sites: Application of a Chemical Transport Model

3.	DATE REPORT PUBLISHED
	MONTH	YEAR
	January	1990

4. FIN OR GRANT NUMBER
FIN B2482

5. AUTHOR(S)

R. L. Erikson
C. J. Hostetler
M. L. Kemner

6. TYPE OF REPORT

Technical

7. PERIOD COVERED *(Inclusive Dates)*
October 1, 1986 to
December 31, 1989

8. PERFORMING ORGANIZATION — NAME AND ADDRESS *(If NRC, provide Division, Office or Region, U.S. Nuclear Regulatory Commission, and mailing address; if contractor, provide name and mailing address.)*

Pacific Northwest Laboratory
P.O. Box 999
Richland, WA   99352

9. SPONSORING ORGANIZATION — NAME AND ADDRESS *(If NRC, type "Same as above"; if contractor, provide NRC Division, Office or Region, U.S. Nuclear Regulatory Commission, and mailing address.)*

Division of Low-Level Waste Management
Office of Nuclear Material Safety and Safeguards
U.S. Nuclear Regulatory Commission
Washington, D. C.   20555

10. SUPPLEMENTARY NOTES

11. ABSTRACT *(200 words or less)*

The geochemical processes of aqueous specification, precipitation, dissolution, and adsorption influence the transport of uranium at uranium mill tailings disposal sites. Traditional transport models involve the use of a single parameter, the retardation factor, to simulate the effects of these geochemical processes. Single parameter models are most applicable to field situations exhibiting no changes in major element chemistry along the flow path. Because of the changes in major element chemistry that occur when acidic leachate contacts a neutralizing soil, a single parameter transport model cannot accurately capture the details of uranium migration at a number of disposal sites. We have used a chemical transport model to qualitatively describe the effects of geochemical mechanisms on uranium transport. The result is a generalized conceptual model that can reproduce the features observed at a number of uranium mill tailings disposal sites.

12. KEY WORDS/DESCRIPTORS *(List words or phrases that will assist researchers in locating the report.)*

Uranium, Geochemistry, Transport
Uranium Mill Tailings

13. AVAILABILITY STATEMENT
Unlimited

14. SECURITY CLASSIFICATION

(This Page)
Unclassified

(This Report)
Unclassified

15. NUMBER OF PAGES

16. PRICE

MOBILIZATION AND TRANSPORT OF URANIUM AT URANIUM MILL TAILINGS DISPOSAL SITES

JANUARY 1990